Day/Night Cycles in the *Euprymna scolopes – Vibrio fischeri* Symbiosis

By

Elizabeth Anne Chapman Heath-Heckman

A dissertation submitted in partial fulfillment of

the requirements for the degree of

Doctor of Philosophy

(Microbiology)

at the

UNIVERSITY OF WISCONSIN – MADISON

2014

Date of final oral examination: 2/11/2014

The dissertation is approved by the following members of the Final Oral Committee:

Margaret McFall-Ngai, Professor, Medical Microbiology and Immunology
Edward Ruby, Professor, Medical Microbiology and Immunology
Caitilyn Allen, Professor, Plant Pathology
William Bement, Professor, Zoology
Heidi Goodrich-Blair, Professor, Bacteriology
Bruce Klein, Professor, Medical Microbiology and Immunology

Dedication

To Nathan, a light to me in dark places

DAY/NIGHT CYCLES IN THE *EUPRYMNA SCOLOPES – VIBRIO FISCHERI* SYMBIOSIS

Elizabeth A.C. Heath-Heckman

Under the Supervision of Professor Margaret J. McFall-Ngai

Day/night cycles, whether they are sunlight, feeding, or other stimuli, are important cues that animal physiology has learned to anticipate by way of circadian rhythms. While sunlight is the most pervasive day/night cycle to which animals are exposed, an organism can learn to anticipate any cycle that occurs with regularity. In the squid/vibrio mutualism, the host squid *Euprymna scolopes* uses light produced by its symbiont *Vibrio fischeri* to avoid predators during its nocturnal foraging. However, through both host and symbiont behaviors, the presentation of light by *V. fischeri* follows a reproducible daily pattern distinct from the presentation of sunlight, suggesting that bacterial luminescence could also act as a daily cue to the host, but this question has yet to be addressed. Using existing transcriptional databases I identified potential circadian regulators called cryptochromes in the host squid, and then determined their transcriptional patterns under normal symbiotic conditions. Using existing *V. fischeri* mutants, I then determined whether bacterial light affected the transcription of cryptochrome genes in the squid symbiotic organ and therefore whether bacterial light could affect circadian rhythms in the host. The presentation of bacterial light to the host makes the squid-vibrio system a powerful tool for the study of symbiont influence on host circadian rhythms due to the presentation of a common circadian cue by the symbiont.

In addition to characterizing the effect of *V. fischeri* on host circadian regulators, I better defined the repertoire of day/night cycles that occur in the symbiosis and their cues. To this end,

I identified and/or further characterized three daily cycles that occur in the squid/vibrio symbiosis. Using qRT-PCR, I first confirmed a daily cycle of transcription of a host galaxin gene in the juvenile and adult light organs and showed by bacterial growth assays that the protein likely functions as a bacterial growth modulator both during symbiosis initiation and during symbiont maintenance. While galaxins have been identified in several invertebrate species, my study is the first to experimentally test a function for this protein family.

Another previously suggested cycle in the squid light organ is that of host chitin production and provision to the symbionts, which then catabolize the polysaccharide. To find the source of this diel chitin provision in the light organ, I treated light organs with a fluorescent chitin-binding protein and localized polymeric chitin to the circulating immune cells, or hemocytes. In addition, I performed a phylogenetic survey of this character throughout the animal kingdom and found that it was apparently lost in the vertebrate lineage. While I did not define a day/night cycle in the hemocytes, this work has served as a framework for further studies delineating the role of chitin utilization by the bacterial symbionts.

The epithelial cells that support bacterial symbionts in the light organ lose their microvilli at some point during the day. Through transmission electron microcopy, I showed that the release of microvilli occurs in juvenile animals at dawn every day and is directly stimulated by the dawn light cue, regardless of symbiotic state. However, the regrowth of these microvilli depends upon symbiotic state, as symbiosis leads to an increased microvillar density, and this phenotype is dependent upon bacterial phosphorylated lipid A presentation to the host. This study is the first to link normal development of a subcellular structure to LPS or the lipid A moiety, and suggests that this mechanism may exist in other systems as well.

Acknowledgements

My thesis, like all those that came before it, would not have possible without the help and support of more people than I could ever name. However, that is not going to stop me from trying.

I have been fortunate to have received a scientific education that started early in my years as an undergraduate at the University of Chicago. There I benefited from the guidance of Dr. Michael LaBarbera, who was the first to introduce me to invertebrate biology and to the idea that scientific curiosity is reason enough to be a scientist. He told me once that the thing he was proud of me for was that I had stopped being afraid of what I wanted to do, which I will always carry with me as an accomplishment and something to strive for.

My research career would not have followed its current trajectory without Dr. Susan Daum, who took me in first as a teaching assistant and then as an undergraduate researcher when I had no research experience and a sometimes unnerving overabundance of enthusiasm about infectious disease. She instilled in me an appreciation for the laboratory and research that I hope to always have. In addition she has proven to be a wonderful collaborator even when I bring her strange squid proteins to test on her strains. Thank you Susan, for everything.

It is perhaps fitting that I have chosen to study symbiosis, since I desperately rely on my friends and family. Whether these interactions are mutualisms or parasitisms may not be clear at times (sorry guys!), but I need to first thank my friends, especially Bethany Rader, for supporting me in lab and out of it, no matter how unhinged any of us became.

Bridging friends and family, my husband Nathan has formed the nucleus of my little family in Madison, managing to simultaneously keep me sane and helping to found new types of astronomy (at least according to the papers). Schatz, you have been the best partner a woman could ask for – it has been a wonderful ten years, here's to a million more.

Last in this section but not least, I have to thank my family – especially my mom, dad, and two brothers - for loving and supporting me no matter what. You may not understand what I do or why I do it, but that has never stopped you from saying that I should do it, something that humbles me every day.

Finally I have to thank the woman who is truly the method in my madness, my advisor Dr. Margaret McFall-Ngai. Margaret, when I barged into your office as a junior in college I was full of unbridled enthusiasm and crazy ideas that would have put off most people, but it never seemed to faze you. I may still be full of crazy ideas, but you shown me how to harness my unfocused energy to become useful to myself and others, a feat without which I would be adrift in a sea of half-formed notions. You have fostered my love for weird invertebrates in a world that sometimes doesn't appreciate them as it should, and so where I would normally have been told to walk the straight and narrow you have shown me how to forge my own path. Now all that remains is to see if I can do it, but no one could have prepared me better than you. Mahalo nui loa Margaret.

And, dear reader, thank you for making it even this far in my thesis - it is perhaps on the long side, but to paraphrase Pascal, I did not have time to write a shorter one.

Table of Contents

List of Figures

Chapter 1

Chapter 2

Chapter 3

Chapter 4

Chapter 5

Appendix B

List of Tables

Chapter 2

Chapter 3

Chapter 5

Chapter 1

Introduction and Thesis Outline

PREFACE:

EACH formulated ideas and wrote the chapter.

"Time is more complex near the sea than in any other place, for in addition to the circling of the sun and the turning of the seasons, the waves beat out the passage of time on the rocks and the tides rise and fall as a great clepsydra."

— John Steinbeck, *Tortilla Flat*

If you ask a person how to tell time, they may often say that it is by clocks or watches (or now, I suppose, phones), but the reason that we feel the need to surround ourselves with these timepieces is to allow us to keep in step with the sun, which rises and sets on a 24-hour cycle. In reality, though our conscious mind requires us to keep time with clock-like accuracy, our bodies are perfectly capable of keeping time without the input of our thinking brain. This feat is accomplished through the use of blue-light receptive proteins that communicate the presence or absence of blue light to what are known as the core clock proteins inside of our cells. The light input then puts into motion a cyclical progression of transcription and degradation of these clock proteins that serves as a pacemaker for the body, controlling about 10% of all transcribed genes and allowing the body to anticipate the rising of sun or other daily events, such as food intake (Eckel-Mahan *et al.*, 2013).

The ability to anticipate daily events is so important to existence that *every* domain of life has the capability to entrain their physiology to day/night cycles, with blue light the most widespread daily cue. Blue light is likely the widely used signal because it has the largest range of penetrance through aquatic environments such as the ocean due to its short wavelength. Since the majority of the history of life has taken place in the oceans, the retention of blue-light signaling in land-dwelling organisms is not surprising. The potency of blue light has major

impacts on human heath. For example, recent studies have shown that the blue light-emitting electronics that humans now favor can severely alter our entrainment to the day/night cycle (Wood *et al.*, 2013), the best cure for which is apparently to go camping for a week (Wright *et al.*, 2013). Further, disease states, such as obesity and diabetes, have strong connections to both aberrant circadian rhythms of the gut and imbalances of the gut microbiota – although possible interactions between these two features have not been studied (Turnbaugh *et al.*, 2006; Velagapudi *et al.*, 2010; Lamia *et al.*, 2011; Tahira *et al.*, 2011).

As odd as it seems at times, we are not the only beings living in our bodies. What we know as our human selves are collections of human, bacterial, archeal, fungal, and protist cells, with viral particles thrown in for good measure. By weight we are predominantly human, but by cell count we are edged out by our symbionts at almost a 10:1 ratio, and at the genetic level we contain 100-fold more bacterial genes than those of human origin (Qin *et al.*, 2010). However, these organisms exist with us intimately and are as subject to day/night rhythms as are our own cells. However, the interplay between host circadian rhythms and symbiont activity has yet to be studied in depth.

In my thesis work, I have striven to study the effect of symbiosis on host daily rhythms and vice versa, using the mutualism between the Hawaiian bobtail squid (*Euprymna scolopes*) and its luminous symbiont *Vibrio fischeri* as a model system. I chose this system in which to study the interplay of rhythms and symbiosis for several reasons, foremost being that this is an association in which the main symbiont output is blue light, presented in close proximity to host cells. Since blue light serves as the predominant circadian input for eukaryotic cells, this fact raises the question of whether this beautiful denizen of the shallows has yet another way to tell time, that is, by the activities of its symbionts.

Circadian Rhythms and Symbiosis

Circadian rhythms are cycles that have a period of about 24 hours and are assisted in maintaining this period by entrainment to daily cues, such as the presence of sunlight or intake of food (Johnson, 1992). In organisms that maintain robust circadian rhythms, which are found in all domains of life (Edgar *et al.*, 2012), these cycles are usually controlled and maintained by transcriptional oscillators that can remain free running in the absence of external cues. However, recent studies have shown that perhaps the most phylogenetically widespread type of circadian rhythm is post-translational (Edgar *et al.*, 2012) and so there may be more types of circadian oscillators than previously thought. These rhythms, in turn, can provide input to many physiological processes; in fact it has been shown that about 10% of an animal's transcriptome is controlled in a circadian manner (Storch *et al.*, 2002).

The set of functions canonically known as the immune system is no exception, with connections between the circadian circuitry and immunity found in such divergent organisms as higher plants (Wang *et al.*, 2011) and mammals (reviewed in (Arjona *et al.*, 2012; Scheiermann *et al.*, 2013)). In mammals, where this connection has been most studied, the influence of time of day on immunity has been apparent since 1927, when Shaw observed that "the leucocytes of man exhibit twice daily a tidal rhythm of about twelve hours' duration which is independent of certain recognized physiological stimuli" (Shaw, 1927). Almost a century later this connection between circulating immune cells and circadian rhythms was supported when it was shown that splenic macrophages in mammals contain free-running circadian clocks that control inflammatory processes (Keller *et al.*, 2009). Indeed, this link is not restricted to mammals,

since it was also shown that the phagocytic activity of immune cells is circadian in the insect *Drosophila melanogaster* (Stone *et al.*, 2012).

The immune system has, until recently, been studied primarily in its role as host defense mechanisms during pathogenic insult. However, the immune system in a mammal likely expends more energy managing and communicating with the microbial communities that beneficially colonize various tissues in the body than defending against dedicated pathogens. In fact, it is possible that the evolution of the adaptive immune system was beneficial because it facilitated interactions with complex beneficial microbial consortia instead of with only one or a few species of mutualists, as is common for invertebrates (McFall-Ngai, 2007). In mammals, most major organ systems, including, but not limited to, the gut, skin, mouth, and reproductive tracts, maintain their own consortia of archaeal, bacterial, fungal, and viral species (Dethlefsen *et al.*, 2007). As such, these consortia have profound effects on the physiology of these organs and organ systems, such as stimulating proper development of the immune system (Bouskra *et al.*, 2008). The gut consortium, which is by far the most well-studied, also assists in the digestion of food and can deliver signals to sites as distant as the mammalian brain (Cryan and Dinan, 2012). Since many aspects of gut physiology, such as processivity and transcription of many genes in gut epithelial and immune cells, is highly circadian (Froy and Chapnik, 2007; Hoogerwerf *et al.*, 2008; Keller *et al.*, 2009), there is likely an interface between the circadian rhythmicity of the gut and the physiological effects of symbionts therein.

While rhythms of the gut have been implicated in diseases such as obesity and diabetes (Lamia *et al.*, 2011; Konturek *et al.*, 2011; Paschos *et al.*, 2012), researchers in gastroenterology have not integrated this information with the known roles of the microbiota in these same disorders (Wen *et al.*, 2008). In addition, recent studies of gut-brain interactions have

demonstrated that behavioral disorders, such as depression, which affect and are affected by circadian rhythms (McCarthy and Welsh, 2012), are also influenced by the microbiota (*e.g.*, (Holzer *et al.*, 2012)). Taken together, the current data strongly implicate host-microbiota interactions in the maintenance of healthy circadian behaviors.

Though the bulk of research on the effect of circadian rhythms on symbiosis has been performed in pathogenic associations (see (Roden and Ingle, 2009; Arjona *et al.*, 2012) for reviews), day/night cycles can and do have a profound effect on mutualisms. The association between corals and their dinoflagellate symbionts is characterized by the transfer of algal photosynthetic products to the host, and so is directly tied to the presentation of exogenous light. This dependence upon light cycles causes both the host (Levy *et al.*, 2011) and symbiont (Sorek *et al.*, 2013) to experience profound circadian regulation of their transcriptomes and physiology. This pattern of parallel host and symbiont diel transcription is also shown in the symbiosis between the Hawaiian bobtail squid and its luminous symbiont *Vibrio fischeri* (Wier *et al.*, 2010). The association requires the presentation of light by *V. fischeri* bacteria to the host squid for nocturnal camouflage. Since both of these symbioses are dependent upon light for their maintenance, it is not surprising that they show evidence of circadian activity, for which exogenous light can be a potent cue. However, other, non-light driven, mutualisms also show similar phenomena, such as the nocturnal spore formation of parrotfish gut symbionts (Flint *et al.*, 2005) and the diurnal variation of bacterial number in the cow rumen (Leedle *et al.*, 1982). Since these symbioses are both tied to food intake and digestion, it is possible that they are integrated into the host circadian cycles through the presentation of food cues, which are also potent circadian inputs, to the host or symbiont.

While both bacterial consortia in contact with hosts and host circadian rhythms have been well studied, the influence of symbionts on host rhythms has only recently begun to be explored. In a way, it is logical that mutualistic symbionts should be able to influence rhythms in the host, as circadian rhythms are often entrained by metabolic cues, which can be profoundly affected by symbiosis. In addition, it has been shown that different organ systems can exhibit different circadian transcriptional profiles (Storch *et al.*, 2002), suggesting that different symbiotic organs can have independent responses to day/night cues. The fact that the mouse gut also shows circadian transcription of many immune genes suggests the idea that gut symbionts may play a role in affecting circadian rhythms in other mammalian hosts (Froy and Chapnik, 2007).

Day/night cycles in the squid-vibrio symbiosis

"May it be a light to you in dark places, when all other lights go out."

— J.R.R. Tolkien, *The Fellowship of the Ring*

The squid-vibrio symbiosis is a monospecific beneficial association between *Euprymna scolopes*, the Hawaiian bobtail squid, and *Vibrio fischeri*, a gram-negative, bioluminescent member of the bacterioplankton. Upon hatching, the juvenile squid acquire their bacterial symbionts from the surrounding seawater, using various chemical cues to facilitate bacterial migration into and subsequent colonization of a specialized set of tissues called the light organ (Nyholm and McFall-Ngai, 2004). Once in the light organ, the symbionts grow in epithelium-lined sacs called crypts where they reach high densities but remain extracellular for the entirety of the symbiosis (Nyholm and McFall-Ngai, 2004). Once the bacteria colonize the organ to a

high density they begin to emit blue light via density-dependent expression of the *lux* operon (K L Visick *et al.*, 2000). Light production is strictly required for the symbiosis to continue, and is thought to allow the squid to camouflage itself during its nocturnal foraging through a process known as counterillumination (Visick *et al.*, 2000; Jones and Nishiguchi, 2004). Counterillumination is a common phenomenon in which an animal produces downwelling light in an intensity and wavelength similar to the light being produced above it to give the illusion of transparency to predators beneath the prey. In return, the squid provides its resident symbionts with metabolites, such as amino acids (Graf and Ruby, 1998), sugars, and glycerol (Wier *et al.*, 2010). Since the benefit to the host is restricted to periods of relative darkness, its utility is strongly tied to the cycle of exogenous light, which is reflected in the many day/night cycles that occur in the symbiosis.

Perhaps the most striking day/night cycle that occurs in the symbiosis is the regulation of symbiont cell number in the light organ. Beginning at only 12 hours post-hatching, at the animal's first dawn, the host squid expels about 90% of the symbionts in the light organ into the surrounding seawater in a process known as venting (Nyholm and McFall-Ngai, 1998), Fig. 1-1. Throughout the remainder of the day, while the squid is buried under the substrate, the remaining bacteria divide to fill the light organ; providing a full complement of symbionts by nightfall when the squid will require the camouflage once more. This process of venting and regrowth occurs *every day* for the remainder of the animal's life and therefore establishes a daily rhythm in the light organ which is directly tied to the cycle of exogenous light (Nyholm and McFall-Ngai, 2004).

Bacterial bioluminescence is a costly process, and so in *V. fischeri* production of light is strongly tied to several quorum-sensing, or density-dependent, signaling systems

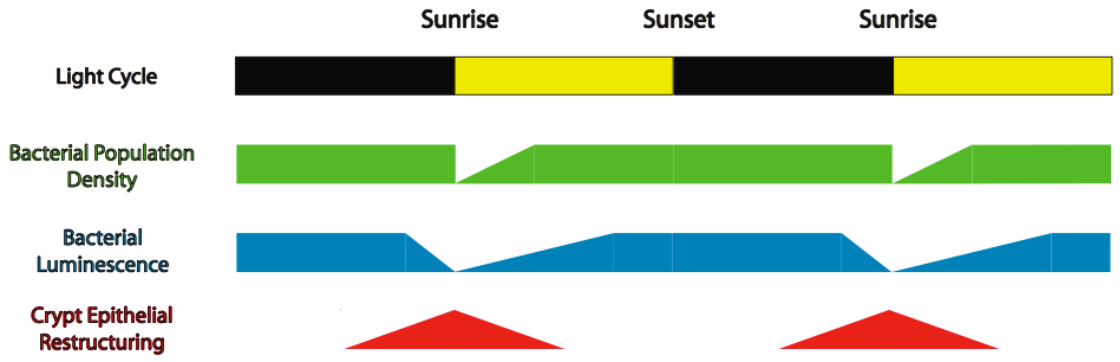

Figure 1-1: Known day/night cycles in the squid-vibrio symbiosis

(Stabb and Dr Karen L Visick, 2013). This is integral to energy conservation by symbionts, since light production by a single cell is not bright enough to be used for counterillumination, and so is only of use to the host when the symbionts are in high density. As such, the cycle of bacterial density established by the dawn light cue also has reprecussions for symbiont luminescence. At venting, bacterial luminescence in the light organ drops markedly, then increases again with bacterial density and remains high through the evening (Nyholm and McFall-Ngai, 2004), Fig. 1-1. However, 2-3 hours before dawn bacterial bioluminescence begins to drop in a density-independent manner (Boettcher *et al.*, 1996). While this decrease in light production can be reversed upon releasing the symbionts from the light organ into oxygen-rich water (Boettcher *et al.*, 1996), little else is currently known about the mechanisms regulating it. The observation of a day/night rhythm of symbiont luminescence implies that the squid cells in the light organ that come into contact with symbionts are exposed to a cycle of blue light very different from that provided by the sun, and so may be entrained differently than other tissues in the host that are only exposed to the solar light cycle.

While my thesis documents the first work to directly link symbiont rhythms and regulation of host transcription, it directly builds upon the finding that transcriptional rhythms exist in both the host and symbiont in the mature symbiosis (Wier *et al.*, 2010). In adult animals about 10% of the host transcriptome is differentially regulated over the day/night cycle in crypt epithelia, with the largest number of genes regulated two hours before dawn. This "anticipation" of the dawn (or perhaps bacterial) light cue is a hallmark of circadian regulation and suggests that a central oscillator may be functioning in the light organ. Several patterns of regulation appear to synergize with those found in the symbiont transcriptomes, such as one appearing to center upon chitin, a polysaccharide that is made in abundance in the marine

environment, and so is easily catabolized by marine bacteria such as *V. fischeri*. Just before dawn there is a significant increase in expression of a host chitin synthetic enzyme and a host chitin breakown enzyme (Wier *et al.*, 2010). At the same time, the symbionts upregulate expression of chitin catabolism and transport proteins, suggesting that the host is provisioning chitin to the symbionts for nutrition, signaling, or perhaps another function.

Another striking set of complementary cycles is the concomitant upregulation of symbiont glycerol ultilization genes and the apparent release of host cell membranes into the crypt spaces where the symbionts reside. The squid light-organ crypts are lined with a simple epithelium, the cells of which elaborate microvilli at their apical ends. Wier *et al*. found that these microvilli and some of the apical portions of the cells were released at or near dawn, but the exact timing was never established (Fig 1-1). In addition, just before dawn the host cells significantly upregulated the expression of transcripts coding for cytoskeletal proteins, suggesting that the host was fortifying the apical portions of the cells before or during this process. The release of host membranes occurred at or near the same time as the symbionts increased transcription of genes needed to catabolize host membranes (glycerol utilization genes), suggesting that a cycle of host membrane release and symbiont utilization of these membrane lipids occurs in the light organ. Host microvilli respond to symbiosis by increasing in number in a reversible manner (i.e. the depletion of symbionts reversed this phenotype), suggesting that symbionts have the ability to modulate the host cytoskeleton in this system (Lamarcq and McFall-Ngai, 1998). However, the connections between the symbiont-modulated increase in host microvillar density and the cycle of microvillar release and regrowth have yet to be examined.

THESIS STRUCTURE:

The main question driving my thesis is: how does symbiosis affect daily rhythms in the squid/vibrio symbiosis? To this end, I have structured this body of work into four main chapters, the first of which describes the behavior of cryptochromes, potential host circadian regulators, in the association, and the subsequent three each describe a day/night cycle that is integral to the symbiosis. Due to the relative novelty of asking my particular question in the symbiosis the three day/night cycles are fairly divergent, but all ultimately lead to a better understanding of the maintenance of the association.

1. How is a potential circadian regulator affected by symbiosis?

   In Chapter 2, I characterize, and examine the effect of symbiosis on transcription of, two squid cryptochrome genes using quantitative RT-PCR, antibody production and utilization, and reverse genetics by way of bacterial mutants. In Appendix B I begin to characterize Period and Timeless, components of the core clock circuitry, in the squid light organ.

2. What is the role of galaxin, an uncharacterized protein, the transcription of which is regulated over the day/night cycle?

   In Chapter 3, I describe a potential function for a squid galaxin in the initiation and maintenance of the symbiosis using qRT-PCR, immunocytochemistry, and bacterial growth inhibition assays.

3. What is the source of chitin in the squid light organ, the provision of which appears to be rhythmic in nature?

   In Chapter 4, I characterize the potential source of chitin in the squid light organ as the circulating hemocytes using a fluorescent chitin-binding probe. In addition, I present a phylogenetic survey to determine the penetrance of this characteristic throughout the animals.

4. What diel morphological changes occur in the epithelia in direct contact with the symbionts?

   In Chapter 5, I examine the timing of microvillar effacement and regrowth in the light-organ crypt epithelia and the effect of symbiosis on the process by transmission electron microscopy and the use of bacterial mutants and purified bacterial products.

REFERENCES:

Arjona, A., Silver, A.C., Walker, W.E., and Fikrig, E. (2012) Immunity's fourth dimension: approaching the circadian-immune connection. *Trends Immunol* **33**: 607–612.

Boettcher, K.J., Ruby, E.G., and McFall-Ngai, M.J. (1996) Bioluminescence in the symbiotic squid *Euprymna scolopes* is controlled by a daily biological rhythm. *J Comp Physiol A* **179**: 65–73.

Bouskra, D., Brézillon, C., Bérard, M., Werts, C., Varona, R., Boneca, I.G., and Eberl, G. (2008) Lymphoid tissue genesis induced by commensals through NOD1 regulates intestinal homeostasis. *Nature* **456**: 507–510.

Cryan, J.F., and Dinan, T.G. (2012) Mind-altering microorganisms: the impact of the gut microbiota on brain and behaviour. *Nat Rev Neurosci*.

Dethlefsen, L., McFall-Ngai, M., and Relman, D.A. (2007) An ecological and evolutionary perspective on human-microbe mutualism and disease. *Nature* **449**: 811–818.

Eckel-Mahan, K.L., Patel, V.R., de Mateo, S., Orozco-Solis, R., Ceglia, N.J., Sahar, S., *et al.* (2013) Reprogramming of the circadian clock by nutritional challenge. *Cell* **155**: 1464–1478.

Edgar, R.S., Green, E.W., Zhao, Y., van Ooijen, G., Olmedo, M., Qin, X., *et al.* (2012) Peroxiredoxins are conserved markers of circadian rhythms. *Nature* **485**: 459–464.

Flint, J.F., Drzymalski, D., Montgomery, W.L., Southam, G., and Angert, E.R. (2005) Nocturnal production of endospores in natural populations of *Epulopiscium*-like surgeonfish symbionts. *J Bacteriol* **187**: 7460–7470.

Froy, O., and Chapnik, N. (2007) Circadian oscillation of innate immunity components in mouse small intestine. *Mol Immunol* **44**: 1954–1960.

Graf, J., and Ruby, E.G. (1998) Host-derived amino acids support the proliferation of symbiotic bacteria. *Proc Natl Acad Sci U.S.A.* **95**: 1818–1822.

Holzer, P., Reichmann, F., and Farzi, A. (2012) Neuropeptide Y, peptide YY and pancreatic polypeptide in the gut–brain axis. *Neuropeptides*.

Hoogerwerf, W.A., Sinha, M., Conesa, A., Luxon, B.A., Shahinian, V.B., Cornelissen, G., *et al.* (2008) Transcriptional Profiling of mRNA Expression in the Mouse Distal Colon. *Gastroenterology* **135**: 2019–2029.

Johnson, B.C. (1992) Nutrient intake as a time signal for circadian rhythm. *J Nutr.* **122**: 1753-1759.

Jones, B.W., and Nishiguchi, M.K. (2004) Counterillumination in the hawaiian bobtail squid, *Euprymna scolopes* Berry (Mollusca : Cephalopoda). *Mar Biol* **144**: 1151–1155.

Keller, M., Mazuch, J., Abraham, U., Eom, G.D., Herzog, E.D., Volk, H.-D., *et al.* (2009) A circadian clock in macrophages controls inflammatory immune responses. *Proc Natl Acad Sci U.S.A.* **106**: 21407–21412.

Konturek, P.C., Brzozowski, T., and Konturek, S.J. (2011) Gut clock: implication of circadian rhythms in the gastrointestinal tract. *J Physiol Pharmacol* **62**: 139–150.

Lamarcq, L.H., and McFall-Ngai, M.J. (1998) Induction of a gradual, reversible morphogenesis of its host's epithelial brush border by *Vibrio fischeri*. *Infect Immun* **66**: 777–785.

Lamia, K.A., Papp, S.J., Yu, R.T., Barish, G.D., Uhlenhaut, N.H., Jonker, J.W., *et al.* (2011) Cryptochromes mediate rhythmic repression of the glucocorticoid receptor. *Nature* **480**: 552–U183.

Leedle, J.A., Bryant, M.P., and Hespell, R.B. (1982) Diurnal variations in bacterial numbers and fluid parameters in ruminal contents of animals fed low- or high-forage diets. *Appl Environ Microbiol* **44**: 402–412.

Levy, O., Kaniewska, P., Alon, S., Eisenberg, E., Karako-Lampert, S., Bay, L.K., *et al.* (2011) Complex diel cycles of gene expression in coral-algal symbiosis. *Science* **331**: 175–175.

McCarthy, M.J., and Welsh, D.K. (2012) Cellular circadian clocks in mood disorders. *J Biol Rhythms* **27**: 339–352.

McFall-Ngai, M. (2007) Adaptive immunity: care for the community. *Nature* **445**: 153.

Nyholm, S.V., and McFall-Ngai, M.J. (1998) Sampling the light-organ microenvironment of *Euprymna scolopes*: description of a population of host cells in association with the bacterial symbiont *Vibrio fischeri*. *Biol Bull* **195**: 89–97.

Nyholm, S.V., and McFall-Ngai, M.J. (2004) The winnowing: establishing the squid-vibrio symbiosis. *Nat Rev Microbiol* **2**: 632–642.

Paschos, G.K., Ibrahim, S., Song, W.L., Kunieda, T., Grant, G., Reyes, T.M., *et al.* (2012) Obesity in mice with adipocyte-specific deletion of clock component Arntl. *Nat Med* **18**: 1768–1777.

Qin, J., Li, R., Raes, J., Arumugam, M., Burgdorf, K.S., Manichanh, C., *et al.* (2010) A human gut microbial gene catalogue established by metagenomic sequencing. *Nature* **464**: 59–65.

Roden, L.C., and Ingle, R.A. (2009) Lights, rhythms, infection: the role of light and the circadian clock in determining the outcome of plant-pathogen interactions. *Plant Cell* **21**: 2546–2552.

Scheiermann, C., Kunisaki, Y., and Frenette, P.S. (2013) Circadian control of the immune system. *Nat Rev Immunol* **13**: 190–198.

Shaw, A.F.B. (1927) The diurnal tides of the leucocytes of man. *J Pathol Bacteriol* **30**: 1–19.

Sorek, M., Yacobi, Y.Z., Roopin, M., Berman-Frank, I., and Levy, O. (2013) Photosynthetic circadian rhythmicity patterns of Symbiodium, the coral endosymbiotic algae. *Proc Biol Sci* **280**: 20122942–20122942.

Stabb, P.E.V., and Visick, D.K.L. (2013) *Vibrio fisheri*: Squid Symbiosis. *The Prokaryotes* 497–532.

Stone, E.F., Fulton, B.O., Ayres, J.S., Pham, L.N., Ziauddin, J., and Shirasu-Hiza, M.M. (2012) The circadian clock protein timeless regulates phagocytosis of bacteria in *Drosophila*. *PLoS Pathog* **8**: e1002445.

Storch, K.F., Lipan, O., Leykin, I., Viswanathan, N., Davis, F.C., Wong, W.H., and Weitz, C.J. (2002) Extensive and divergent circadian gene expression in liver and heart. *Nature* **417**: 78–83.

Tahira, K., Ueno, T., Fukuda, N., Aoyama, T., Tsunemi, A., Matsumoto, S., *et al.* (2011) Obesity alters the expression profile of clock genes in peripheral blood mononuclear cells. *Arch Med Sci* **7**: 933–940.

Turnbaugh, P.J., Ley, R.E., Mahowald, M.A., Magrini, V., Mardis, E.R., and Gordon, J.I. (2006) An obesity-associated gut microbiome with increased capacity for energy harvest. *Nature* **444**: 1027–1031.

Velagapudi, V.R., Hezaveh, R., Reigstad, C.S., Gopalacharyulu, P., Yetukuri, L., Islam, S., *et al.* (2010) The gut microbiota modulates host energy and lipid metabolism in mice. *J Lipid Res* **51**: 1101–1112.

Visick, K.L., Foster, J., Doino, J., McFall-Ngai, M., and Ruby, E.G. (2000) *Vibrio fischeri lux* genes play an important role in colonization and development of the host light organ. *J Bacteriol* **182**: 4578–4586.

Wang, W., Barnaby, J.Y., Tada, Y., Li, H., Toer, M., Caldelari, D., *et al.* (2011) Timing of plant immune responses by a central circadian regulator. *Nature* **470**: 110–U126.

Wen, L., Ley, R.E., Volchkov, P.Y., and Stranges, P.B. (2008) Innate immunity and intestinal microbiota in the development of Type 1 diabetes. *Nature*.

Wier, A.M., Nyholm, S.V., Mandel, M.J., Massengo-Tiasse, R.P., Schaefer, A.L., Koroleva, I., *et al.* (2010) Transcriptional patterns in both host and bacterium underlie a daily rhythm of anatomical and metabolic change in a beneficial symbiosis. *Proc Natl Acad Sci U.S.A.* **107**: 2259–2264.

Wood, B., Rea, M.S., Plitnick, B., and Figueiro, M.G. (2013) Light level and duration of exposure determine the impact of self-luminous tablets on melatonin suppression. *Appl Ergon* **44**: 237–240.

Wright, K.P., McHill, A.W., Birks, B.R., Griffin, B.R., Rusterholz, T., and Chinoy, E.D. (2013) Entrainment of the human circadian clock to the natural light-dark cycle. *Curr Biol* **23**: 1554–1558.

Chapter 2

Bacterial Bioluminescence Regulates Expression of a Host Cryptochrome Gene in the Squid–Vibrio Symbiosis

PREFACE:

Published in *mBio* in April 2013 as:

Heath-Heckman, E.A.C., Peyer, S.M., Whistler, C.A., Apicella, M.A., Goldman, W.E., and McFall-Ngai, M.J. "Bacterial Bioluminescence Regulates Expression of a Host Cryptochrome Gene in the Squid-Vibrio Symbiosis"

EACH, CAW, and MJM formulated ideas and planned experiments. MAA and WEG contributed reagents. EACH performed all experiments with the exception of the sequencing of *escry1,* which was performed by SMP. EACH and MJM wrote and edited the chapter.

ABSTRACT:

The symbiosis between the squid *Euprymna scolopes* and its luminous symbiont *Vibrio fischeri* is characterized by daily transcriptional rhythms in both partners and daily fluctuations in symbiont luminescence. In this study, we sought to determine whether symbionts affect host transcriptional rhythms. We identified two transcripts in host tissues (*escry1* and *escry2*) that encode cryptochromes, proteins that influence circadian rhythms in other systems. Both genes cycled daily in the head of the squid with a similar pattern to that of other animals, in which expression of certain *cry* genes is entrained by environmental light. *escry1* expression cycled in the symbiont-colonized light organ with 8-fold up-regulation coincident with the rhythms of bacterial luminescence, which are offset from the day-night light regime. Colonization of the juvenile light organ by symbionts was required for induction of *escry1* cycling. Further, analysis with a bacterial mutant strain defective in light production showed that symbiont luminescence is essential for cycling of *escry1*; this defect could be complemented by presentation of exogenous blue light. However, blue light exposure alone did not induce cycling in non-symbiotic animals, but addition of molecules of the symbiont cell envelope to light-exposed animals did recover significant cycling activity, showing that light acts in synergy with other symbiont features to induce cycling. While symbiont luminescence may be a character specific to rhythms of the squid-vibrio association, resident microbial partners could similarly influence well-documented daily rhythms in other systems, such as the mammalian gut.

In mammals, biological rhythms of the intestinal epithelium and the associated mucosal immune system regulate such diverse processes as lipid trafficking and immune response to pathogens. While these same processes are affected by the diverse resident microbiota, the extent

to which these microbial communities control, or are controlled by, these rhythms has not been addressed. This study provides evidence that the presentation of three bacterial products (lipid A, peptidoglycan monomer, and blue light) is required for cyclic expression of a cryptochrome gene in the symbiotic organ. The finding that bacteria can directly influence the transcription of a gene encoding a protein implicated in the entrainment of circadian rhythms provides the first evidence for the role of bacterial symbionts in influencing, and perhaps driving, peripheral circadian oscillators in the host.

INTRODUCTION:

Biologists have studied the role of endogenous circadian rhythms in a wide array of biological processes. Although direct evidence is not yet available, recent data hint that a host's bacterial partners may affect, or be affected by, these rhythms. For example, numerous studies have demonstrated that immune competence requires intact circadian rhythms (see, *e.g.* ((Lee and Edery, 2008; Keller *et al.*, 2009; Wang *et al.*, 2011; Silver *et al.*, 2012)), and recent discoveries have shown that the normal function of an animal's immune system relies on interactions with the microbiota (reviewed in (Hooper *et al.*, 2012)). In addition, the gut, where most bacterial partners reside, has strong circadian rhythms on an array of processes from peristaltic activity to underlying molecular mechanisms (Konturek *et al.*, 2011). Transcriptomic data have shown that gene expression patterns of cells of the mucosal immune system of the gut, and the epithelial cells that line the gut, are strongly circadian (Froy and Chapnik, 2007; Hoogerwerf *et al.*, 2008). As the gut microbes provide a principal and critical input to this system, they likely impact, and/or are impacted by, the associated rhythms. Further, disease states, such as obesity and diabetes, have strong connections to both aberrant circadian rhythms of the gut and imbalances of the gut microbiota – although possible interactions between these two features have not been studied (Turnbaugh *et al.*, 2006; Velagapudi *et al.*, 2010; Lamia *et al.*, 2011; Tahira *et al.*, 2011). In this study, using the model association between the Hawaiian squid *Euprymna scolopes* and luminous symbiont *Vibrio fischeri* (strain ES114) (Fig. 2-1A, B), we asked: can microbial symbionts directly influence daily rhythms of a host animal?

While circadian rhythms can be entrained by many daily events, the day-night cycle of environmental light is the most well-documented cue, or Zeitgeber (Foster and Helfrich-Forster,

2001). One family of proteins implicated in the control of light entrainment of circadian rhythms in animals is the group of blue-light receptors called cryptochromes. They occur as components of the central oscillator, which resides in the animal brain, as well as in peripheral oscillators, such as in gut tissues (Foster and Helfrich-Forster, 2001). Cryptochromes are evolutionarily derived from the photolyases, which are DNA-repair enzymes (Fig. 2-1D). Whereas all vertebrate cryptochromes arose from the same evolutionary event, invertebrate cryptochromes typically fall into one of two clades, each of which is the product of an independent evolutionary derivation of photolyases (Yuan *et al.*, 2007; Reitzel *et al.*, 2010). Members of one clade (Cry1) are light-responsive and lead to degradation of repressors of the core clock machinery, and the others (Cry2) are light-independent transcriptional repressors of the core clock genes (Oztürk *et al.*, 2007). All cryptochromes have the conserved amino acids critical for function, as well as the characteristic domain structure of photolyases . However, cryptochromes have a defining C-terminal extension that does not occur in the photolyases. Whereas the role of cryptochromes in circadian rhythms have been well studied in many invertebrate groups (Ikeno *et al.*, 2008; Zhu *et al.*, 2008; Reitzel *et al.*, 2010; Mueller *et al.*, 2010; Ikeno, Numata, *et al.*, 2011; Ikeno, Katagiri, *et al.*, 2011; Merlin *et al.*, 2013), the identification of *cry* gene sequences and in one case the expression pattern of a single cryptochrome (Connor and Gracey, 2011) are the only examples available for these genes in the Lophotrochozoa, the superphylum of animals that contains the squid host *E. scolopes* and its relatives.

V. fischeri occurs as an extracellular symbiont in deep crypt spaces of the light organ of *E. scolopes* (Fig. 2-1B). The host animal has strong rhythms on its behavior; as a nocturnal predator, it remains buried in the sand during the day and emerges at night to forage in the water column (Fig. 2-1C). Host and symbiont cells within the adult light organ have rhythmic patterns

of gene expression that underlie day-night activities of the partners in the symbiosis (Wier *et al.*, 2010). Some behavioral evidence suggests the night-active host animal uses the luminescence of the bacterial symbiont as an antipredatory camouflage in a process known as counterillumination (Jones and Nishiguchi, 2004). Studies of the juvenile light organ have shown that the animal has molecular mechanisms by which to detect and respond to the bacterial luminescence (Tong *et al.*, 2009). Mutant symbionts defective in light emission are incapable of sustaining a symbiosis, and are also defective in inducing full light-organ development (Visick *et al.*, 2000), which is principally triggered by derivatives of symbiont MAMPs (microbe-associated molecular patterns). MAMPs are a class of molecules, specific to microbes that trigger host animal responses. In the development of the squid-vibrio system, the lipid A moiety of lipopolysaccharide and the peptidoglycan monomer TCT (or tracheal cytotoxin) are the MAMPs known to be active in inducing host light organ morphogenesis (Koropatnick *et al.*, 2004). Further, transcriptomic studies of the juvenile light organ revealed that colonization by luminous *V. fischeri* cells is required for normal symbiont-induced changes in host gene expression (Chun *et al.*, 2008). Particularly relevant here is the finding that the luminescence output of the animal is on a daily rhythm (Fig. 2-1C), which has key features of a circadian rhythm (Boettcher *et al.*, 1996). In this rhythm, luminescence peaks at night, when the animal is active. As such, light presentation by symbionts in the organ occurs with nearly the opposite timing of the exogenous cues of environmental light.

Transcriptional databases of the light organ (Chun *et al.*, 2006) revealed the expression of two genes that encode proteins with high sequence similarity to the known invertebrate cryptochromes. This finding offered the opportunity to investigate and compare the role of cryptochromes in host squid rhythms in response to exogenous (environmental light) and

endogenous (bioluminescence) light cues. Of broader significance, the presence of cryptochromes offered the opportunity to determine if bacterial symbionts and their luminescence can operate as critical features in the elaboration of host rhythms.

Here we characterize phylogenetic relationships of the two cryptochrome genes identified in *E. scolopes* and activity of these host genes in response to interactions with the bacterial partner. Taken together, these data contribute to our understanding of the extent to which bacterial partners can be integrated into the control of the biological rhythms of their animal hosts.

MATERIALS AND METHODS:

General Methods

Adult *Euprymna scolopes* were collected and maintained as previously described (Montgomery and McFall-Ngai, 1993). Juveniles from this breeding colony were collected within 15 min of hatching and placed into filter-sterilized Instant Ocean (FSIO, Aquarium Systems, Mentor, OH, USA). For all experiments, animals were maintained on a 12 h light/dark cycle. Uncolonized juveniles were maintained in FSIO. Symbiotic juveniles were exposed to 5000 *V. fischeri* cells per mL of FSIO overnight. Colonization of the host animals by the wild-type strain was monitored by taking luminescence readings using a TD 20/20 luminometer (Turner Designs, Sunnyvale, CA); uncolonized animals and animals colonized with the *Δlux* mutant were also checked with the luminometer to ensure that the light organs had not been colonized by wild-type strains. To determine colony-forming units (CFU) per light organ, tissues were homogenized in FSIO and dilutions of the homogenate were plated onto LBS medium (LB agar containing 2% wt/vol NaCl). Strains that were used include the wild-type strain ES114 (Boettcher and Ruby, 1990), the light-deficient mutant EVS102 ((55), *Δlux*), and the lysine auxotroph VCW3F6 ((Whistler *et al.*, 2007), *lysA:TnKan)*. All reagents were obtained from Sigma-Aldrich (St. Louis, MO) unless otherwise noted.

Exogenous Blue-Light and MAMPs Stimuli

To determine whether the decrease in *escry1* expression seen in *Δlux*-colonized animals was due to the lack of bacterial luminescence and not another consequence of deleting the *lux* operon (*e.g.*, change in oxygen utilization by the symbionts), the ventral surfaces of the animals

colonized by *Δlux* bacteria were exposed to exogenous blue light to mimic exposure of the tissues to bacterial luminescence. The animals were placed directly above 470 nm blue LED light arrays (Super Bright LEDs, St. Louis, MO) on ring stands, with 2 mm plexiglass heat shields to maintain the water temperature throughout the experiment at ~23° C. The blue LEDs were turned on at 6 h past dawn to mimic induction of blue light production following a light cue-induced expulsion of the bacteria, and then turned off at 22 h past dawn to mimic the decrease in luminescence seen in animals before dawn (Boettcher *et al.*, 1996). The ambient day-night light cycle was maintained as in other experiments. In experiments to determine whether non-symbiotic animals would respond to the blue LED light, with the exception of not being exposed to *V. fischeri* cells, the animals were treated similarly to those that were colonized by *Δlux* mutants. Lipid A and the peptidoglycan monomer were prepared as previously described (J S Foster *et al.*, 2000; Koropatnick *et al.*, 2004). For experiments where MAMPs were added, they were introduced directly into the seawater.

Identification of Cryptochrome Sequences from Transcriptional Databases

A Cry2-like sequence was identified by a tblastn search against the EST database of the juvenile-host light organ (Chun *et al.*, 2006) using *Drosophila* Cry (Table 2-1). Sequence for Cry1 was identified in transcriptional libraries of the host light organ by a tblastn search using *Drosophila* Cry (Table 2-1). These sequences were used for primer design for subsequent sequence analysis.

Table 2-1. Proteins used to construct the cryptochrome phylogeny in figure 2-1

Sequence	NCBI/JGI Protein Accession
A. egypti CRY1	157104635
A. gambiae CRY1	158301399
A. gambiae CRY2	78191297
A. mellifera CRY2	136255185
A. millepora CRY1	145881069
A. pernyi CRY1	13022111
A. pernyi CRY2	133754342
A. thaliana 6-4 PHR	18400841
B. impatiens CRY2	350420124
C. teleta CRY1	JGI: 226189
C. teleta CRY2	JGI: 178510
D. melanogaster 6-4 PHR	1304062
D. melanogaster CRY	24648152
D. plexippus 6-4 PHR	133754344
D. plexippus CRY1	62001759
D. plexippus CRY2	77166866
D. rerio 6-4 PHR	18858473
D. rerio CRY1a	55251266
D. rerio CRY1b	148540005
D. rerio CRY2a	63100688
D. rerio CRY2b	66910245
D. rerio CRY3	40254688
D. rerio CRY4	27882257
E. scolopes CRY1	This Study
E. scolopes CRY2	This Study
G. gallus CRY1	45383636
G. gallus CRY2	45383642
G. gallus CRY4	110626125
L. gigantea CRY1	JGI: 143285
L. gigantea CRY2	JGI: 131547
M. musculus CRY1	6681031
M. musculus CRY2	27312016
N. vectensis 6-4 PHR	156393374
N. vectensis CRY2	156353900

T. castaneum CRY2	134032019
X. laevis 6-4 PHR	147906624
X. laevis CRY1	147901097
X. laevis CRY2b	15341194
X. laevis CRY4	148226272

Rapid Amplification of cDNA Ends (RACE)

Preparation of RNA for 5' and 3' RACE was performed using the GeneRacer kit (Life Technologies, Grand Island, NY). Reverse transcription for RACE was performed using the SuperScript III RT kit and RACE reactions were performed using Platinum Taq DNA polymerase according to the manufacturer's instructions (Life Technologies, Grand Island, NY) using gene-specific primers found in Table 2-2. PCR products of interest were separated by gel electrophoresis, excised from the gel, and purified using the QIAEX II gel extraction kit (Qiagen, Valencia, CA). The purified PCR products were cloned using the TOPO TA Cloning Kit for Sequencing and transformed into TOP-10 chemically competent *E. coli* cells (Life Technologies, Grand Island, NY). The resulting transformants were prepared for sequencing with the QIAprep spin miniprep kit (Qiagen, Valencia, CA) and screened for the correct insert by plasmid digestion with EcoRI (Fermentas, Glen Burnie, MD). Plasmid inserts were sequenced using the M13F and R primers (Life Technologies, Grand Island, NY).

Protein Alignment and Phylogenetic Analysis

Sequences obtained by RACE were assembled into contigs using the CAP3 Sequence Assembly program (http://pbil.univ-lyon1.fr/cap3.php). The resulting sequences were analyzed by BLAST searches of GenBank using the default parameters (Altschul *et al.*, 1990). The cDNA sequence was translated using the ExPASy Translate tool (http://web.expasy.org/ translate/). Protein translation of the cDNA sequence was analyzed for domain structure using the Pfam website (http://pfam.sanger.ac.uk/). Alignments of cryptochrome sequences were generated using MUSCLE (Edgar, 2004) and the CLC sequence viewer (http://www.clcbio.com/index.php?id=28).

Table 2-2. Primers used in this study

Primer Name	**Sequence (5'-3')**
escry1 qRT F	GAAAGCCAACTGCATCATCGGCAA
escry1 qRT R	ATGCTCAATGGGTGGAAGCCAAAC
escry2 qRT F	TGTTGGATGCTGACTGGAGTGTGA
escry2 qRT R	AAAGCCAACAGGGCAGTAGCAATG
es40S qRT F	AATCTCGGCGTCCTTGAGAA
es40S qRT R	GCATCAATTGCACGACGAGT
escry1 5' RACE primary	AAAAGCCGAACTAGACACCCACATCC
escry1 5' RACE nested	AGACACCCACATCCAATTACCAGCAC
escry1 3' RACE	GGATGTGGGTGTCTAGTTCGGCTTTT
escry2 5' RACE primary	GCTGTACTTCGCATGGTAAGTCTGTG
escry2 5' RACE nested	TGTCTGATGAAGTCGCCATTCGGA

Specific, unambiguously aligned regions were selected for tree reconstruction to ensure that only evolutionarily conserved sequences were used to reconstruct the tree. With the full dataset, we then performed maximum likelihood analysis in PhyML 3.0 (60) with the WAG model.

RNA and cDNA Preparation

Whole juvenile animals were stored in RNALater RNA stabilization Reagent (Qiagen, Valencia, CA) for 24h at 4°C and then at -80°C until ready for RNA extraction. RNA was extracted from light organs, whole heads, or eyes using the RNeasy Fibrous Tissue Mini Kit (Qiagen, Valencia, CA) after homogenizing tissues in a TissueLyser LT (Qiagen, Valencia, CA). Three to six biological replicates were used per condition per experiment. The samples were treated with the Ambion TURBO DNA-*free* kit (Life Technologies, Grand Island, NY) to remove any contaminating DNA. The samples were then quantified using a Qubit 2.0 Fluorometer (Life Technologies, Grand Island, NY) and 5 µL were separated on a 1% agarose gel to ensure the quality of the RNA. If not used immediately, samples were aliquoted and then stored at -80°C. cDNA synthesis was performed with SMART MMLV Reverse Transcriptase (Clontech, Mountain View, CA) according to the manufacturer's instructions, and then reactions were diluted to a concentration of 2.08 ng/µL using nuclease-free water and stored at 4°C.

Quantitative Reverse Transcripase PCR

All qRT-PCR assays were performed in compliance with the MIQE Guidelines (Bustin *et al.*, 2009). Gene-specific primers were designed to *escry1*, *escry2*, and the *Euprymna scolopes* 40S ribosomal RNA sequence was used as a control for equal well loading (Table 2-2). For each experiment, negative controls were run without template and with cDNA reactions run with no

reverse transcriptase to ensure the absence of chromosomal DNA in the reaction wells. The efficiencies of all qRT-PCR primer sets were between 95 and 100%. Data were analyzed using the ΔΔCq method (Pfaffl, 2001). qRT-PCR was performed on *E. scolopes* cDNA using iQSYBR Green Supermix or SsoAdvanced SYBR Green Supermix (BioRad, Hercules, CA) in an iCycler Thermal Cycler or a CFX Connect Real-Time System (BioRad, Hercules, CA). Amplification was performed under the following conditions: 95°C for 5 min, followed by 45 cycles of 95°C for 15 sec, 60°C for 15 sec, and 72°C for 15 sec. Each reaction was performed in duplicate and contained 0.2 μM primers and 10.4 ng cDNA. To determine whether a single amplicon resulted from the PCR reactions, the presence of one optimal dissociation temperature for each PCR reaction was assayed by incrementally increasing the temperature every 10 sec from 60 to 89.5°C. Each reaction in this study had a single dissociation peak. Standard curves were created using a 10-fold dilution series of the PCR product with each primer set.

Western Blotting

A polyclonal antibody to EsCRY1 was produced in rabbit (Genscript, Piscataway, NJ) to two unique peptides within the EsCry1 sequence (CFGIEPECEEQKKPI and CGSCLPNHQENPELL), chosen for their predicted antigenicity and lack of similarity to other *E. scolopes* or *V. fischeri* proteins. Protein samples for western blotting were prepared as described previously (Troll *et al.*, 2010). Protein concentrations of the samples were then determined using a Qubit 2.0 Fluorometer (Life Technologies, Grand Island, NY). The proteins were separated on a 10% SDS-PAGE gel with 40 μg of protein per lane and then transferred onto a nitrocellulose membrane with a Mini Trans-Blot Electrophoretic Transfer Cell (BioRad, Hercules, CA) per the manufacturer's instructions. The membrane was blocked overnight at room temperature (RT) as

previously described (Troll *et al.*, 2010). The antibody was diluted 1:250 in blocking solution and incubated with the membrane for 3h at RT. The blot was then exposed to secondary antibody, washed, and developed as previously described (Troll *et al.*, 2010).

Immunocytochemistry

Light organs were fixed, permeabilized, and blocked as described previously (Troll *et al.*, 2009). The light organs were then incubated with a 1:250 dilution of the anti-EsCry1 antibody in blocking solution for 8 days at 4°C, and then rinsed 4 x 1h in 1% Triton X-100 in marine PBS and incubated overnight in blocking solution at 4°C. Samples were then incubated with a 1:50 dilution of fluorescein-conjugated goat anti-rabbit secondary antibody (Jackson ImmunoResearch Laboratories, West Grove, PA) in blocking solution in the dark at 4°C overnight. Samples were then counterstained with rhodamine or Alexa-633 phalloidin (Life Technologies, Grand Island, NY), as described previously (Troll *et al.*, 2009) and mounted for confocal microscopy. Samples were analyzed on a Zeiss LSM 510.

Statistics

All experimental data were log transformed to provide a normally distributed data set and then analyzed in R (version 2.12.1, R Foundation for Statistical Computing, Vienna, Austria [www.R-project.org]) by one-way ANOVA followed by a Tukey's pairwise comparison. Shapiro-Wilk and Levene tests were used to ensure the normal distribution and homoscedasticity of the residuals, respectively.

Nucleotide sequence accession numbers: Nucleotide sequence accession numbers were as follows: EsCry1, KC261598 and EsCry2, KC261599.

RESULTS:

Two cryptochrome genes are expressed in the *E. scolopes* light organ

We identified two candidate cryptochrome (*cry*) sequences in existing transcriptional databases produced from the *E. scolopes* light organ (Chun *et al.*, 2006). Rapid amplification of cDNA ends (RACE) and subsequent BLAST and alignment analyses showed that the two transcripts are likely homologs of known cryptochromes (Fig. 2-1, 2-2 and 2-3). The derived amino-acid sequences of full-length transcripts have the typical structure of cryptochrome (Cry) proteins with photolyase and FAD-binding domains characteristic of members of this protein family. In addition, both protein sequences have the conserved tryptophan residues that coordinate flavin binding (Zoltowski *et al.*, 2013) and conserved serine residues, whose phosphorylation is implicated in protein-protein interactions (Sanada *et al.*, 2004). Phylogenetic analyses placed the *E. scolopes* Cry proteins, with high confidence, within the two major invertebrate cryptochrome clades (Fig. 2-1C). The data provide evidence that the light organ expresses the same number of cryptochrome transcripts as the head and that the predicted proteins occur in phylogenetic relationships characteristic of the cryptochromes of most invertebrate species.

***escry1* expression in the light organ is influenced by symbiosis**

To characterize the regulation of expression of the *escry* genes in the light organ, we performed real-time quantitative reverse transcriptase PCR (qRT-PCR) on symbiont-colonized juvenile light organs, ~2 d post hatch, at four times over the day-night cycle (Fig. 2-4). These points were chosen to avoid the daily, non-circadian venting of symbionts that

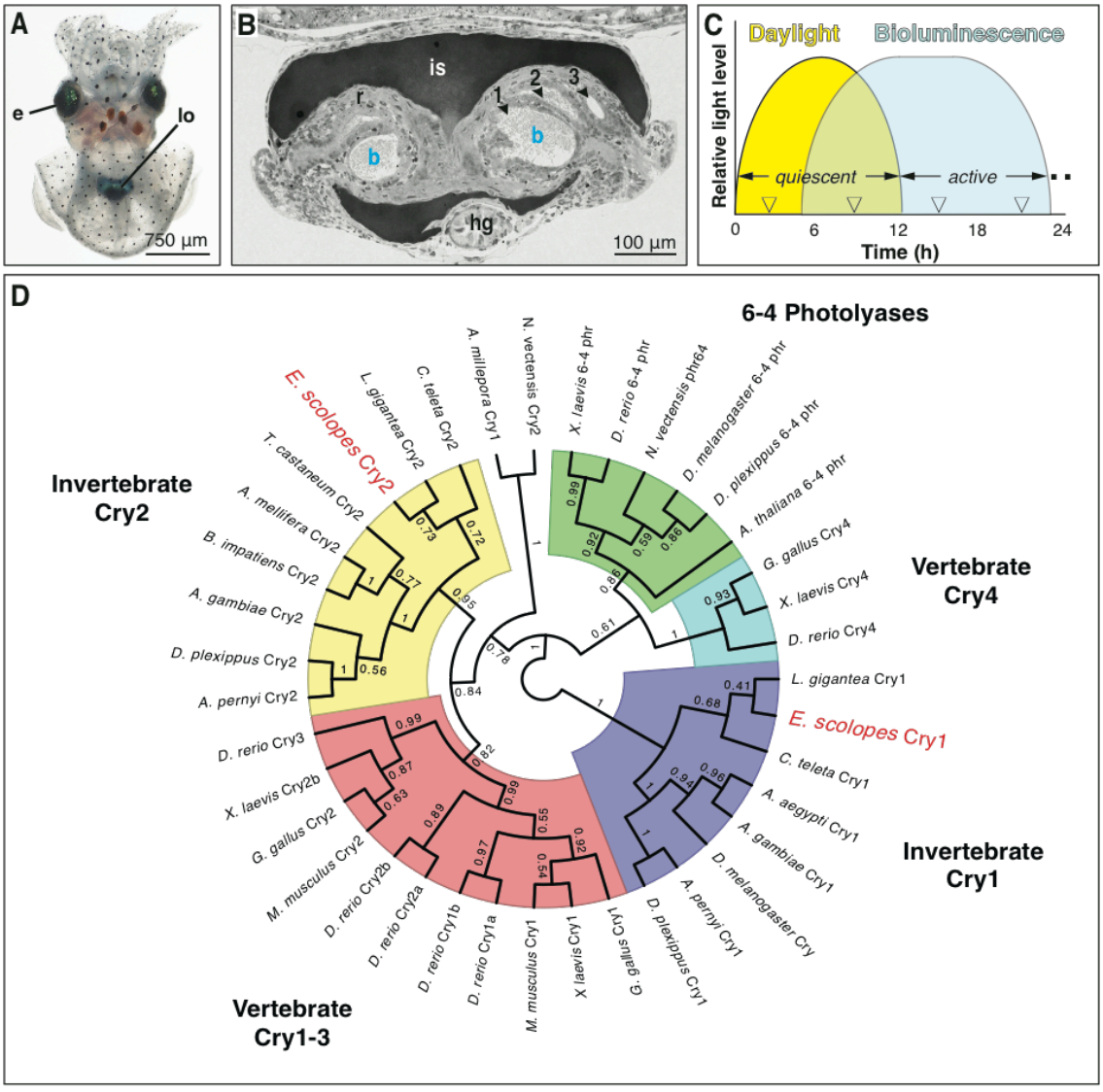
A
e
lo
750 µm
B
is
r
1
2
3
b
b
hg
100 µm
C
Daylight
Bioluminescence
Relative light level
quiescent
active
0
6
12
18
24
Time (h)
D
6-4 Photolyases
Vertebrate Cry4
Invertebrate Cry1
Vertebrate Cry1-3
Invertebrate Cry2
E. scolopes Cry2
E. scolopes Cry1
A. millepora Cry1
N. vectensis Cry2
X. laevis 6-4 phr
D. rerio 6-4 phr
N. vectensis phr64
D. melanogaster 6-4 phr
D. plexippus 6-4 phr
A. thaliana 6-4 phr
G. gallus Cry4
X. laevis Cry4
D. rerio Cry4
L. gigantea Cry1
C. teleta Cry1
A. aegypti Cry1
A. gambiae Cry1
D. melanogaster Cry
A. pernyi Cry1
D. plexippus Cry1
G. gallus Cry1
X. laevis Cry1
M. musculus Cry1
D. rerio Cry1a
D. rerio Cry1b
D. rerio Cry2a
D. rerio Cry2b
M. musculus Cry2
G. gallus Cry2
X. laevis Cry2b
D. rerio Cry3
A. pernyi Cry2
D. plexippus Cry2
A. gambiae Cry2
B. impatiens Cry2
A. mellifera Cry2
T. castaneum Cry2
L. gigantea Cry2
C. teleta Cry2

Fig. 2-1. The cryptochromes in the symbiotic organ of *E. scolopes*. **A.** The juvenile animal. e, eyes; lo, light organ, seen through ventral mantle tissue. **B.** A light micrograph of a cross section of the juvenile light organ. The interior of the organ contains three epithelium-lined crypts (1, 2, 3), each harboring bacteria (b) in the crypt lumen. Surrounding the light organ, and controlling light emission from the organ into the environment, are the ink sac (is) and reflector (r); hindgut (hg). **C.** Light cycles experienced by *E. scolopes*. The squid is exposed to bright exogenous light (Daylight) during its diurnal quiescent period and bacterial luminescence of the light organ (Bioluminescence) during the night, when the host is active (not to scale). **D.** Phylogenic relationships of *E. scolopes* cryptochromes. An unrooted, maximum-likelihood cladogram resolves the relative positions of EsCry1 and EsCry2 proteins within the animal cryptochrome/6-4 photolyase radiation. Bootstrap values after 500 replicates are shown at each node. Relevant families of proteins are grouped by color; *E. scolopes* sequences are highlighted in red.

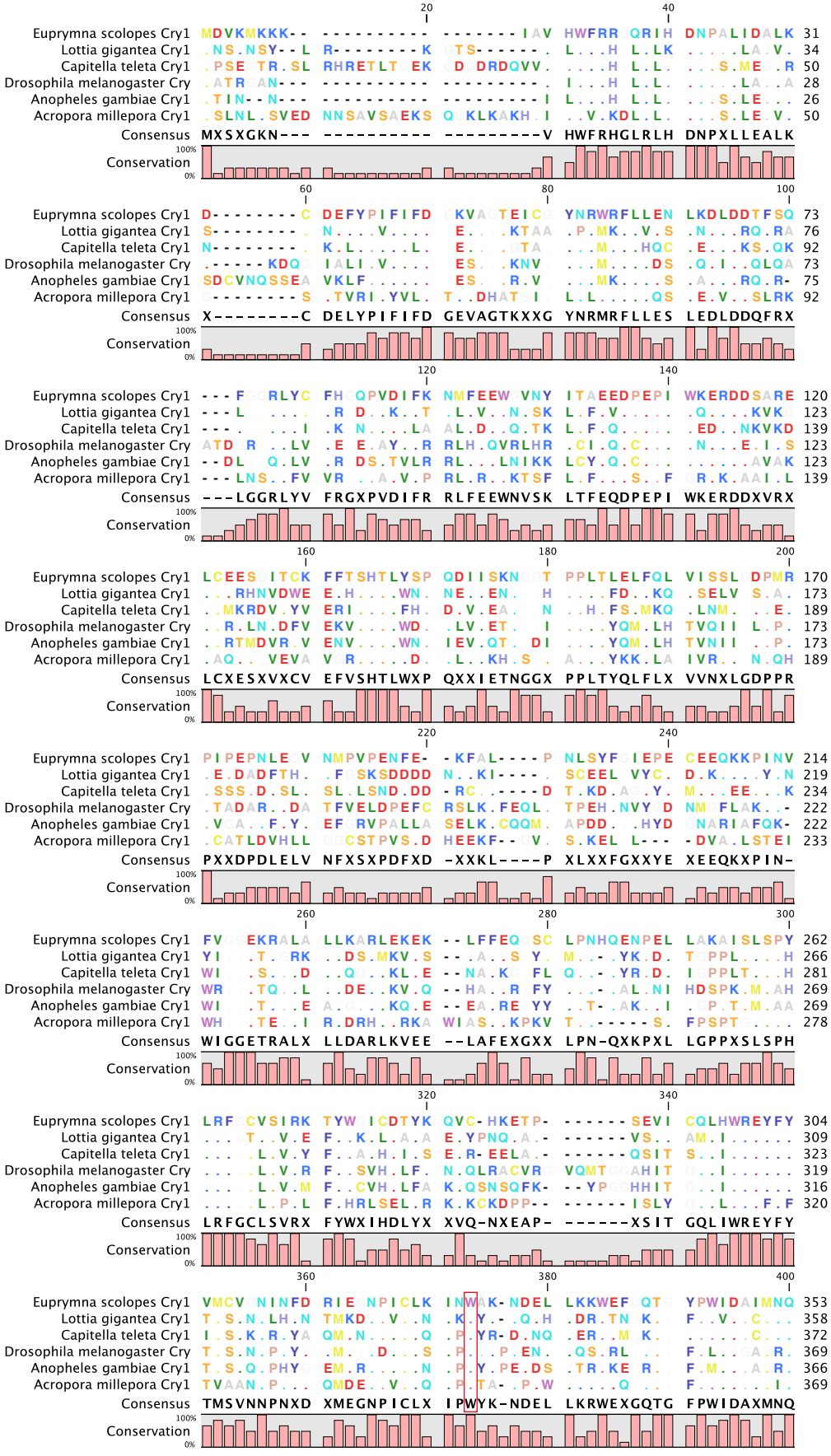
Euprymna scolopes Cry1
Lottia gigantea Cry1
Capitella teleta Cry1
Drosophila melanogaster Cry
Anopheles gambiae Cry1
Acropora millepora Cry1
Consensus
Conservation
100%
0%

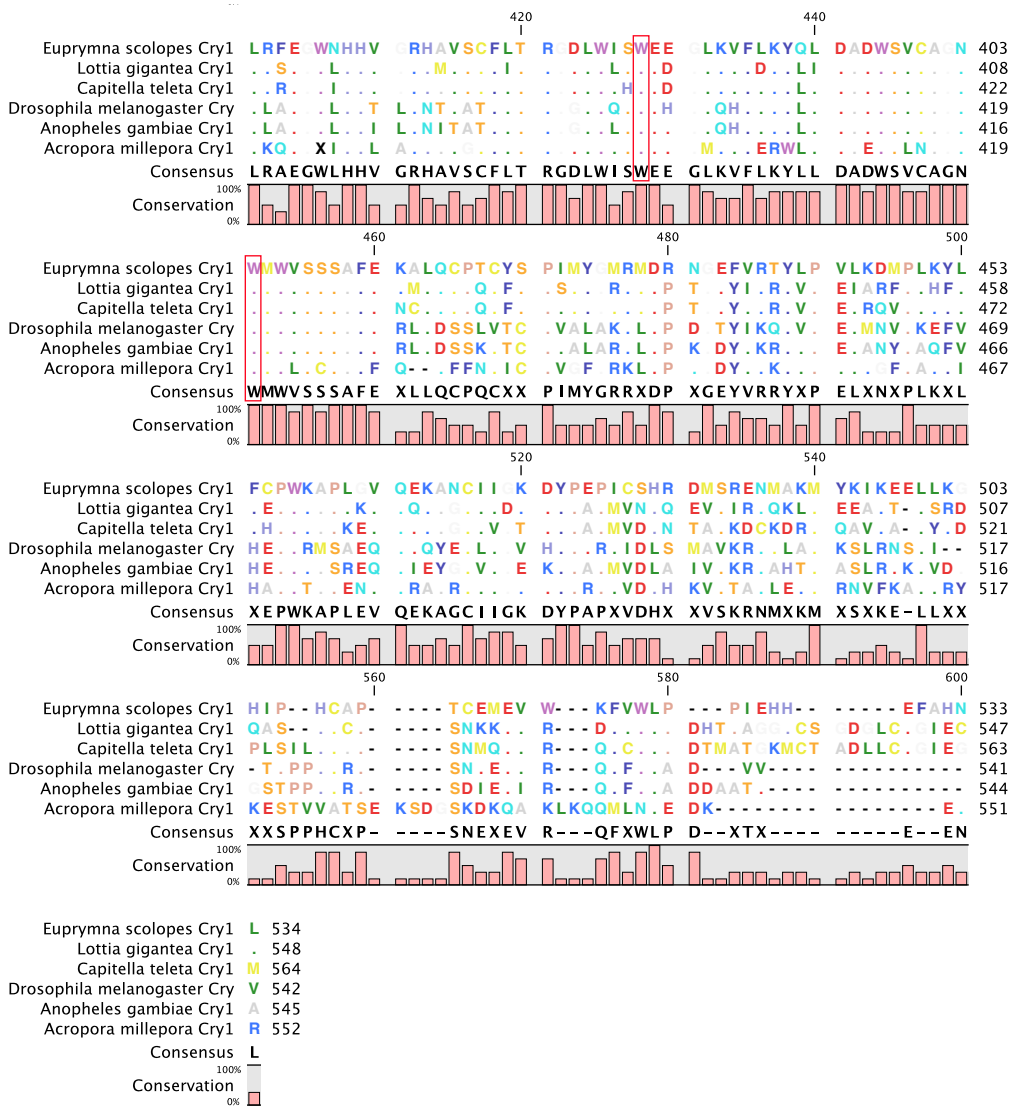

Fig. 2-2. Alignment of EsCry1 and other Cry1 proteins. Species names are shown to the left of the alignment and the consensus sequence is shown at the bottom of each line. Dashes (-) indicate gaps in the alignment and dots (.) indicate identity to the above residue. Boxes around particular residues indicate conservation of amino acids shown to be important for cryptochrome function in other studies.

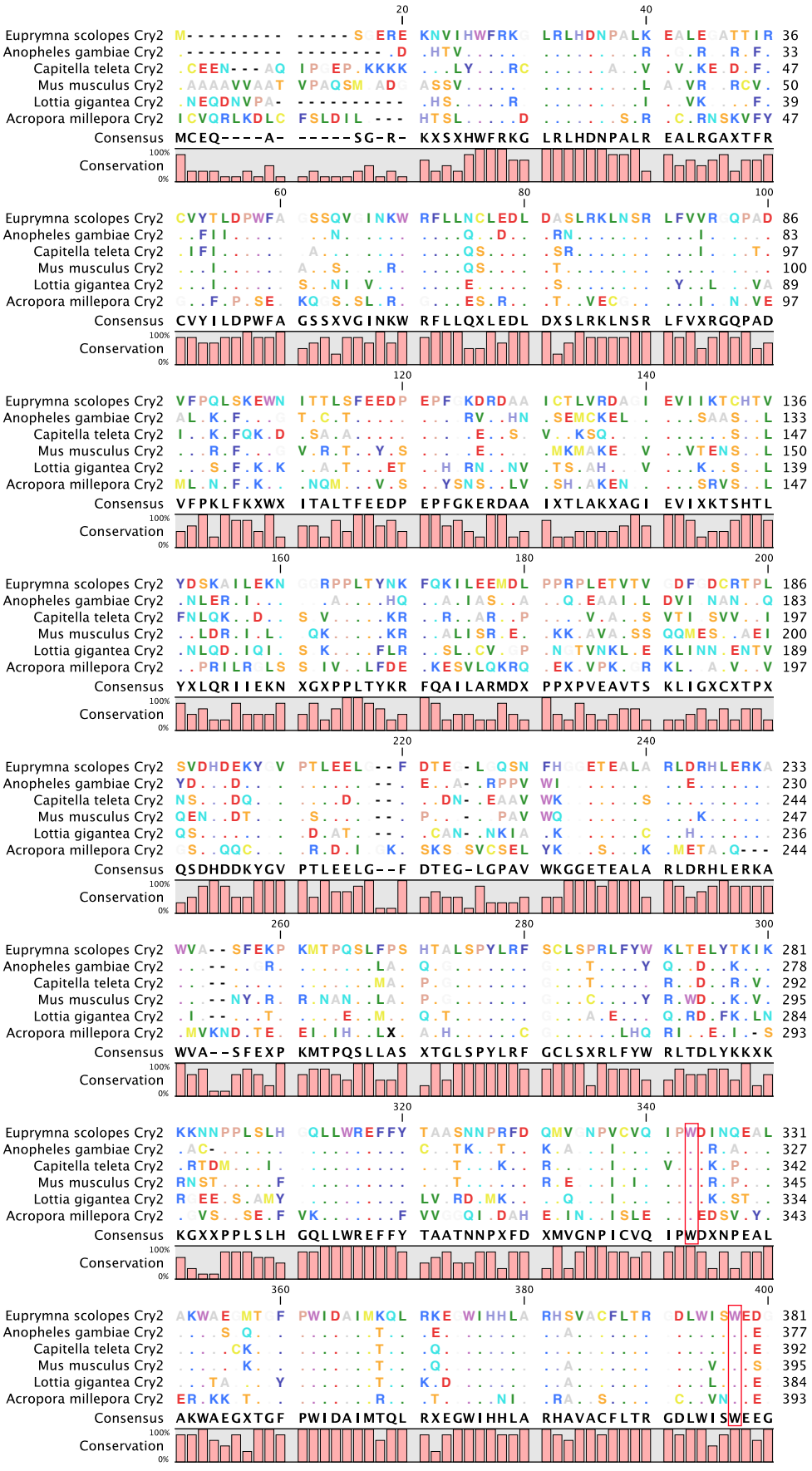
Euprymna scolopes Cry2
Anopheles gambiae Cry2
Capitella teleta Cry2
Mus musculus Cry2
Lottia gigantea Cry2
Acropora millepora Cry2
Consensus
Conservation
100%
0%

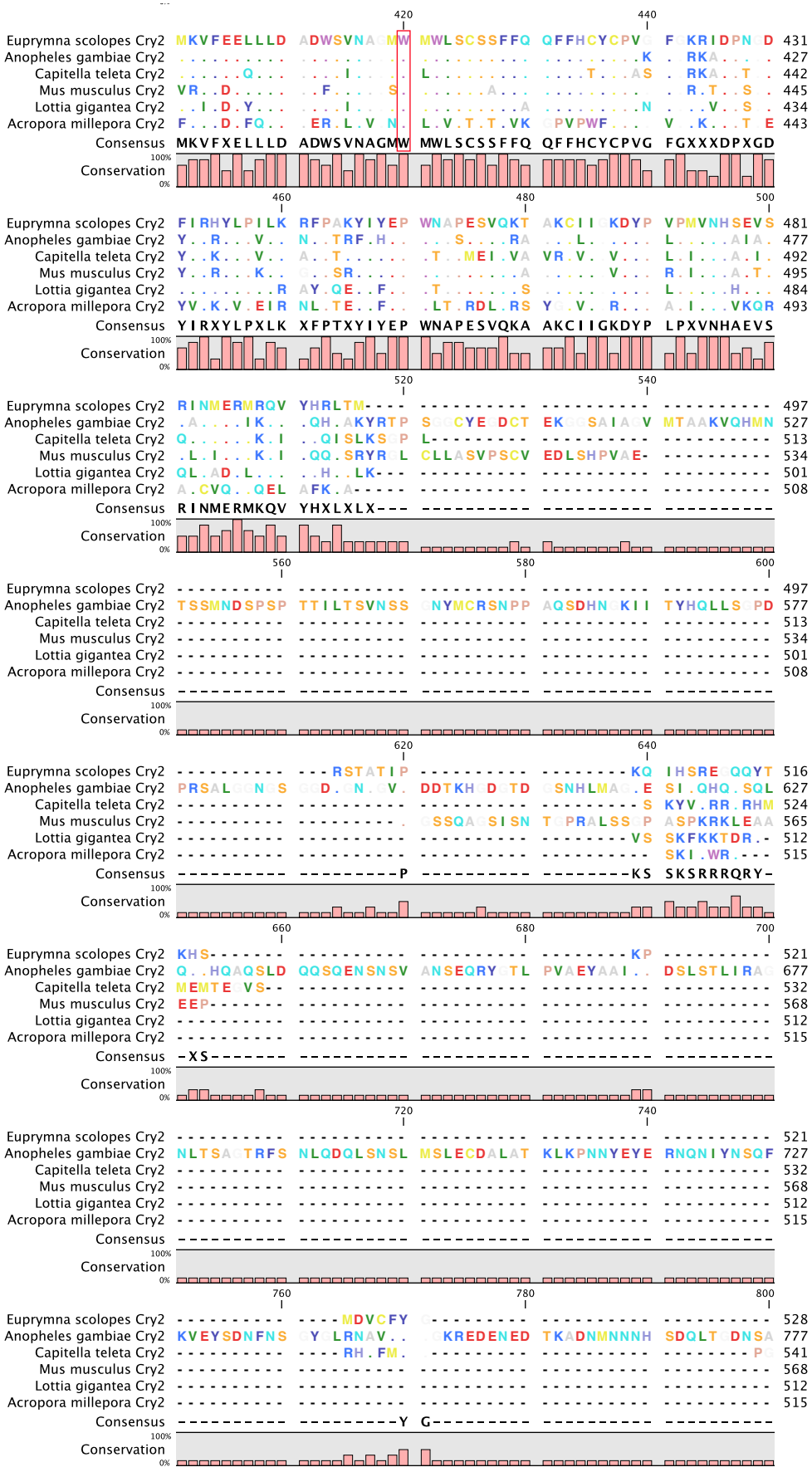
Euprymna scolopes Cry2
Anopheles gambiae Cry2
Capitella teleta Cry2
Mus musculus Cry2
Lottia gigantea Cry2
Acropora millepora Cry2
Consensus
Conservation
100%
0%
420
440
460
480
500
520
540
560
580
600
620
640
660
680
700
720
740
760
780
800

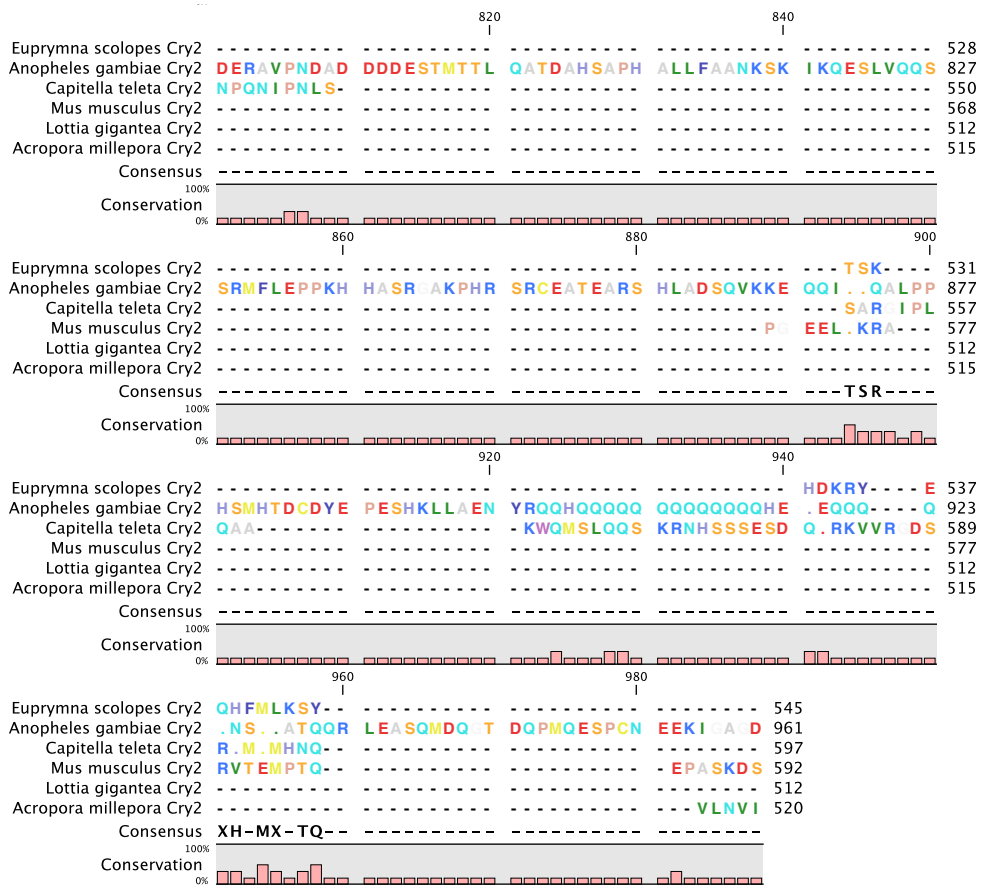

Fig. 2-3. Alignment of EsCry2 and other Cry2 proteins. Species names are shown to the left of the alignment and the consensus sequence is shown at the bottom of each line, above a bar graph showing the degree of conservation at each amino acid residue. Dashes (-) indicate gaps in the alignment and dots (.) indicate identity to the above residue. Boxes around particular residues indicate conservation of amino acids shown to be important for cryptochrome function in other studies.

occurs with a dawn light cue (Graf and Ruby, 1998), and to capture the extremes of the luminescence cycle of the light organs (Boettcher *et al.*, 1996). To compare patterns of *cry* expression in the light organ with those occurring in other invertebrates (Glossop and Hardin, 2002) we also performed qRT-PCR on the heads of the same juvenile animals, which contain tissues that typically have cycling *cry* expression in animals. Whereas the patterns of message levels for *escry1* and *escry2* showed statistically significant variation over the day in the head as observed in other systems (Glossop and Hardin, 2002), *i.e.*, in synchrony with environmental light, only *escry1* mRNA levels varied over the day/night cycle in the light organ (Fig. 2-4A). Further, peak mRNA levels in the light organ were observed in periods of high light-organ luminescence, *i.e.*, shifted ~6 h+ from that observed in the head (Fig. 2-4A) (Boettcher *et al.*, 1996). Light organs extracted in the field from mature wild-caught animals show a expression profile similar to that of the lab-raised symbiotic juveniles, providing evidence that the pattern of *escry1* expression is neither life-stage specific nor due to laboratory conditions (Fig. 2-4B). To determine whether the induction of rhythms is developmentally regulated by the onset of symbiosis, we characterized diel patterns of mRNA abundance in uncolonized juvenile squid. Animals that lacked symbionts did not show the same diel variation in *escry1* mRNA levels observed in symbiotic animals (Fig 2-4C), although the light organs did show an intriguing statistically significant decrease in message at the time when luminescence would be increasing, if the animals had been colonized. These data provide evidence that *escry1* expression cycles in the light organ in a manner consistent with induction by symbiosis.

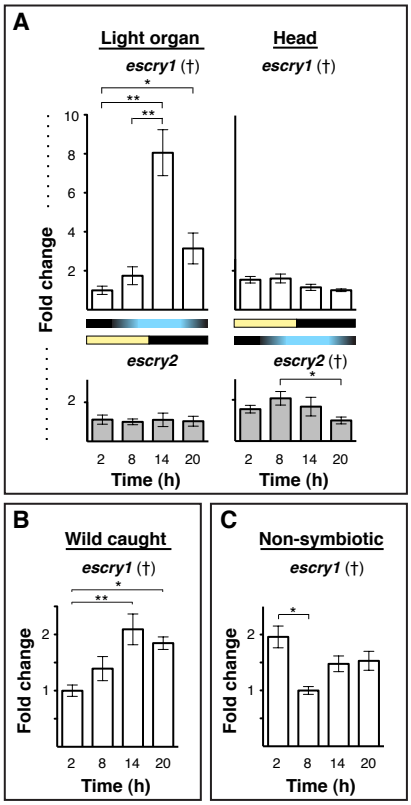

Fig. 2-4. Day/night cycle variation in *E. scolopes* cryptochrome expression. **A.** The expression of es*cry1* and es*cry2* in the squid light organ and head over four points in the day/night cycle. Graphs indicate the relative expression of *escry1* and *escry2* as measured by qRT-PCR. Yellow and black bars denote the cycle of exogenous light, and the blue and black bars show the cycle of bacterial light production in the light organ. **B.** Expression of es*cry1* in the light organs of mature squid caught in the wild and maintained in natural light. **C.** es*cry1* expression over the day/night cycle in non-symbiotic light organs. All data were normalized to the time point of lowest expression in each graph. Error bars represent the standard error of the mean. N= 2 to 6 biological replicates and 2 technical replicates per condition. † = ANOVA p-value < 0.05. * = pairwise comparison $p < 0.05$, ** = pairwise comparison $p < 0.01$.

Abundant EsCry1 localizes to the apical surfaces of light-organ epithelial cells that are adjacent to the symbiont

To determine if the EsCry1 protein was produced in close proximity to bacterial light in the light organ (Fig. 2-5A), we made an antibody to a peptide sequence unique to EsCry1. In extracts of the light organ, the antibody cross-reacted with a low-abundance protein species in the soluble fraction (S) at a molecular mass of ~63 kD, the size of the predicted full length of EsCry1 (Fig. 2-5B), and similar to that of Cry1 proteins in other invertebrates (Wier *et al.*, 2010; Connor and Gracey, 2011); no cross reactivity was detected in the membrane fraction (M). The antibody also detected another protein at a molecular mass of ~42 kD, which is consistent with a common breakdown product of invertebrate Cry1 proteins detected in a western blot (see *e.g.*, {FanjulMoles:2004ks}).

In analyses of light organ tissues by confocal immunocytochemistry, the EsCry1 antibody showed cross reactivity in the cells of the crypt epithelia that surround the symbiotic partner (Fig. 2-5C). The labeling occurred throughout these cells, but often showed concentration at the apical surfaces (Fig. 2-5C, D). Comparisons of immune cross reactivity revealed no detectable differences in protein abundance or localization among uncolonized animals and those colonized by wild-type or *Δlux V. fischeri* (Fig. 2-5D).

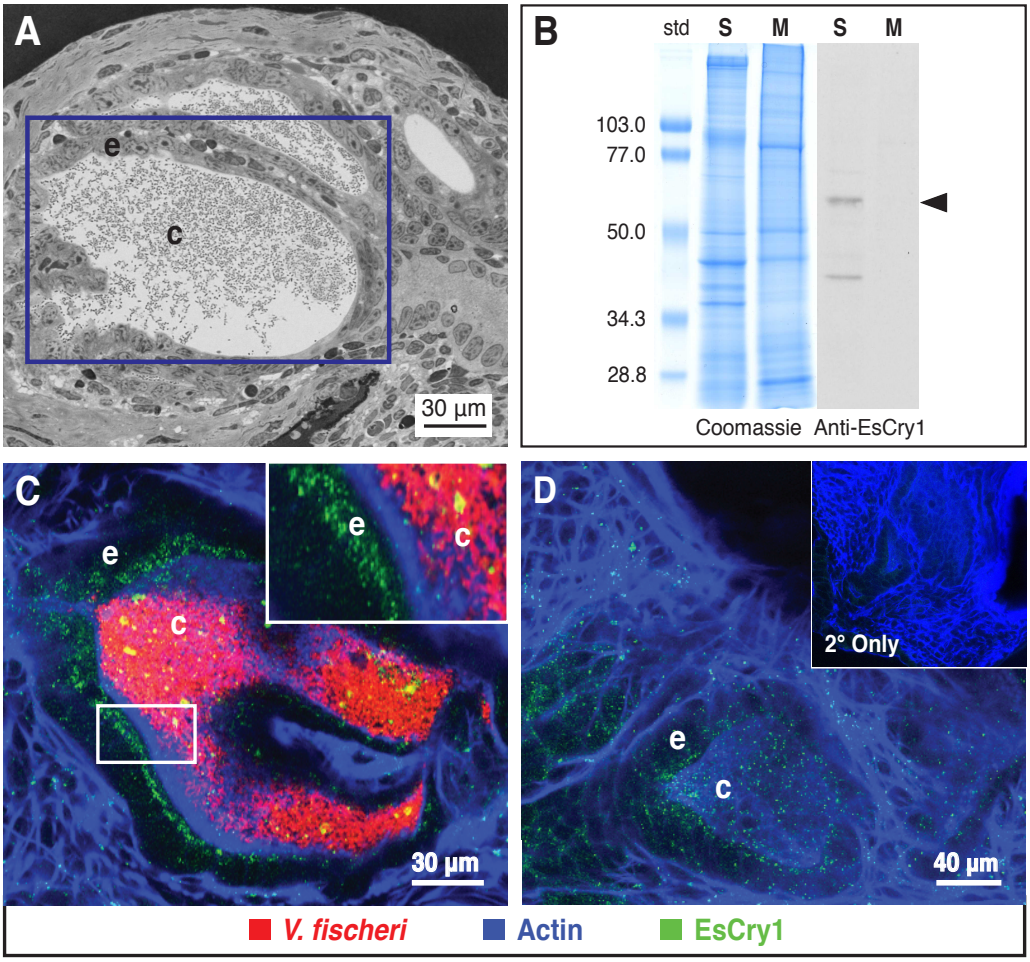
A
e
c
30 µm
B
std
S
M
S
M
103.0
77.0
50.0
34.3
28.8
Coomassie
Anti-EsCry1
C
e
c
e
c
30 µm
D
2° Only
e
c
40 µm
V. fischeri
Actin
EsCry1

Fig. 2-5. EsCry1 protein production in the light organ. **A.** Light micrograph of a cross section of the *E. scolopes* light organ, shown in Fig. 2-1B. The purple box denotes the placement of crypt 1, which is comprised of an epithelial cell layer (e) surrounding a population of *V. fischeri* bacteria in the crypt lumen (c). **B.** A western blot showing the immunoreactivity of the anti-EsCry1 antibody. Both aqueous soluble (S) and membrane (M) protein extracts from whole squid were run on SDS-PAGE gels and either stained with coomassie blue (Coomassie) or transferred to a membrane and exposed to an anti-EsCry1 antibody (Anti-EsCry1). An arrowhead shows a major band at the predicted molecular weight of 62.3 kD. Standards to the left (std) are shown in kD. **C.** A confocal micrograph of a 48-h colonized light organ stained with the anti-EsCry1 antibody. **D.** A confocal micrograph showing a 48-h uncolonized light organ crypt stained with the anti-EsCry1 antibody. The inset contains a negative control where the light organ was only stained with a secondary antibody (2° Only). In C and D, anti-EsCry1 = green, *V. fischeri* cells = red, filamentous actin = blue, e = crypt epithelium, c = crypt lumen.

Peak expression of *escry1* requires symbiont luminescence

Because the *escry1* mRNA levels reflected diel patterns of symbiont luminescence and Cry protein localized near the site where symbionts reside in the light organ, we used *V. fischeri* mutants *(Δlux*) defective in light production (Fig. 2-6A) to determine whether symbiont luminescence is critical for the induction of *escry1* mRNA cycling (Glossop and Hardin, 2002). At the time of highest *escry1* expression in symbiotic animals, *i.e.*, 14 h past "dawn" (see Fig. 2-4A), expression of this gene in animals colonized by the *Δlux* mutants was not significantly different from that of uncolonized animals (Fig. 2-6C). Genetic complementation of *lux* genes has been shown to restore normal host responses (Visick *et al.*, 2000), but here we sought to isolate the effect of light exposure from other potential effects of luminescence, particularly influences on the oxygen environment. Thus, to complement the light defect phenotypically, we used exposure to exogenous blue light (Fig. 2-6B). mRNA levels of *Δlux* colonized animals complemented with exogenous blue light had a fold-change in *escry1* mRNA levels similar to that of animals colonized with wild-type *V. fischeri* (Fig. 2-6D). At 2 d post colonization, the density of *Δlux* bacteria in the light organ was about 10% of the wild-type strains, similar to values previously reported (Fig. 2-6F**,** (Visick *et al.*, 2000)). A lysine auxotroph (*lysA:TnKan*) that colonizes the light organ to the same extent as *Δlux* (Whistler *et al.*, 2007), but exhibits per-cell luminescence similar to that of wild-type, also induced significantly higher *escry1* expression than the *Δlux* bacteria (Fig. 2-6D), providing further evidence that the presence of bacterial light, not wild-type bacterial density, increases *escry1* expression. Finally, we characterized expression of *escry1* in the head and determined that it was not affected by colonization state or strain (Fig. 2-6E), suggesting that the symbionts do not induce a systemic host response that influences the behavior of the genes in the head.

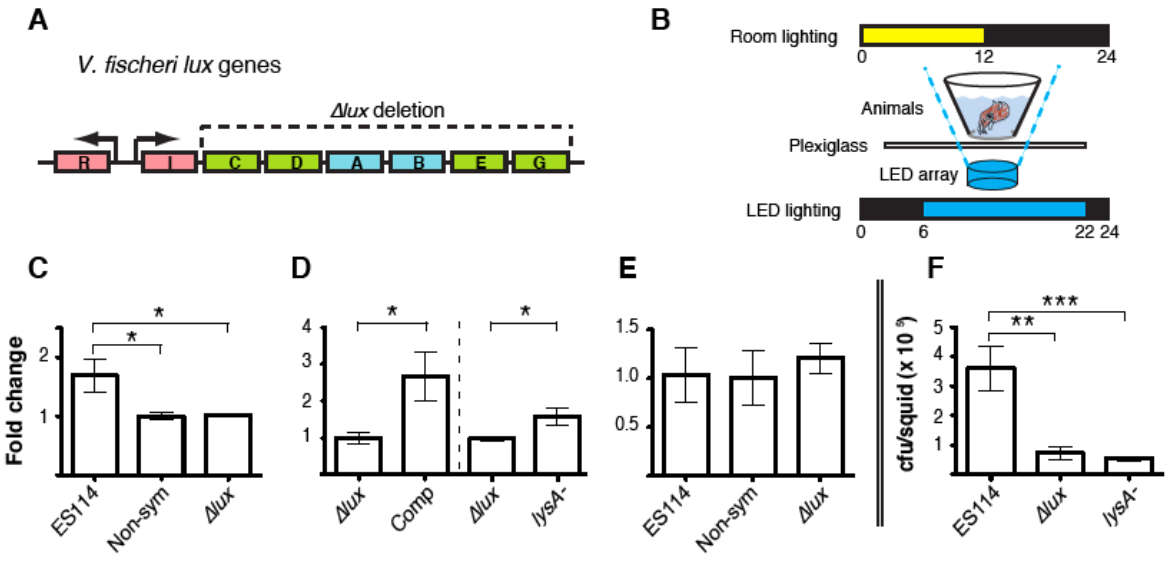
A
V. fischeri lux genes
Δlux deletion
R
I
C
D
A
B
E
G
B
Room lighting
0
12
24
Animals
Plexiglass
LED array
LED lighting
0
6
22 24
C
Fold change
ES114
Non-sym
Δlux
D
Δlux
Comp
Δlux
lysA-
E
ES114
Non-sym
Δlux
F
cfu/squid (x 10 9)
ES114
Δlux
lysA-

Fig. 2-6. The effect of bacterial light on *escry1* expression. **A.** Organization of the *V. fischeri lux* genes. Regulatory genes are in red, genes encoding luciferase enzyme subunits are in blue, and genes encoding substrate subunits are in green. The dotted line denotes the genes deleted in the *Δlux* mutant used in this study. **B.** Experimental setup for complementation of the *Δlux* mutant. Briefly, squid were placed above a blue LED array with a heat-dissipating plexiglass shield, with the overhead and LED light schedule as shown. **C.** Expression of es*cry1* at 14h in the light organs of animals colonized by ES114 (ES114), no bacteria (Non-Sym), or the *Δlux* mutant (*Δlux)* as measured by qRT-PCR. **D.** Expression of es*cry1* at 14h in the light organs of animals colonized with *Δlux* bacteria (*Δlux),* or colonized with *Δlux* and exposed to exogenous blue light (Comp). To the right of the dotted line, expression in animals at 14h colonized by the *Δlux* mutant (*Δlux*), or a lysine auxotroph (*lysA*-). **E.** Expression of es*cry1* in the eyes of animals whose light organs were analyzed in (A). Data within each expression graph were normalized to the condition of lowest expression within each separate experiment. Error bars are the standard error of the mean. N = 3 to 4 biological replicates per condition for each experiment. **F.** Number of bacteria per light organ of squid colonized with ES114 (ES114), the *Δlux* mutant (*Δlux*), or the *lysA*- mutant (*lysA*) at 14h. N = 10 animals per condition. For all graphs, * = $p < 0.05$, ** = $p<0.01$, and *** = $p<0.001$ by an ANOVA, followed by a post-hoc Tukey's pairwise comparison.

Symbiont MAMPs enable light to induce *cry1* cycling in the light organ

Because the data showed that bacterial luminescence is essential for peak *cry* expression in the organ, we sought to determine whether light alone was sufficient to induce the cycling of *escry1* expression. When we exposed the light organs of non-symbiotic animals to a cycle of exogenous blue light of a wavelength similar to that emitted by wild-type bacterial symbionts, *escry1* expression did not cycle (Fig. 2-7A). Exposure to exogenous blue light and derivatives of symbiont MAMPs, specifically the lipid A component of LPS and the peptidoglycan monomer (tracheal cytotoxin, or TCT), however, did induce cycling (Fig. 2-7B). However, treatment with only TCT or lipid A did not induce cycling of *escry1* expression (Fig. 2-8).

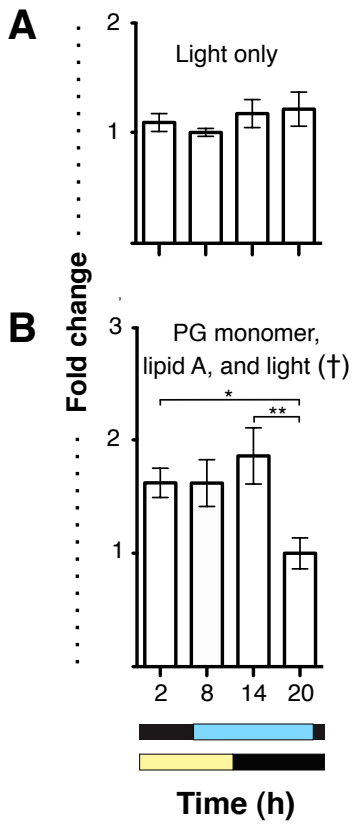

Fig. 2-7 The effect of MAMPs and light on *escry1* expression. **A.** Expression of *escry1* in the light organs of uncolonized animals exposed to exogenous blue light at four time points over the day/night cycle. **B.** *escry1* light-organ expression in animals exposed to exogenous blue light, 10 μM peptidoglycan monomer, and 10 ng/mL *V. fischeri* lipid A in seawater. Graphs indicate the relative expression of *escry1* as measured by qRT-PCR. Yellow and black bars denote the cycle of exogenous white (overhead) light, and the blue and black bars show the schedule of blue LED light presentation. All data were normalized to the time point of lowest expression in each graph. Error bars represent the standard error of the mean. N= 3 to 6 biological replicates and 2 technical replicates per condition. † = ANOVA p-value < 0.05. * = pairwise comparison $p < 0.05$. ** = pairwise comparison $p < 0.01$

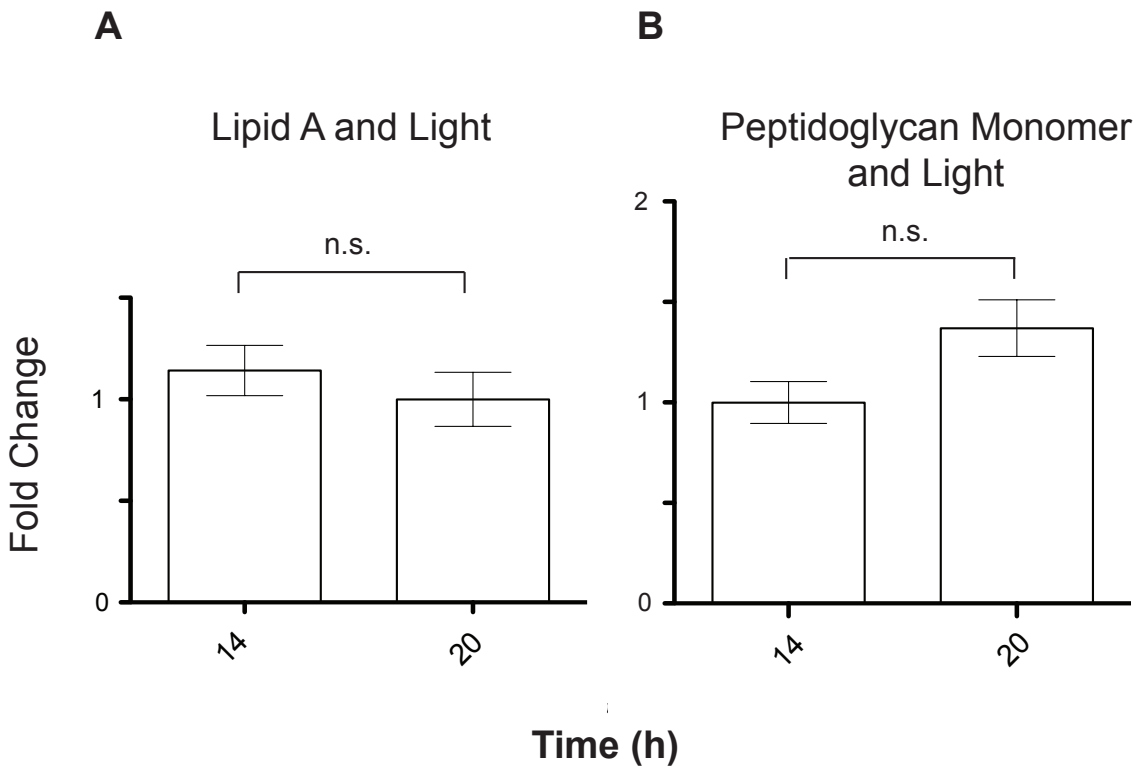

Fig. 2-8. The effect of lipid A or peptidoglycan monomer addition on light organ *escry1* expression. A. Expression of *escry1* in the light organs of uncolonized animals treated with 10 ng/mL *V. fischeri* lipid A in seawater exposed to exogenous blue light at two time points over the day/night cycle. B. *escry1* light-organ expression in animals exposed to exogenous blue light and 10 μM peptidoglycan monomer in seawater. Graphs indicate the relative transcription of *escry1* as measured by qRT-PCR. Blue LED light and room light presentation were the same as in figure 5. All data were normalized to the time point of lowest expression in each graph. Error bars represent the standard error of the mean. N= 3 biological replicates and 2 technical replicates per condition.

DISCUSSION:

The data presented in this study provide evidence that bacterial symbionts in the *E. scolopes* light organ influence the expression of a single cryptochrome gene and that therefore luminescence of the symbionts may provide input to a circadian oscillator in the host. In the larger context, these data suggest the possibility that the microbial partners of a symbiosis can be integrated into the biology of the host through an influence on daily rhythms.

The cephalopod *E. scolopes* belongs to the Phylum Mollusca, which occurs in the Lophotrochozoa, one of the three superphyla of animals. No previous studies on the presence of cryptochromes have been reported for other cephalopods, and while they have been reported in other lophotrochozoans (Connor and Gracey, 2011), none of these identified transcripts have been characterized. The data presented here, along with the identification of cryptochrome genes from full-genome sequences from other species of this group, suggest that the lophotrochozoans typically have two genes encoding cryptochromes. However, because of the small number of species examined thus far, other members of this superphylum may have fewer or more *cry* genes. Our data for the phylogenetic relationships of the *E. scolopes cry* genes inside and outside of the Lophotrochozoa agree with previous studies on cryptochrome radiation (Yuan *et al.*, 2007; Reitzel *et al.*, 2010), showing support for two main cryptochrome clades within the invertebrates.

With the finding that symbiont luminescence entrains host rhythms, this study expands the known roles for cryptochrome proteins with both the finding that bacterial symbionts affect rhythms and that luminescence is the critical feature. As in *E. scolopes*, the different cryptochrome genes of an animal species often have different expression patterns in response to external stimuli (Chaves *et al.*, 2011). For example, only one of two cryptochromes is regulated by the cycles of the moon in moonlight-responsive corals (Levy *et al.*, 2007). Also, in migrating

monarch butterflies, only the expression of one of two cryptochromes (cry2) is regulated during sun compass orientation (Merlin *et al.*, 2009), and the regulation and biochemistry behind these differences in input response is currently being studied in this system (Song *et al.*, 2007; Zhu *et al.*, 2008; Gegear *et al.*, 2010). In *E. scolopes*, both *cry* genes cycle with environmental light in the head and both *cry* genes are expressed in the light organ, but only *escry1* cycles in response to bioluminescence. Thus, further study in the squid-vibrio system is needed to determine the mechanism of function and downstream effects of these proteins on central and peripheral oscillators.

The data presented here suggest the possibility that *escry1* localizes specifically to the apical surfaces of cells interacting directly with symbionts, and that presentation of symbiont MAMPs enables *cry* responses to luminescence. The mechanism by which MAMP presentation primes the light-organ crypt cells to interact with light remains to be determined, but the system apparently ensures that the crypt cells respond solely to light presented in the context of the bacterial symbiont and not to environmental light presented on the day/night cycle.

The data presented here suggest a number of areas for future research efforts in the squid-vibrio system. A likely fruitful area will be to determine the extent to which *escry1* influences the various daily rhythms that have been described. In addition to the early studies of rhythms on bioluminescence (Boettcher *et al.*, 1996), recent analyses of the transcriptomes of the symbiont and its supporting host epithelium at several points over the day-night cycle revealed a profound daily rhythm on gene expression in both partners (Wier *et al.*, 2010). The data showed that 9.6% of the total available host transcriptome is regulated over the day/night cycle, similar to the proportion (~8%) of the total transcriptome controlled by the circadian clock in the tissues of other animals (Keller *et al.*, 2009; Hughes *et al.*, 2009). The transcriptomic rhythms in the squid-

vibrio system reflected cyclic changes in the ultrastructure of crypt epithelial cells and in symbiont metabolism (Wier *et al.*, 2010). Finally, the cryptochromes are not the only blue light receptors in the host light organ. An earlier study of the system demonstrated that the light organ expresses the genes encoding rhodopsin as well as other key members of the visual transduction cascade, and that the light organ has the physiological potential to respond to light similarly to the eye (Tong *et al.*, 2009). How light perception by rhodopsin and cryptochrome function and are integrated in the same organ remains to be determined.

An influence of bacterial symbionts on host rhythms is unlikely to be unique to the squid-vibrio system. The conservation of both bacterial-epithelial interactions and circadian gene regulation across the metazoa suggests that symbiont-induced circadian rhythms may be widespread. For example, although such influences have not been studied directly as yet, evidence is mounting that the microbiome of mammals is critical to host rhythms. For example, in the epithelia-immune-microbiota axis of the gut, the transcriptomes of both immune and epithelial components of the gut (Froy and Chapnik, 2007; Hoogerwerf *et al*., 2008; Keller *et al*., 2009) are on a profound circadian rhythm controlled by the clock genes (*e.g*., cry (Lamia *et al*., 2011; Narasimamurthy *et al*., 2012)). It would be surprising if these critical oscillations of gut function had no impact on the activity of the microbiota and, perhaps, as in the squid-vibrio system, the microbiota are actually essential for normal entrainment of biological rhythms. An early suggestion of this connection was that the gut-associated circadian clocks are entrained by food, and the microbiota are essential for the speed and efficiency of digestion (Velagapudi *et al*., 2010). Most recently, certain disease states, such as diabetes (Wen *et al*., 2008), obesity (Manco *et al*., 2010), depression (Holzer *et al*., 2012), and sleep disorders (Gonzalez *et al*., 2011), have become linked not only to perturbations in the circadian rhythms but, significantly, to imbalances

in the microbiota (Tremaroli and Bäckhed, 2012). An emerging hypothesis is that the host and its microbiota work together to develop and maintain biological rhythms that are essential to the homeostasis of the symbiosis. The complexity of the mammalian systems presents a significant challenge to the study of their rhythms. The study of simpler systems, such as the squid-vibrio system and the *Drosophila* gut community, may provide valuable insight into the rules governing symbiont influence on host rhythms.

ACKNOWLEDGEMENTS:

We thank N. Bekiares, B. Krasity, and N. Kremer for comments on the manuscript, and A. Schaefer for design of the LED array for complementation of bacterial luminescence. This work was supported by grants from National Institutes of Health (NIH) R01-RR12294 (to EG Ruby and MM-N) and R01-AI50661 (to MM-N), and National Science Foundation IOS 0517007 (to MM-N & EGR) and IOS 0715905 (to MM-N). EACH-H was supported by NRSA T-32 GM07215.

REFERENCES:

Altschul, S.F., Gish, W., Miller, W., and Myers, E.W. (1990) Basic local alignment search tool. *J Mol Biol* **215**: 403-410.

Boettcher, K.J., and Ruby, E.G. (1990) Depressed light emission by symbiotic *Vibrio fischeri* of the sepiolid squid *Euprymna scolopes. J Bacteriol* **172**: 3701–3706.

Boettcher, K.J., Ruby, E.G., and McFall-Ngai, M.J. (1996) Bioluminescence in the symbiotic squid *Euprymna scolopes* is controlled by a daily biological rhythm. *J Comp Physiol A* **179**: 65–73.

Bustin, S.A., Benes, V., Garson, J.A., Hellemans, J., Huggett, J., Kubista, M., *et al.* (2009) The MIQE guidelines: minimum information for publication of quantitative real-time PCR experiments. *Clin Chem* **55**: 611–622.

Chaves, I., Pokorny, R., Byrdin, M., and Hoang, N. (2011) The cryptochromes: blue light photoreceptors in plants and animals. *Annu Rev Plant Biol.* **62**: 335-364.

Chun, C.K., Scheetz, T.E., Bonaldo Mde, F., Brown, B., Clemens, A., Crookes-Goodson, W.J., *et al.* (2006) An annotated cDNA library of juvenile *Euprymna scolopes* with and without colonization by the symbiont *Vibrio fischeri*. *BMC genomics* **7**: 154.

Chun, C.K., Troll, J.V., Koroleva, I., Brown, B., Manzella, L., Snir, E., *et al.* (2008) Effects of colonization, luminescence, and autoinducer on host transcription during development of the squid-vibrio association. *Proc Natl Acad Sci U.S.A.* **105**: 11323–11328.

Connor, K.M., and Gracey, A.Y. (2011) Circadian cycles are the dominant transcriptional rhythm in the intertidal mussel *Mytilus californianus*. *Proc Natl Acad Sci U.S.A.* **108**: 16110–16115.

Edgar, R.C. (2004) MUSCLE: a multiple sequence alignment method with reduced time and space complexity. *BMC Bioinformatics* **5**: 113.

Foster, J.S., Apicella, M.A., and McFall-Ngai, M.J. (2000) *Vibrio fischeri* lipopolysaccharide induces developmental apoptosis, but not complete morphogenesis, of the *Euprymna scolopes* symbiotic light organ. *Dev Biol* **226**: 242–254.

Foster, R.G., and Helfrich-Forster, C. (2001) The regulation of circadian clocks by light in fruitflies and mice. *Philos Trans R Soc Lond B Biol Sci* **356**: 1779–1789.

Froy, O., and Chapnik, N. (2007) Circadian oscillation of innate immunity components in mouse small intestine. *Mol Immunol* **44**: 1954–1960.

Gegear, R.J., Foley, L.E., Casselman, A., and Reppert, S.M. (2010) Animal cryptochromes mediate magnetoreception by an unconventional photochemical mechanism. *Nature*. **463**: 804-807

Glossop, N.R.J., and Hardin, P.E. (2002) Central and peripheral circadian oscillator mechanisms in flies and mammals. *J Cell Sci* **115**: 3369–3377.

Gonzalez, A., Stombaugh, J., and Lozupone, C. (2011) The mind-body-microbial continuum. *Dialogues Clin Neurosci* **13**: 55-62.

Graf, J., and Ruby, E.G. (1998) Host-derived amino acids support the proliferation of symbiotic bacteria. *Proc Natl Acad Sci U.S.A.* **95**: 1818–1822.

Holzer, P., Reichmann, F., and Farzi, A. (2012) Neuropeptide Y, peptide YY and pancreatic polypeptide in the gut–brain axis. *Neuropeptides*. **46**: 261-274.

Hoogerwerf, W.A., Sinha, M., Conesa, A., Luxon, B.A., Shahinian, V.B., Cornelissen, G., *et al.* (2008) Transcriptional Profiling of mRNA Expression in the Mouse Distal Colon. *Gastroenterology* **135**: 2019–2029.

Hooper, L.V., Littman, D.R., and Macpherson, A.J. (2012) Interactions Between the Microbiota and the Immune System. *Science* **336**: 1268–1273.

Hughes, M.E., DiTacchio, L., Hayes, K.R., Vollmers, C., Pulivarthy, S., Baggs, J.E., *et al.* (2009) Harmonics of Circadian Gene Transcription in Mammals. *PLoS Genet* **5**.

Ikeno, T., Katagiri, C., Numata, H., and Goto, S.G. (2011) Causal involvement of mammalian-type cryptochrome in the circadian cuticle deposition rhythm in the bean bug *Riptortus pedestris*. *Insect Mol Biol* **20**: 409–415.

Ikeno, T., Numata, H., and Goto, S.G. (2008) Molecular characterization of the circadian clock genes in the bean bug, *Riptortus pedestris*, and their expression patterns under long- and short-day conditions. *Gene* **419**: 56–61.

Ikeno, T., Numata, H., and Goto, S.G. (2011) Photoperiodic response requires mammalian-type cryptochrome in the bean bug *Riptortus pedestris*. *Biochem Biophys Res Commun* **410**: 394–397.

Jones, B.W., and Nishiguchi, M.K. (2004) Counterillumination in the hawaiian bobtail squid, *Euprymna scolopes* Berry (Mollusca : Cephalopoda). *Mar Biol* **144**: 1151–1155.

Keller, M., Mazuch, J., Abraham, U., Eom, G.D., Herzog, E.D., Volk, H.-D., *et al.* (2009) A circadian clock in macrophages controls inflammatory immune responses. *Proc Natl Acad Sci U.S.A.* **106**: 21407–21412.

Konturek, P.C., Brzozowski, T., and Konturek, S.J. (2011) Gut clock: implication of circadian rhythms in the gastrointestinal tract. *J Physiol Pharmacol* **62**: 139–150.

Koropatnick, T.A., Engle, J.T., Apicella, M.A., Stabb, E.V., Goldman, W.E., and McFall-Ngai, M.J. (2004) Microbial factor-mediated development in a host-bacterial mutualism. *Science* **306**: 1186–1188.

Lamia, K.A., Papp, S.J., Yu, R.T., Barish, G.D., Uhlenhaut, N.H., Jonker, J.W., *et al.* (2011)

Cryptochromes mediate rhythmic repression of the glucocorticoid receptor. *Nature* **480**: 552–U183.

Lee, J.-E., and Edery, I. (2008) Circadian regulation in the ability of *Drosophila* to combat pathogenic infections. *Curr Biol* **18**: 195–199.

Levy, O., Appelbaum, L., Leggat, W., Gothlif, Y., Hayward, D.C., Miller, D.J., and Hoegh-Guldberg, O. (2007) Light-responsive cryptochromes from a simple multicellular animal, the coral *Acropora millepora*. *Science* **318**: 467–470.

Manco, M., Putignani, L., and Bottazzo, G.F. (2010) Gut microbiota, lipopolysaccharides, and innate immunity in the pathogenesis of obesity and cardiovascular risk. *Endocr Rev*. **6**: 817-844.

Merlin, C., Beaver, L.E., Taylor, O.R., Wolfe, S.A., and Reppert, S.M. (2013) Efficient targeted mutagenesis in the monarch butterfly using zinc-finger nucleases. *Genome Res* **23**: 159–168.

Merlin, C., Gegear, R.J., and Reppert, S.M. (2009) Antennal circadian clocks coordinate sun compass orientation in migratory monarch butterflies. *Science* **325**: 1700–1704.

Montgomery, M.K., and McFall-Ngai, M.J. (1993) Embryonic development of the light organ of the sepiloid squid *Euprymna scolopes* Berry. *Biol Bull* **184**: 296–308.

Mueller, W.E.G., Wang, X., Schroeder, H.C., Korzhev, M., Grebenjuk, V.A., Markl, J.S., *et al.* (2010) A cryptochrome-based photosensory system in the siliceous sponge *Suberites domuncula* (Demospongiae). *FEBS J* **277**: 1182–1201.

Narasimamurthy, R., Hatori, M., Nayak, S.K., Liu, F., Panda, S., and Verma, I.M. (2012) Circadian clock protein cryptochrome regulates the expression of proinflammatory cytokines. *Proc Natl Acad Sci U.S.A.* **109**: 12662–12667.

Oztürk, N., Song, S.-H., Ozgür, S., Selby, C.P., Morrison, L., Partch, C., *et al.* (2007) Structure and function of animal cryptochromes. *Cold Spring Harb Symp Quant Biol* **72**: 119–131.

Pfaffl, M.W. (2001) A new mathematical model for relative quantification in real-time RT-PCR. *Nucleic Acids Res* **29**: e45.

Reitzel, A.M., Behrendt, L., and Tarrant, A.M. (2010) Light Entrained Rhythmic Gene Expression in the Sea Anemone *Nematostella vectensis*: The Evolution of the Animal Circadian Clock. *PLoS One* **5**.

Sanada, K., Harada, Y., Sakai, M., Todo, T., and Fukada, Y. (2004) Serine phosphorylation of mCRY1 and mCRY2 by mitogen-activated protein kinase. *Genes Cells* **9**: 697–708.

Silver, A.C., Arjona, A., Walker, W.E., and Fikrig, E. (2012) The Circadian Clock Controls Toll-like Receptor 9-Mediated Innate and Adaptive Immunity. *Immunity* **36**: 251–261.

Song, S.-H., Oztürk, N., Denaro, T.R., Arat, N.Ö., Kao, Y.-T., Zhu, H., *et al.* (2007) Formation and function of flavin anion radical in cryptochrome 1 blue-light photoreceptor of monarch

butterfly. *J Biol Chem* **282**: 17608–17612.

Tahira, K., Ueno, T., Fukuda, N., Aoyama, T., Tsunemi, A., Matsumoto, S., *et al.* (2011) Obesity alters the expression profile of clock genes in peripheral blood mononuclear cells. *Arch Med Sci* **7**: 933–940.

Tong, D., Rozas, N.S., Oakley, T.H., Mitchell, J., Colley, N.J., and McFall-Ngai, M.J. (2009) Evidence for light perception in a bioluminescent organ. *Proc Natl Acad Sci U.S.A.* **106**: 9836–9841.

Tremaroli, V., and Bäckhed, F. (2012) Functional interactions between the gut microbiota and host metabolism. *Nature* **489**: 242-249.

Troll, J.V., Adin, D.M., Wier, A.M., Paquette, N., Silverman, N., Goldman, W.E., *et al.* (2009) Peptidoglycan induces loss of a nuclear peptidoglycan recognition protein during host tissue development in a beneficial animal-bacterial symbiosis. *Cell Microbiol* **11**: 1114–1127.

Troll, J.V., Bent, E.H., Pacquette, N., Wier, A.M., Goldman, W.E., Silverman, N., and McFall-Ngai, M.J. (2010) Taming the symbiont for coexistence: a host PGRP neutralizes a bacterial symbiont toxin. *Environ Microbiol* **12**: 2190–2203.

Turnbaugh, P.J., Ley, R.E., Mahowald, M.A., Magrini, V., Mardis, E.R., and Gordon, J.I. (2006) An obesity-associated gut microbiome with increased capacity for energy harvest. *Nature* **444**: 1027–1031.

Velagapudi, V.R., Hezaveh, R., Reigstad, C.S., Gopalacharyulu, P., Yetukuri, L., Islam, S., *et al.* (2010) The gut microbiota modulates host energy and lipid metabolism in mice. *J Lipid Res* **51**: 1101–1112.

Visick, K.L., Foster, J., Doino, J., McFall-Ngai, M., and Ruby, E.G. (2000) *Vibrio fischeri lux* genes play an important role in colonization and development of the host light organ. *J Bacteriol* **182**: 4578–4586.

Wang, W., Barnaby, J.Y., Tada, Y., Li, H., Toer, M., Caldelari, D., *et al.* (2011) Timing of plant immune responses by a central circadian regulator. *Nature* **470**: 110–U126.

Wen, L., Ley, R.E., Volchkov, P.Y., and Stranges, P.B. (2008) Innate immunity and intestinal microbiota in the development of Type 1 diabetes. *Nature* **455:** 1109-1113.

Whistler, C.A., Koropatnick, T.A., Pollack, A., McFall-Ngai, M.J., and Ruby, E.G. (2007) The GacA global regulator of *Vibrio fischeri* is required for normal host tissue responses that limit subsequent bacterial colonization. *Cell Microbiol* **9**: 766–778.

Wier, A.M., Nyholm, S.V., Mandel, M.J., Massengo-Tiasse, R.P., Schaefer, A.L., Koroleva, I., *et al.* (2010) Transcriptional patterns in both host and bacterium underlie a daily rhythm of anatomical and metabolic change in a beneficial symbiosis. *Proc Natl Acad Sci U.S.A.* **107**: 2259–2264.

Yuan, Q., Metterville, D., Briscoe, A.D., and Reppert, S.M. (2007) Insect cryptochromes: Gene duplication and loss define diverse ways to construct insect circadian clocks. *Mol Biol Evol* **24**: 948–955.

Zhu, H., Sauman, I., Yuan, Q., Casselman, A., Emery-Le, M., Emery, P., and Reppert, S.M. (2008) Cryptochromes define a novel circadian clock mechanism in monarch butterflies that may underlie sun compass navigation. *PLoS Biol* **6**: 138–155.

Zoltowski, B.D., Vaidya, A.T., Top, D., Widom, J., Young, M.W., and Crane, B.R. (2013) Structure of full-length Drosophila cryptochrome (vol 480, pg 396, 2011). *Nature* **496**: 252–252.

Chapter 3

Shaping the microenvironment: Evidence for the influence of a host galaxin on symbiont acquisition and maintenance in the squid-vibrio symbiosis

PREFACE:

Submitted to *Environmental Microbiology* in December 2013 as:

Heath-Heckman, E.A.C., Gillette, A.A., Augustin, R., Gillette, M.X., Goldman, W.E., and McFall-Ngai, M.J. "Shaping the microenvironment: A host galaxin influences symbiont acquisition and maintenance in the squid-vibrio symbiosis"

EACH, AAG, and MJM formulated ideas and planned experiments. WEG contributed reagents, and S. Daum donated strains and space for the MRSA MIC experiments. AAG produced the data for Figs 3-1, 3-4, 3-5, 3-8, and Table 3-3 as well as assisting in the data collection for Fig. 3-7 and 3-9. MXG assisted with the plating experiments in Fig. 3-11. RA instructed EACH and AAG in the MIC assay. EACH performed all other experiments and performed all data analysis. EACH and MJM wrote and edited the chapter.

ABSTRACT:

Most bacterial species make transitions between habitats, such as switching from free-living to symbiotic niches. We provide evidence that a galaxin protein, EsGal1, of the squid *Euprymna scolopes* participates in both: (i) selection of the specific partner *Vibrio fischeri* from the bacterioplankton during symbiosis onset and, (ii) modulation of *V. fischeri* growth in symbiotic maintenance. We identified two galaxins in transcriptomic databases and showed by qRT-PCR that one (*esgal1*) was dominant in the light organ. Further, *esgal1* expression was upregulated by symbiosis, and to a lesser extent by exposure to symbiont cell-envelope molecules. Confocal immunocytochemistry of juvenile animals localized EsGal1 to the apical surfaces of light-organ epithelia and surrounding mucus, the environment in which *V. fischeri* cells aggregate before migration into the organ. Growth assays revealed that a peptide derived from EsGal1 arrested growth of Gram-positive bacterial cells, which represent the cell type first 'winnowed' during initial selection of the symbiont. The EsGal1-derived peptide also significantly decreased the growth rate of *V. fischeri* in culture. Further, when animals were exposed to an anti-EsGal1 antibody, symbiont population growth was significantly increased. These data provide a window into how hosts select symbionts from a rich environment and govern their growth in symbiosis.

INTRODUCTION:

A new field of ecology focuses on how microbial communities are structured in natural habitats, and how microbes within those communities transition between different niches (Fuhrman, 2009; Needham *et al.*, 2013). One common niche transition occurs when marine microbes move from planktonic habitats to persistent associations with animal partners (Gallo and Hooper, 2012; Bulgarelli *et al.*, 2013). The light-organ symbiosis between *Euprymna scolopes*, the Hawaiian bobtail squid, and *Vibrio fischeri*, a luminescent Gram-negative marine bacterium, is a horizontally transmitted association, i.e., acquired each generation (for review, see (Stabb and Visick, 2013)). The symbionts colonize deep light-organ tissues, or crypts, within hours of the host's hatching, taking up residence along the apical surfaces of the crypt epithelia. The host responds to a variety of cues presented by *V. fischeri* in the crypts, including luminescence and microbe-associated molecular patterns (MAMPs), notably cell envelope molecules (for review see (McFall-Ngai *et al.*, 2010; McFall-Ngai *et al.*, 2012). Transitions of *V. fischeri* between membership in the bacterioplankton to the symbiotic niche occur both at the onset of the symbiosis, when *V. fischeri* is recruited *into* animal tissues, and each day of the association with the venting of ~90% of the symbiont population *out of* the light organ at dawn, when *V. fischeri* cells cycle into the planktonic niche.

How the bacterioplankton is winnowed in the selection of the specific symbiotic partner at onset of the association has been a continuing focus of studies of the squid-vibrio system. Soon after hatching, juvenile *E. scolopes* begin to ventilate, and environmental microbial communities, as well as the products they release, flow over superficial ciliated epithelial fields that are specific to the juvenile light organ. The epithelia begin to shed mucus within minutes in

response to environmental peptidoglycan (PGN). *V. fischeri* is then enriched along these tissues by first attaching to the cilia and then aggregating (Altura *et al.*, 2013). Whereas Gram-positive environmental bacteria appear not to associate with this ciliated field, all tested Gram-negative bacterial cells have the capacity to adhere (Nyholm and McFall-Ngai, 2003; Altura *et al.*, 2013). Through the recruitment process, however, all non-specific Gram-negative bacteria are gradually lost from the aggregating cells such that, by about 3 h, only a small population of *V. fischeri* cells remains (Altura *et al.*, 2013).

While this stepwise dominance of *V. fischeri* on the ciliated surface is not well understood, recent research has provided some insight. The shed mucus is acidic (Kremer *et al.*, 2013) and contains abundant biomolecules typically associated with 'antimicrobial' activity, including nitric oxide (Davidson *et al.*, 2004) and a peptidoglycan-recognition protein, which has an amidase activity that breaks down PGN (Troll *et al.*, 2010). In addition, a recent comparison of the host transcriptome in 3-h animals exposed or not exposed to *V. fischeri* revealed robust changes in gene expression in response to the presence of the symbiont (Kremer *et al.*, 2013). The data suggest that some of the upregulated genes encode proteins with activities that shape the chemical environment of the mucus to favor *V. fischeri*. A role for host biomolecules as critical determinants of host-symbiont interactions is not without precedent; they have been widely studied as features that can structure and modulate behaviors of host-associated microbial communities (de Oliveira *et al.*, 2012; Shnit-Orland *et al.*, 2012). For example, host factors function in symbiont attraction in the legume-rhizobia symbioses (Redmond *et al.*, 1986), in the structuring of symbiont communities in the mammalian gut (Cash *et al.*, 2006), and in maintaining specificity in nematode-microbe associations (Bulgheresi *et al.*, 2011).

In this study, we have explored the possible roles of another host biomolecule, a protein known as galaxin, in shaping the transition to a symbiotic habitat by *V. fischeri*. Galaxins were first reported in other symbiotic associations. For example, several studies on corals have correlated galaxin activity with the process of calcification of the exoskeleton (Fukuda *et al.*, 2003; Watanabe *et al.*, 2003), and galaxin transcripts have also been identified in the body wall of *Riftia pachyptila* (Sanchez *et al.*, 2007), although their function remains unexplored. In the squid-vibrio system, previous studies of symbiont-induced changes in host gene expression showed that transcripts encoding putative galaxin proteins are upregulated at first colonization of the light organ by the symbionts (Chun *et al.*, 2008), and are regulated over the day/night cycle in the adult light organ (Wier *et al.*, 2010). Here we characterize in depth one of the host-squid galaxins, EsGalaxin1 (EsGal1), the prominent isoform in the host light organ, during the selection of the symbiont in onset of the partnership and during the maintenance of the mature association as a balanced system.

MATERIALS AND METHODS:

General Methods

Adult *Euprymna scolopes* were collected and maintained as previously described (Wollenberg and Ruby, 2012). Juveniles from the breeding colony were collected within 15 min of hatching. Aposymbiotic (Apo) animals were maintained in *V. fischeri*-free, unfiltered seawater, while other juveniles were exposed to ~5,000 colony-forming units (CFU) /mL of the *V. fischeri* strain ES114 (Boettcher and Ruby, 1990) overnight to produce the symbiotic (Sym) condition. Colonization of the symbiotic juvenile squid was determined by measuring luminescence output of the symbionts with a TD 20/20 luminometer (Turner Designs, Sunnyvale, CA); aposymbiotic squid were also analyzed to ensure that their light organs had not been colonized. In experiments with *V. fischeri* surface molecules, the lipid A and the peptidoglycan monomer (also called tracheal cytotoxin, or TCT) were prepared as previously described (Foster *et al.*, 2000; Koropatnick *et al.*, 2004) and exposed to animals at 10 ng/mL and 10 μM, respectively for 48 h with the water + MAMPs replaced every 24h. Symbiont depletion from the light organ was performed with antibiotics as previously described (Doino and McFall-Ngai, 1995). In experiments examining the role of symbiont light production in *esgal1* upregulation, animals were colonized with the light-deficient *V. fischeri* strain EVS102 (Δ*lux*) (Bose *et al.*, 2008) as described above and a subset of the exposed squid were plated to ensure colonization. All reagents were obtained from Sigma-Aldrich (St. Louis, MO) unless otherwise noted. All animal experiments conform to the relevant regulatory standards established by the University of Wisconsin – Madison.

Identification of galaxin gene sequences from the EST database and subsequent analyses

Two galaxin gene sequences were identified by a tblastn search against the expressed sequence tag (EST) database of the juvenile-host light organ (Chun *et al.*, 2006) using *Galaxea fasicularis* galaxin as the query sequence (Fukuda *et al.*, 2003). The identified sequences in the EST database sequence were used for primer design for subsequent rapid amplification of cDNA ends (RACE) to obtain the full sequence of the open-reading frame.

Preparation of RNA for 5' RACE (Rapid Amplification of cDNA Ends) was performed using the GeneRacer kit (Life Technologies, Grand Island, NY). Reverse transcription for RACE was performed using the SuperScript III RT kit and RACE reactions were performed using Platinum Taq DNA polymerase according to the manufacturer's instructions (Life Technologies, Grand Island, NY) with gene-specific primers (Table 3-1). PCR products of interest were separated by gel electrophoresis, excised from the gel, and purified using the QIAEX II gel extraction kit (Qiagen, Valencia, CA). The purified PCR products were cloned using the TOPO TA Cloning Kit for Sequencing and transformed into TOP-10 chemically competent *E. coli* cells (Life Technologies, Grand Island, NY). The resulting transformants were prepared for sequencing with the QIAprep spin miniprep kit (Qiagen, Valencia, CA) and screened for the correct insert by plasmid digestion with EcoRI (Fermentas, Gen Burnie, MD). Plasmid inserts were sequenced using the M13F and -R primers (Life Technologies, Grand Island, NY).

Sequences obtained by RACE were assembled into contigs using the CAP3 sequence assembly program (http://pbil.univ-lyon1.fr/cap3.php). The resulting full-length sequence was analyzed by BLAST searches of GenBank using the default parameters. The cDNA sequence was translated using the ExPASy Translate tool (http://web.expasy.org/translate/), and the resulting derived amino acid sequence was examined for a putative repeat structure using

Table 3-1: Primers used in this study

Name	Sequence (5'-3')
esgal1 qRT F	gaactcgaatctgttgttctggcg
esgal1 qRT R	gttggtttcatggtaacacggcca
esgal2 qRT F	tgtggcggaaatgtctacaaccca
esgal2 qRT R	tggcgtccttgctttgatctgact
es40S qRT F	aatctcggcgtccttgagaa
es40S qRT R	gcatcaattgcacgacgagt
esgal1 RACE primary	tggtttcatggtaacacggccagc
esgal1 RACE nested	acacggccagcacaacacaaagca

RADAR (Rapid Automatic Detection and Alignment of Repeats), http://www.ebi.ac.uk/Tools/pfa/radar/). Signal peptide prediction was performed using the SignalP 4.1 Server (http://www.cbs.dtu.dk/services/SignalP/), and a potential N-glycosylation site was identified using the NetNGlyc 1.0 Server (http://www.cbs.dtu.dk/services/NetNGlyc/). Potential for antimicrobial activity was assayed *in silico* with the APD2 antimicrobial peptide predictor (http://aps.unmc.edu/AP/prediction/prediction_main.php). The *Galaxea fasicularis*, *Acropora palmata*, and *Balanoglossus clavigerus* sequences used in this study were derived from the NCBI protein database. Amino acids from the first three putative repeats of the proteins were aligned using MUSCLE (Edgar, 2004) and the subsequent alignment was visualized with the CLC Sequence viewer (CLC Bio, Cambridge, MA, http://clcbio.com/index.php?id=28).

RNA and cDNA preparation and quantitative-reverse-transcriptase PCR (qRT-PCR)

Whole juvenile animals were stored in RNALater RNA stabilization reagent (Qiagen, Valencia, CA) for 24h at 4°C and then transferred to -80°C for extended storage until RNA extraction. RNA was extracted from light organs using the RNeasy Fibrous Tissue Kit (Qiagen, Valencia, CA) after homogenizing the organs in a TissueLyser LT (Qiagen, Valencia, CA). Three to four biological replicates were used per experiment. The extracts were treated with the Ambion TURBO DNA-*free* kit (Life Technologies, Grand Island, NY) to remove any contaminating genomic DNA. The RNA extracts were then quantified using a Qubit 2.0 Fluorometer (Life Technologies, Grand Island, NY) and 5 μL of each preparation were separated on a 1% agarose gel to ensure the integrity of the RNA. If not used immediately, the RNA extracts were aliquoted and stored at -80°C. cDNA synthesis was performed with SMART MMLV Reverse

Transcriptase (Clontech, Mountain View, CA) according to the manufacturer's instructions, and then each cDNA synthesis reaction was diluted to a concentration of 2.08 ng/μL using nuclease-free water and stored at 4°C.

All qRT-PCR assays were performed in compliance with the MIQE guidelines (Bustin *et al.*, 2009). Gene-specific primers were designed for *esgal1* and *2*, and for the *Euprymna scolopes* 40S ribosomal RNA sequence, which was used as a control for equal well loading (Table 3-1). For each qRT-PCR experiment, wells without a template and with cDNA reactions run with no reverse transcriptase as a template were run as negative controls to ensure the absence of chromosomal DNA in the reaction wells. The efficiencies of all qRT-PCR primer sets were between 95 and 105%. Data were analyzed using the ΔΔCq method (Pfaffl, 2001). qRT-PCR was performed on light organ cDNA using iQSYBR Green Supermix or SsoAdvanced SYBR Green Supermix (BioRad, Hercules, CA) in a CFX Connect Real-Time System (BioRad, Hercules, CA). Amplification was performed under the following conditions: 95°C for 5 min, followed by 45 cycles of 95°C for 15 sec, 60°C for 15 sec, and 72°C for 15 sec. Each reaction was performed in duplicate and contained 0.2 μM primers and 10.4 ng of cDNA. To determine whether each PCR reaction resulted in a single amplicon, the presence for one optimal dissociation temperature for each PCR reaction was assayed by incrementally increasing the temperature every 10 sec from 60 to 89.5°C. Each reaction in this study had a single dissociation peak. Standard curves were created using a 10-fold dilution of the PCR product with each primer set.

Western blotting and immunocytochemistry (ICC)

A polyclonal antibody to EsGal1 was produced in rabbit (Genscript, Piscataway, NJ) to two unique peptides within the EsGal1 sequence (GNRTYDPQFQIC and CKYRAYDTDNFR), chosen for their predicted antigenicity, surface exposure, and lack of similarity to other known, predicted *E. scolopes* or *V. fischeri* proteins. Protein samples for western blotting were prepared as described previously (Troll *et al.*, 2010). Concentrations of the protein samples were determined using a Qubit 2.0 Fluorometer (Life Technologies, Grand Island, NY). The proteins were separated on 12.5% SDS-PAGE gel with 25 μg of protein per lane and then transferred onto a PVDF membrane with a Mini Trans-Blot Electrophoretic Transfer Cell (BioRad, Hercules, CA) per the manufacturer's instructions. The membrane was blocked overnight at room temperature (RT) as previously described (Troll *et al.*, 2010). The antibody was diluted 1:1000 in blocking solution and incubated with the membrane for 3 h at RT. The blot was then exposed to secondary antibody, washed, and developed as previously described (Troll *et al.*, 2010).

For ICC, light organs were fixed, permeabilized, and blocked as described previously (Troll *et al.*, 2009). Briefly, the organs were incubated with a 1:500 dilution of the EsGal1 antibody in blocking solution of 1% goat serum, 1% TritonX100, and 0.5% bovine serum albumin in marine PBS (50 mM sodium phosphate, 0.45 M sodium chloride, pH 7.4) for 7 to 14 d at 4°C, and then rinsed 4 x 1 h in 1% Triton X-100 in marine PBS, and incubated overnight in blocking solution at 4°C. Samples were then incubated with a 1:50 dilution of a fluorescein-conjugated goat anti-rabbit secondary antibody (Jackson ImmunoResearch Laboratories, West Grove, PA) in blocking solution in the dark at 4°C overnight. The light organs were then counterstained with rhodamine phalloidin as previously described (Troll *et al.*, 2009), mounted on glass slides, and examined on a Zeiss LSM 510 confocal microscope. For mucus secretion

assays, samples were prepared as previously described (Kremer *et al.*, 2013). Briefly, juvenile squid were fixed in Bouin's solution for 3 h at room temperature and then washed 4 x 1 h in mPBS at 4°C. The samples were then treated as for the above ICC experiments, except for the use of Alexa 633-conjugated wheat germ agglutinin as a counterstain to visualize host mucus. (Life Technologies, Carlsbad, CA). Fluorescence intensities were quantified using the Zeiss LSM 510 software.

Minimum Inhibitory Concentration (MIC) assays

To determine the minimal (growth) inhibitory concentration for the galaxin repeat-derived peptides, we performed micro-dilution susceptibility assays (Fedders and Leippe, 2008). Briefly, a two-fold serial dilution of each peptide was carried out in 96-well plates in 10 mM sodium phosphate buffer, with the addition of 345 mM NaCl for marine strains, pH 8.0. One hundred CFU of a log-phase bacterial culture were added to each peptide dilution and incubated overnight at 28°C for marine bacteria and 37°C for non-marine strains. After incubation, the MIC was defined as the peptide dilution where no visible bacterial growth was detected after incubation. The values are expressed as the median of at least two experiments, each performed in duplicate, with a divergence of not more than one dilution step. The following bacterial strains were used: *Bacillus subtilis* 1009, *Bacillus megaterium* 1006, *Escherichia coli* MG1665 K12 (Blattner *et al.*, 1997), CNJ 771 (*Exiguaobacterium aestuarii*-like) (Gontang *et al.*, 2007), CNJ 778 (*Bacillus megaterium*-like) (Gontang *et al.*, 2007), CNJ 803 (*Bacillus algicola*-like) (Gontang *et al.*, 2007), *Vibrio fischeri* ES114 (Boettcher and Ruby, 1990), *Photobacterium leiognathi* Ln1a (Dunlap, 1985), and *Vibrio parahemolyticus* KNH1 (Nyholm *et al.*, 2000). Marine bacteria were grown in SWT medium (Boettcher and Ruby, 1990), whereas *B. subtilis*,

B. megaterium, and *E. coli* were grown in LB medium with (wt/vol) 1% tryptone, 0.5% yeast extract, and 1% NaCl.

Bacterial growth assays

Overnight cultures of *V. fischeri* strain ES114 (Boettcher and Ruby, 1990) were diluted 1:500 and then grown to OD_{600} 0.2 at room temperature with shaking in LBS (LB with sodium chloride) medium with (wt/vol) 1% tryptone, 0.5% yeast extract, and 2% NaCl, and 50 mM Tris-HCl, pH 7.5. The cultures were then diluted with LBS 1:9 to reach an OD_{600} of about 0.02. Ten µL of the bacterial culture were then added to 190 µL of 10% LBS medium in a 96-well microtiter plate containing 17 µM EsGal1R3 or ApGalR2 (Genscript, Piscataway, NJ, sequences can be found in table 3-3), or no addition as a control. The plate was then placed in a Tecan Genios Pro plate reader (Tecan Group, Männedorf, Switzerland) and incubated at 27°C with shaking for 18 h, with OD_{600} readings taken every 15 min. Sample wells were also run without added bacteria to ensure that no contamination occurred. Bacterial doubling times were calculated using the equation $G= [\log(N-n)/\log(2)]*(T-t)$ where N is the OD_{600} at time T (final) and n is the OD_{600} at time t (initial).

Measurement of bacterial length

Cultures of RFP-expressing *V. fischeri* (Strain ES114 containing the plasmid pVSV208 (Dunn *et al.*, 2006) were grown as for the bacterial growth assays for 18 h, and were then visualized using a Zeiss AxioImager.M2 epifluorescence microscope. Bacterial length was then measured using Zeiss software.

In vivo antibody adsorption

Newly hatched juvenile squid were placed in seawater containing 5000 CFU/mL *V. fischeri* strain ES114 cells/mL filter-sterilized Instant Ocean (FSIO) for 3 h, and were then washed three times in FSIO to remove any non-attached bacteria. The juvenile squid were then either placed into FSIO containing a 1:500 dilution of the α-EsGal1 antibody or FSIO containing an equal concentration of purified rabbit IgG (Genscript, Piscataway, NJ) and then animal luminescence was measured and light organ bacterial density was determined by dilution plating of light organ homogenates on LBS agar at 6 and 8 h post-bacterial exposure.

Statistics

All qRT-PCR data were log transformed to provide a normally distributed data set and then analyzed in R (version 2.12.1; R Foundation for Statistical Computing, Vienna, Austria [http://R=project.org]) by one-way ANOVA followed by a Tukey's pairwise comparison. Shapiro-Wilk and Levene tests were used to ensure the normal distribution and homoscedasticity of the residuals, respectively.

Nucleotide accession numbers

EsGal1 has been submitted to Genbank with the submission ID 1681541.

RESULTS:

Features of the *esgal* genes and of EsGalaxin1 (EsGal1), the principal galaxin of the light organ

We identified two *esgal* sequences, *esgal1* and *esgal2*, in the *E. scolopes* transcriptomic databases. Using qRT-PCR to examine expression in different tissues of the animal, we confirmed that the *esgal1* gene is the most highly expressed galaxin gene in both the juvenile and adult light organs. Thus, for this study, we explored aspects of *esgal1* gene expression and the EsGal1 protein patterns in the squid-vibrio symbiosis. An unexpected finding was that *esgal1* expression is ~250X higher in the light organ than in the accessory nidamental gland (ANG), another less well-studied symbiotic organ. The ANG contains a consortium of bacteria thought to play a role in protection of the eggs during host development (Collins *et al.*, 2012). The expression of *esgal2* showed the opposite pattern in that it was ~250X higher in the ANG than in the light organ (Fig. 3-1).

To examine the biochemical characteristics of the EsGal1 protein more fully, we verified the full-length coding sequence for EsGal1 by 5'RACE. *esgal1* is predicted to encode a 13.1 kD protein with a pI of ~10. RADAR analysis of the sequence predicted that the protein has three tandem repeats (Fig. 3-2A) anchored by dicysteine pairs. SignalP analysis predicted a signal peptide, suggesting that the protein is secreted. The high predicted pI, repeat structure, and abundant cysteines (12.3%) suggested that the protein could be antimicrobial (Fedders and Leippe, 2008).

BLAST analysis (NCBI) of the derived amino-acid sequence of the protein revealed 25 proteins with some similarity to EsGal1 (Table 3-2), with the closest match being to a galaxin occurring in the coral *Acropora millepora* (E-value = $4e^{-13}$). Examination of full-length

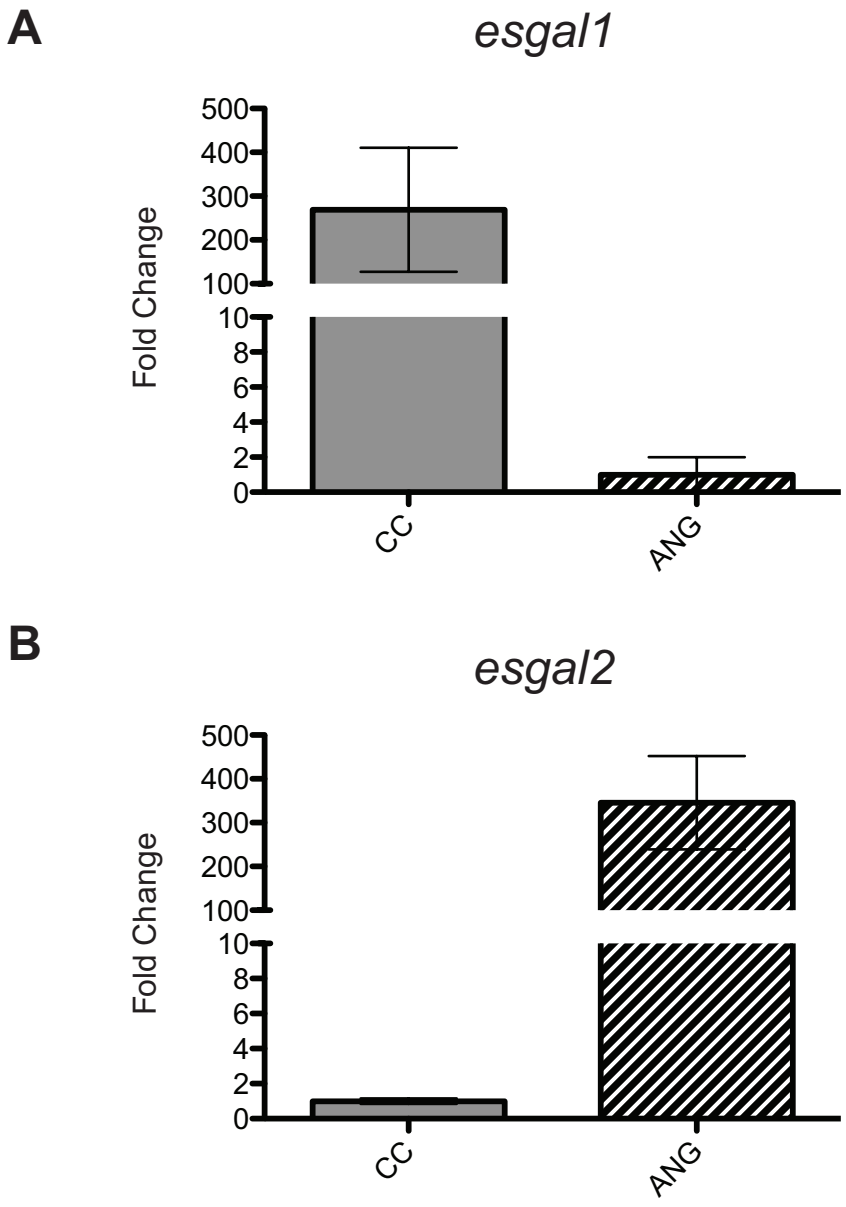

Fig. 3-1. Expression of *esgal1* and *esgal2* in symbiotic organs of adult squid. Expression, as measured by qRT-PCR, of *esgal1* (A) and *esgal2* (B) in the bacteria-containing epithelia of the adult light organ, or central core (CC) and the female-specific accessory nidamental gland (ANG). Data are normalized to the condition of lowest expression. Values +/- SEM, and n=3 biological replicates and 2 technical replicates per condition.

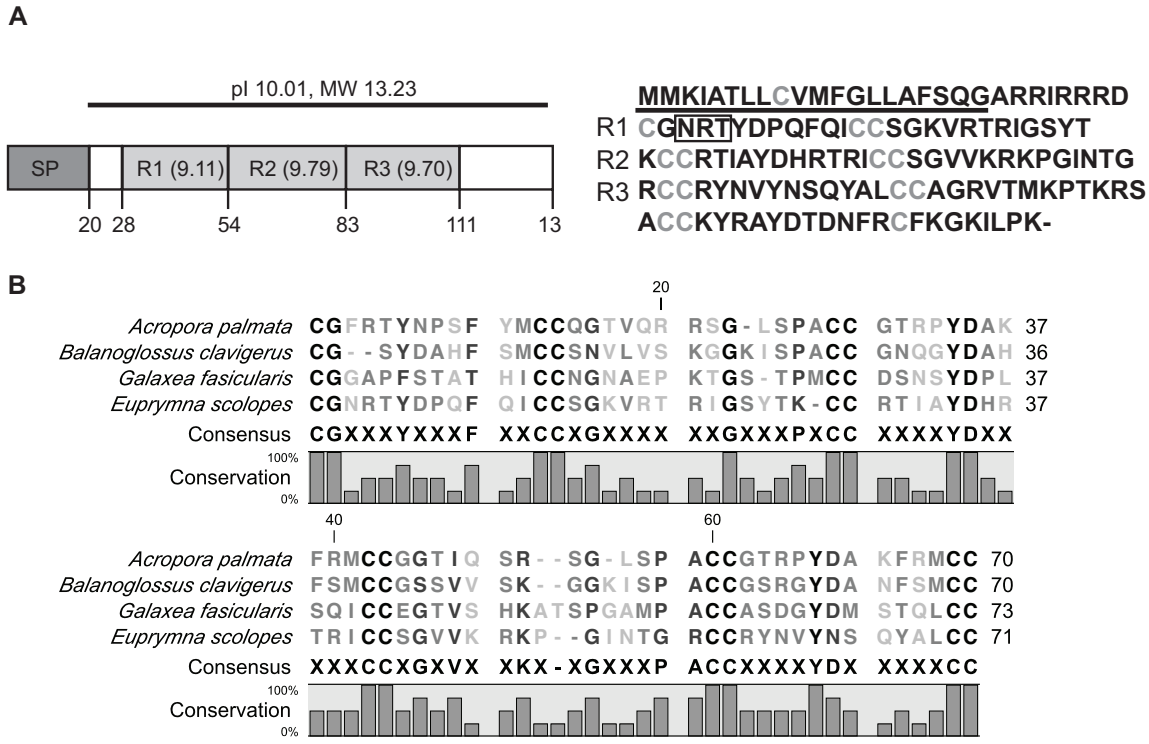

Fig. 3-2. Biochemical properties of the EsGal1 protein. (A) The structure of the protein. Left, major regions, with amino acid position indicated by the numbers below. M_r, molecular mass; pI, predicted isoelectric point; R1-3, predicted repeats and their pIs; SP, predicted signal peptide. Right, the derived amino acid sequence of EsGal1 R1-R3, with the RADAR-predicted repeat structure; predicted signal peptide, underlined; predicted N-glycosylation site, boxed; cysteines, gray. (B) MUSCLE alignment of portions of galaxin sequences from *Acropora palmata, Balanoglossus clavigerus, E. scolopes*, and *Galaxea fasicularis*, with the consensus sequence and graphical representation of conservation at each amino acid residue shown below the alignment.

Table 3-2. Galaxin sequences and their relevant features, including predicted repeat structure and antimicrobial activity

Organism	Accession	Length (AA)	pI	Repeats	Repeat Length	Number of Repeats	# of Antimicrobial Repeats / Total	Signal Peptide
Acropora millepora	297718761	338	5.45	yes	26	9	n/a*	yes
Acropora millepora	297718763	660	8.33	yes	27	15	15 of 15	yes
Acropora millepora	297718765	582	4.82	yes	40	8	n/a*	yes
Acropora palmata	282476131	223	8.78	yes	26	5	5 of 5	yes
Acropora palmata	282469886	223	8.72	yes	25	5	5 of 5	yes
Balanoglossus clavigerus	311135555	193	9.23	yes	26	6	5 of 6	yes
Branchiostoma floridae	260831180	828	6.93	yes	42	12	n/a*	yes
Caenorhabditis remanei	308257573	254	6.42	yes	28	6	n/a*	yes
Capitella teleta	JGI 200308	348	4.61	yes	25	11	n/a*	yes
Capitella teleta	JGI 205037	207	4.9	yes	25	6	n/a*	yes
Capitella teleta	JGI 113664	361	6.21	yes	25	10	n/a*	yes
Ciona intestinalis	198432839	692	6.23	yes	87	8	n/a*	yes
Ciona intestinalis	198428686	557	4.29	yes	49	11	n/a*	yes
Ciona intestinalis	198428682	776	3.76	yes	45	13	n/a*	yes
Ciona intestinalis	198428684	572	4.19	yes	44	11	n/a*	no

E. scolopes	n/a	133	9.98	yes	28	3	3 of 3	yes
Galaxea fascicularis	26106077	343	4.95	yes	27	10	n/a*	yes
Hydra magnipapillata	221103150	342	8.35	yes	27	9	5 of 9	yes
Hyriopsis cumingii	312836609	158	7.71	yes	27	5	3 of 5	yes
Lottia gigantea	JGI 153896	116	8.14	yes	26	2	1 of 2	no
Lottia gigantea	JGI 167440	693	8.64	yes	24	7	n/a*	no
Lottia gigantea	JGI 235558	467	8.13	yes	25	9	n/a*	yes
Montastraea faveolata	282524973	225	6.81	yes	22	6	n/a*	yes
Saccoglossus kowalevskii	187145257	171	9.18	yes	25	4	3 of 4	yes
Salpingoeca	326435182	350	4.09	yes	16	6	n/a*	no
Salpingoeca	326434627	232	4.42	yes	32	5	n/a*	yes
Sipunculus nudus	326358366	109	10.44	yes	26	3	3 of 3	yes

sequences revealed a protein family with an array of sizes, from 116 to 828 amino acids (Table 3-2). Our alignment with portions of other galaxin proteins (Figs. 3-2B and 3-3) revealed that EsGal1 shares with the other family members the conserved repeat structure and a number of residues, which suggests that these regions of the protein are critical to structure and function of galaxins.

Patterns of *esgal1* expression

To characterize the regulation of expression of *esgal1* over early light-organ development, we performed qRT-PCR on both aposymbiotic and symbiotic light organs collected at six time points over the first 2 d of colonization of the juvenile squid (Fig. 3-4A). These points were chosen to determine when the regulation of *esgal1* begins after colonization and then how long after colonization the regulation persists. The *esgal1* mRNA levels were higher in the symbiotic than the aposymbiotic light organs; significant upregulation began at 10 h post-hatching and persisted over the first two days of the symbiosis. In addition, symbiotic light-organ expression of *esgal1* increased two fold between 10 and 14 h post-hatching, whereas we observed no difference in expression in aposymbiotic light organs, suggesting that symbiosis is increasing expression rather than expression being downregulated in aposymbiotic animals. To determine if galaxin expression is more prevalent in symbiotic tissues than other portions of the squid, we analyzed *esgal1* expression in six different tissues of the adult squid and found that relative expression of *esgal1* is 100-1000 fold higher in *V. fischeri*-containing tissue (central core) than in any other tissue sampled (Fig. 3-4B).

In the squid-vibrio symbiosis, certain symbiont-induced host phenotypes are reversible upon depletion of symbionts from a colonized organ after 12 h, i.e, they require persistent

Euprymna scolopes

MMKIATLLCVMFGLLAFSQGARRIRRRDCGNRTYDPQFQICCSGKVRTRIGSYT
KCCRTIAYDHRTRICCSGVVKRKPGINTGRCCRYNVYNSQYALCCAGRVTMKP
TKRSACCKYRAYDTDNFRCFKGKILPK

Balanoglossus clavigerus (FN987614.1)

MGKKLVALILLFIVVDSFVSTDAWRRRRRRRRSSSGGSPPSGGGGGNPPVGC
GSYDAHFSMCCSNVLVSKGGKISPACCGNQGYDAHFSMCCGSSVVSKGGKIS
PACCGSRGYDANFSMCCGSSVVSKGGKISPGCCGSRGYDANFNMCCGSNVV
SKGGKISPACCGSVGYDARFSMCCYGIVRSRVGISPSC

Galaxea fasicularis (BAC41519.1)

MSPTVSICFCSALFAVFSSCASFPRDTLSADSENVPNKLETRYRRQAPVPPVVS
YCGGAPFSTATHICCNGNAEPKTGSTPMCCDSNSYDPLSQICCEGTVSHKATS
PGAMPACCASDGYDMSTQLCCNDNVMHKPTGPTALPGCCGDHSYDASVQLC
CDSNVVPKMGSLSACCGPNSYDTNTTLCCDSNVAFVSGPQAQCCGSQGYDG
ATQLCCDSNVLPKPGATGACCGSQSYTQDTHLCCEGVIVLKAGPSFACCGSAS
YNQSSSLCCGATVVAKTPSKPVCCGSTSYNPVTEICCDGHVGTRAGLTSPTCC
GGAVFDAATAKCCDGVPVFNVPSCAGLA

Acropora palmata (GW202476.1)

MFKSSLTVFFLILFAHSCNAHSLTEQVEPIEIPGENRESSVVETTGAIEVPDEDN
GDKTNVGEKDFEGQKSVKSRQRRAVCGFRTYNPSFYMCCQGTVQRRSGLSP
ACCGTRPYDAKFRMCCGGTIQSRSGLSPACCGTRPYDAKFRMCCGGTLQSRS
GLSPACCGTRPYDAQFRMCCGGTIQSRSGLSPACCGTRPYDAQISHVLWRYY
TKQIQIETRMLRD

Fig. 3-3. Sequences of the Galaxin proteins used in the alignment in Fig. 1. Full-length protein sequences of the proteins (with Genbank identifying numbers in parentheses) are given, with the repeats used for the alignment highlighted in yellow.

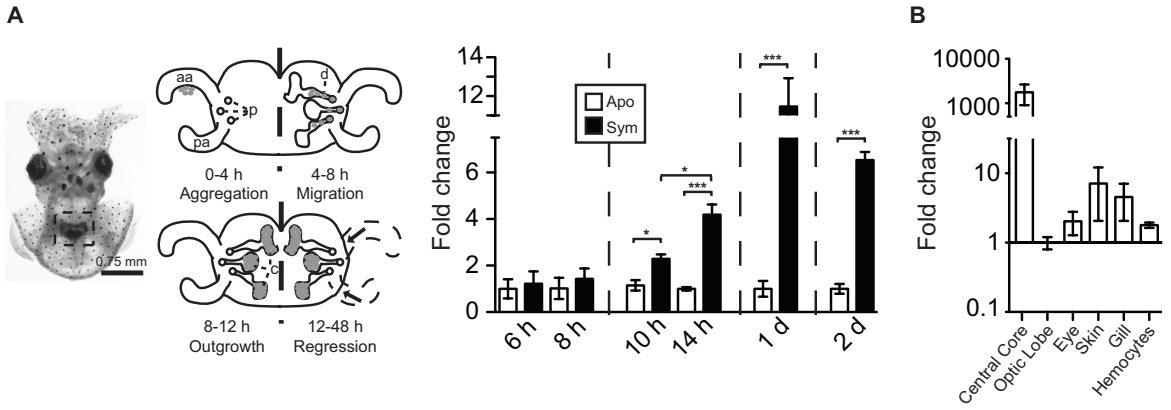

Fig. 3-4. Patterns of *esgal1* expression. (A) Top, a ventral view of the juvenile animal, with relevant features. Left, the light organ (box), seen through translucent ventral mantle tissue. Center, stages of early symbiosis development. The acquisition of symbionts from the seawater is facilitated by anterior (aa) and posterior (pa) epithelial 'appendages' of a superficial ciliated epithelium. Symbionts (gray) accumulate along these epithelia in the first hours after exposure (Aggregation). They then migrate into pores (p), through the ducts (d) into the crypt spaces (c) (Migration). In the crypts, the symbionts proliferate to fill the spaces (Outgrowth). At 12 h, the symbionts deliver an irreversible morphogenic signal that leads to the eventual loss of the ciliated epithelia (Regression). Right, the expression of *esgal1* in the light organ at time points over the first 2 d in apo- and symbiotic animals. Significant differences (*, <0.05; ***, <0.001) between conditions by an ANOVA followed by a Tukey's pairwise comparison. (B) Expression of *esgal1* in six tissues of adult animals. Central Core refers to the bacteria-containing epithelia of the adult light organ. Relative qRT-PCR values (+/- SEM). All data are normalized to the condition of lowest level of expression; n=3 biological replicates and 2 technical replicates per condition.

interaction with the symbiont (Lamarcq and McFall-Ngai, 1998; Nyholm *et al.*, 2002), while some are irreversibly established after a 12-h colonization (Doino and McFall-Ngai, 1995; Davidson *et al.*, 2004). To address if persistent colonization of the light organ by symbionts is necessary for *esgal1* regulation, we depleted colonized animals of their symbionts with antibiotics at 24 h post-hatching and then compared *esgal1* expression levels in these depleted light organs 24 h later, i.e, at 48 h post hatching, to those of symbiotic and aposymbiotic animals. Depletion of symbionts did not significantly alter the expression of the *esgal1* transcript from the symbiotic level of expression under the conditions used (Fig. 3-5A), suggesting that the persistence of viable symbionts in the light organ is not necessary for the regulation of *esgal1,* or that any change in expression requires significantly longer than other reversible phenotypes.

We explored signals from *V. fischeri* that might regulate *esgal1* expression. Because the bacterial products lipid A and TCT induce many host phenotypes in the squid-vibrio system (McFall-Ngai *et al.*, 2010), we determined if these products are also responsible for the regulation of *esgal1*. While exposure to TCT and lipid A increased expression of *esgal1* in the light organ on average ~1.75-fold (Fig. 3-5B), the response was only ~20% of the increase observed in symbiotic relative to aposymbiotic organs. One other inducer of host phenotypes is symbiont light production (McFall-Ngai *et al.*, 2012). However, *V. fischeri* mutants defective in light production showed no defect in *esgal1* upregulation (Fig. 3-5C).

Localization and abundance of EsGal1 in the juvenile animal

The EsGal1 antibody recognized apical cytoplasmic and perinuclear sites in the epithelia of the light organ, including the appendages and ducts, but did

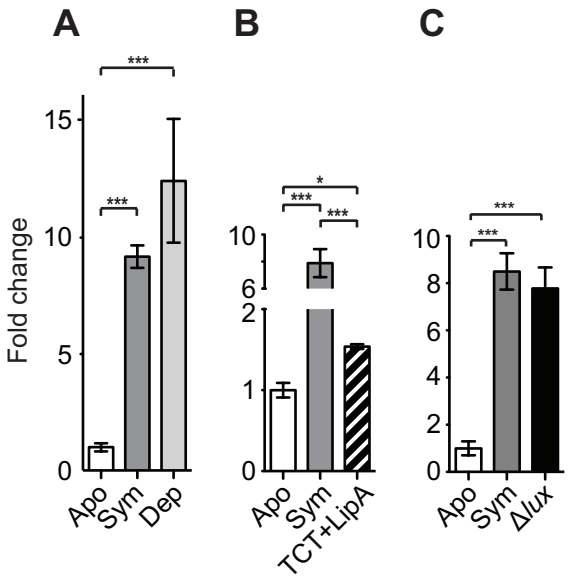

Fig. 3-5. The influence of experimental manipulation on *esgal1* expression. Expression, as measured by qRT-PCR, at 48 h in the light organ of animals remaining uncolonized (Apo) or colonized with *V. fischeri* strain ES114 (Sym) compared with: (A) animals colonized with *V. fischeri* for 24 h and then antibiotically depleted of their symbionts (Dep); (B) treated with the bacterial products TCT and lipid A (TCT+LipA) (see Materials and Methods for details); (C) animals colonized with mutants defective in light production (*Δlux*). Data are normalized to the time point of lowest expression. Values +/- SEM; Significant differences (* = $p < 0.05$, ** = $p<0.01$, *** = $p<0.001$) between conditions by an ANOVA followed by a Tukey's pairwise comparison; n = 3 to 4 biological replicates and 2 technical replicates per condition.

not label internal musculature (Fig. 3-6A, A'). The apical localization, in conjunction with the presence of a signal peptide in the *esgal1*-derived amino acid sequence, suggested that the protein is secreted, which was confirmed by localization of EsGal1 to the mucus outside of the light organ (Fig. 3-6B). In quantification of labeling of EsGal1 antibody in apo- and symbiotic animals, although the two conditions had the same signal intensity in the duct cells, the epithelial appendages of symbiotic light organs had about twice the signal intensity (Fig. 3-6A', inset). We also observed antibody reactivity in the symbiont-containing crypts (Fig. 3-6C). Reactivity localized to perinuclear sites inside of the epithelial cells and to the extracellular crypt spaces where the symbionts reside, suggesting secretion of the protein into symbiont-containing regions. We observed no staining in samples exposed to rabbit IgG as a negative control (Fig. 3-7 A-C). When we performed a western blot analysis on squid proteins using the EsGal1 antibody, we observed several specific bands, one of which corresponded to the predicted molecular weight (Fig. 3-7D). The existence of multiple bands may be due to the putative N-glycosylation site on the EsGal1 protein (Fig. 3-2A), the modification of which could alter the migration of the protein on an SDS gel, or due to the abundant dicysteine bonds that may not have been fully reduced before protein preparation.

To determine whether epithelial localization of EsGal1 protein was unique to the light organ, we performed immunocytochemistry with the antibody on other host tissues (Fig. 3-8). The antibody recognized cytoplasmic and perinuclear sites in all epithelial tissues exposed to seawater, including the tentacles and gills, but did not label internal tissues, such as the white body (the haematopoietic organ of the animal) or musculature of the tentacles. Symbiotic state of the light organ did not detectably alter the localization of EsGal1 in any non-symbiotic tissue.

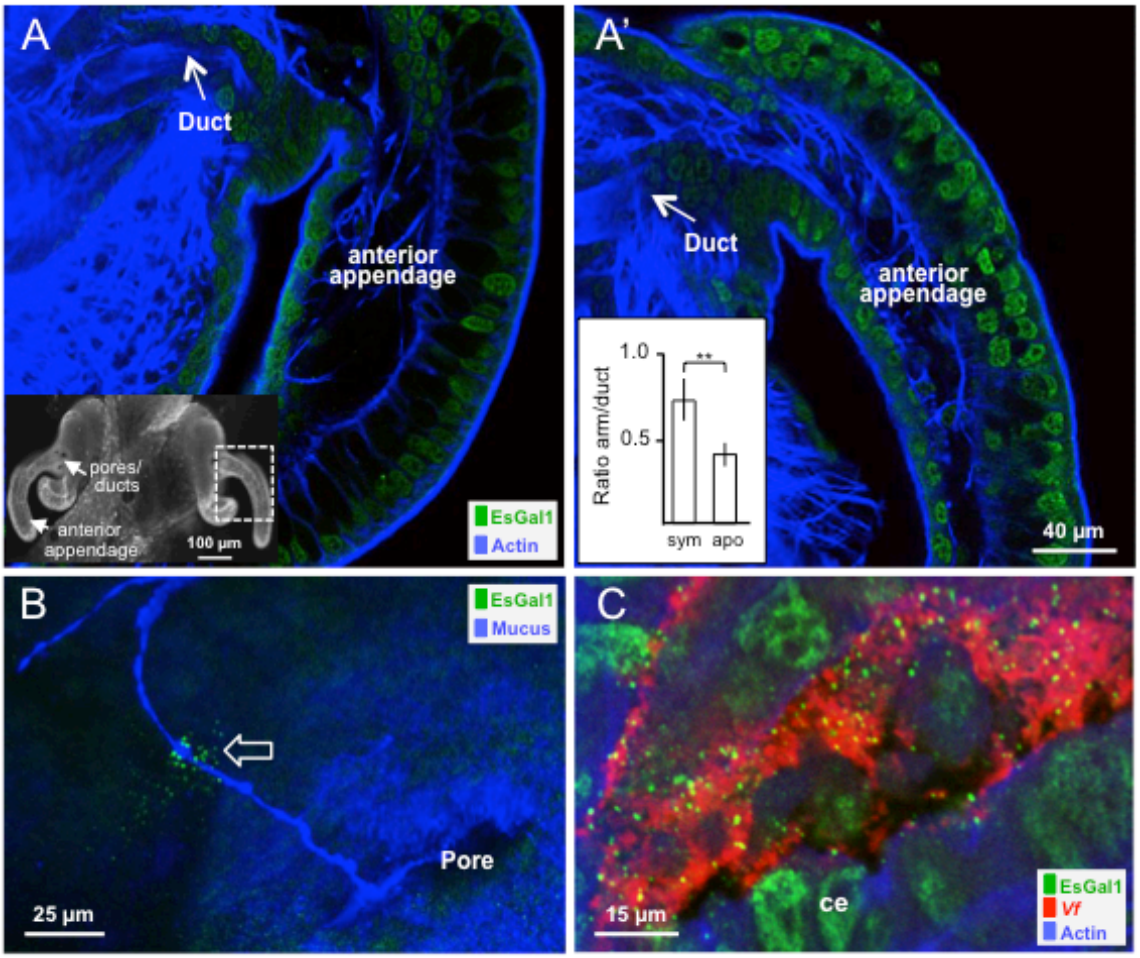

Fig. 3-6. Localization and abundance of EsGal1 in the juvenile light organ. Light organs from 24 h uncolonized (A) and colonized (A') juveniles probed with the EsGal1 antibody, showing the relative abundance of reactive material in each condition. Labeling of tissue actin (phalloidin) was used as a counterstain. Inset in A, confocal micrograph of the entire organ showing regions explored by ICC. Inset graph in A', relative fluorescent intensity; ** = $p<0.01$ by an unpaired t-test after log transformation to ensure normality. (B) EsGal1 localization to the mucus outside of the hatchling juvenile light organ. Open arrow, EsGal1 in contact with a mucus strand outside of the light-organ pore. (C) EsGal1 secretion into crypt spaces of the colonized organ. ce, crypt epithelium; Vf, *Vibrio fischeri.*

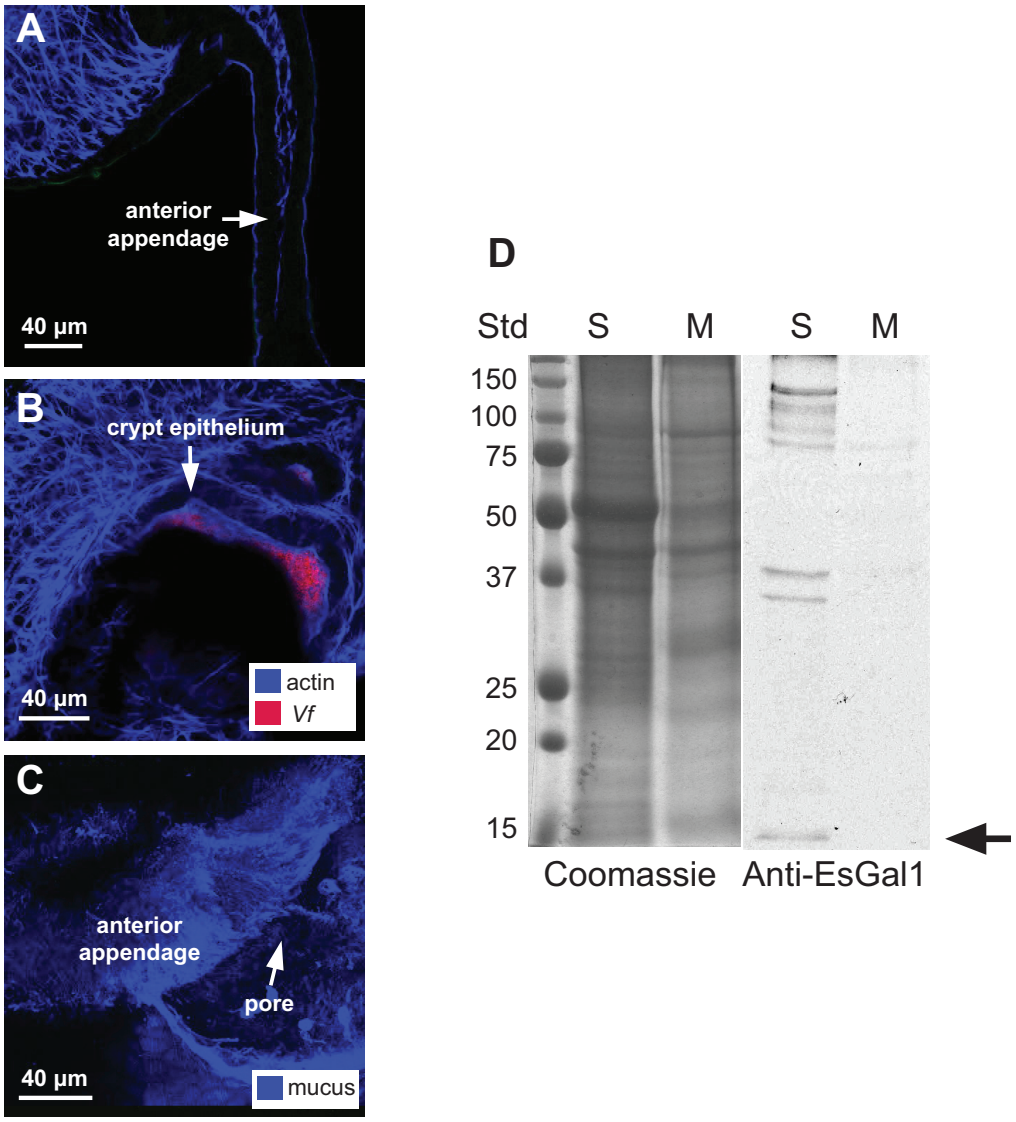

Fig. 3-7 Controls for antibody staining. (A-C) Juvenile squid light organs stained with IgG as a negative control for antibody in the animals shown in Fig. 3-6. Shown are portions of the light organ including (A) the anterior appendage, (B) the colonized crypt spaces, and (C) the mucus outside of the light organ. No IgG staining (green) is shown. (D), Western blot performed with the anti-EsGal1 antibody on aqueous soluble (S) and SDS-soluble, or membrane, (M) fractions. The arrow denotes a band at the predicted molecular weight. Molecular weight standards in kDa are shown at left.

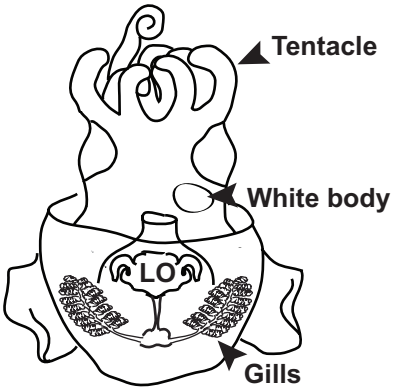
Tentacle
White body
LO
Gills

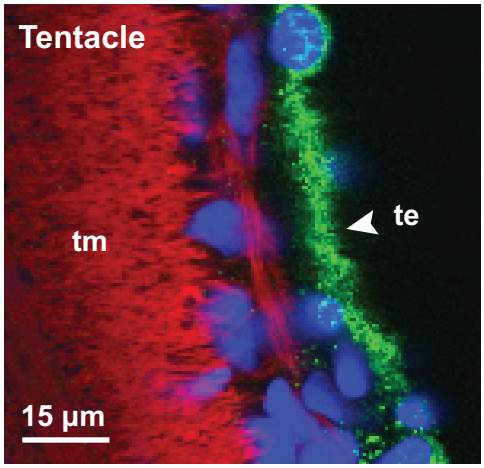
Tentacle
tm
te
15 µm

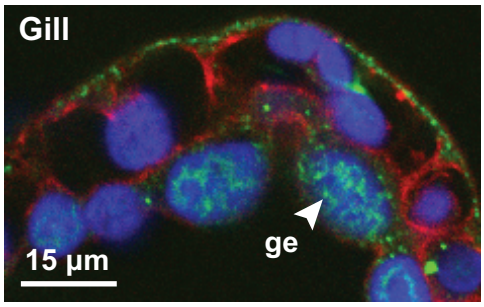
Gill
ge
15 µm

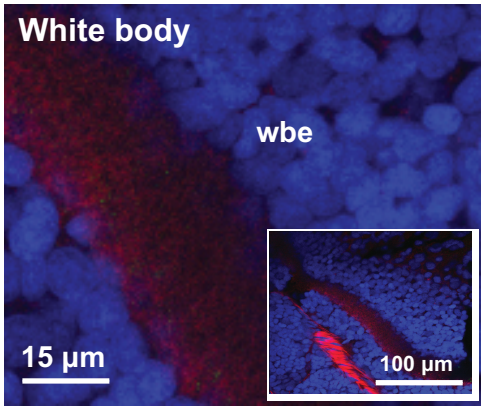
White body
wbe
15 µm
100 µm

Fig. 3-8. Localization of EsGal1 in whole juvenile squid. Top, diagram of a juvenile *E. scolopes*, showing the tissues examined in the remainder of the figure. Multiple tissues of 24 h *E. scolopes* that were examined for production of the EsGal1 protein by confocal immunocytochemistry, including the tentacles, the gills, and the main haematopoietic organ known as the white body. Day-old symbiotic juvenile *E. scolopes* were exposed to the anti-EsGal1 antibody (green), and counterstained with phalloidin (red, actin cytoskeleton) and TOTO-3 (blue, nuclei). The anti-EsGal1 antibody stained the nuclei and apical portions of epithelial cells most brightly (white arrowheads). Aa – anterior appendage, d – ducts, ge – gill epithelium, pa – posterior appendage, te – tentacle epithelium, tm – tentacle musculature, wbe – white body epithelium.

Evidence for antimicrobial activity of EsGal1

Due to the small size, basic pI, presence of a secretion signal, and numerous cysteines in EsGal1, we hypothesized that the protein acts as an anti-microbial effector, a class of molecules that tend to share all of these properties (Fedders and Leippe, 2008). To determine whether the protein might have such activity, we synthesized the third of the three repeats present in the EsGal1 protein (EsGal1R3, Table 3-3) that, by *in silico* analysis, was predicted to be the most likely region of the protein to be antimicrobial, and characterized its ability to inhibit bacterial growth. The third repeat of EsGal1 was chosen because of its high net charge and hydrophobic residue ratio, as well as its significant sequence similarity to a known oyster defensin, all determined with the APD2 antimicrobial peptide calculator and predictor (see Experimental Procedures). EsGal1R3 affected the growth of Gram-positive bacteria at concentrations as low as 27 nM (Table 3-3), and was about 10 to 100 times more effective against non-marine species than non-marine species under the assay conditions used. However, EsGal1R3 did not inhibit the growth of Gram-negative marine species, including *V. fischeri*, in MIC assays. To determine whether antimicrobial activity was a shared characteristic of galaxin proteins from other species, we also synthesized a peptide corresponding to the predicted repeat 2 from *Acropora palmata* galaxin (ApGalR2), which we chose for its basic pI and predicted antimicrobial capabilities, and determined its ability to inhibit bacterial growth under the same conditions used for assays with EsGal1R3. ApGalR2 did not exhibit any capacity to inhibit the growth of marine bacteria and was, at most effective, 10-fold less active than EsGal1R3 against non-marine strains.

As EsGal1R3 showed promise as an antimicrobial, we tested its activity against a known pathogen of interest, Methicillin-resistant *S. aureus* (MRSA) using strains from S. Daum at the University of Chicago. We found that EsGal1 was active against all MRSA strains tested

(MRSA, MRSA strains with Vancomycin resistance, and a MRSA strain with daptomycin resistance, Table 3-4), suggesting that this peptide may be of use as an antimicrobial agent in healthcare settings.

Because of the influence of day/night cycles on the symbiont growth in the association (Nyholm and McFall-Ngai, 2004; Wier *et al.*, 2010) and the potential that EsGal1 has to modulate bacterial growth, we also measured *esgal1* gene expression at two time points over the day/night cycle in both juvenile light organs and adult central cores, i.e., the epithelial tissue of the adult light organ that supports the symbiont. In both sample groups, we found an upregulation of *esgal1* at 2 h after dawn (Fig. 3-9), a time point coincident with the rapid symbiont growth in the organ that immediately follows the venting of 90% of the symbionts (Graf and Ruby, 1998; Nyholm and McFall-Ngai, 1998). These data suggest that in both juvenile and adult animals *esgal1* is upregulated when the bacterial symbionts are rapidly dividing in the light organ.

Although the MIC assay showed that EsGal1R3 does not inhibit growth of *V. fischeri* except at high concentrations, we hypothesized that in lower concentrations, the peptide could modulate the rate of bacterial growth in the light organ. We first tested the growth response of *V. fischeri* to sub-inhibitory concentrations of the peptide under *in vitro* culture conditions. We observed that exposure to EsGal1R3 over 18 h both delayed the start of exponential growth of *V. fischeri* by approximately 2 h and decreased its growth rate 1.5-fold once in exponential phase growth (Fig. 3-10 A,B). While the most robust result was obtained using 17.4 μM EsGal1R3 (half of the concentration determined to be inhibitory), the peptide showed a dose-dependent ability to modulate the growth of *V. fischeri* at a concentration as low as 8.2 μM (Fig. 3-11).

TABLE 3-3. Antimicrobial activity of EsGal1R3 and ApGal R2

Strain Characteristics and Strain	EsGal1 R3 MIC (μM) - RCCRYNVYNNSQ YALCCAGRVTMK PTKRS	ApGal R2 MIC (μM) - VQRRSGLSPACCGTRP YDAKFRMCCGGT	Source
Gram-positive			
Non-marine			
B. megaterium	0.027	0.287	This Study
B. subtilis	0.5375	4.76	This Study
Marine			
B. algicola CNJ 803	4.3	>152.29	(Gontang *et al.*, 2007)
B. megaterium-like CNJ 778	6.88	>152.29	(Gontang *et al.*, 2007)
E. aestuorii CNJ 771	3.44	>152.59	(Gontang *et al.*, 2007)
Gram-negative			
Non-marine			
E. coli	1.72	76.145	(Blattner *et al.*, 1997)
Marine			
P. leiognathi	>137.5	>152.29	(Dunlap, 1985)
V. fischeri ES114	34.4	>152.29	(Boettcher and Ruby, 1990)
V. parahaemolyticus	137.5	>152.29	(Nyholm *et al.*, 2000)

TABLE 3-4. Anti-Staphylococcal Activity of EsGal1R3

Strain	Phenotype	MIC (μM)
923	MRSA	2.15
MI	VRSA	1.72
Q2283	VISA	1.075
2902	Daptomycin-resistant	3.44

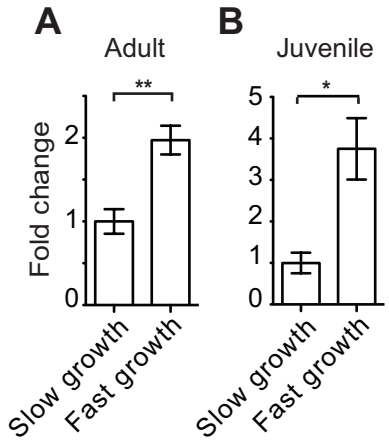

Fig. 3-9. Daily changes in *esgal1* expression with variation in light-organ symbiont growth rate. *esgal1* expression in wild-caught adult (A) and juvenile (B) light organs during periods of slow and rapid bacterial growth, approximately 12-14 h before dawn and 2 h after dawn, respectively. All data are normalized to the condition of lowest expression. Error bars denote the standard error of the mean. * = $p<0.05$ and ** = $p<0.01$ by an unpaired t-test after log transformation to ensure normality.

The growth curve (Fig. 3-10A) had a higher terminal optical density (OD) for the EsGal1R3 exposed cells, which suggested that either smaller cells or more numerous cells had resulted from the conditions. Measurements of the cells showed an average decrease in their length of about 20% (Fig. 3-10C), similar to the decrease in size noted in *V. fischeri* cells adapted to the crypts of the light organ (Ruby and Asato, 1993).

To determine whether EsGal1 might affect *V. fischeri* growth during onset of the association, we co-incubated the animals during colonization with the EsGal1 antibody to adsorb the protein from the environment, a proven approach to the study of interactions of the symbiont with host biomolecules (Aeckersberg *et al.*, 2001; Kremer *et al.*, 2013). In the treated hatchlings, we observed a 2.5-fold increase in symbiont luminescence (Fig. 3-10D) and a 1.6-fold increase in bacterial density (Fig. 3-10E) at 8 h post-bacterial exposure as compared to the negative control.

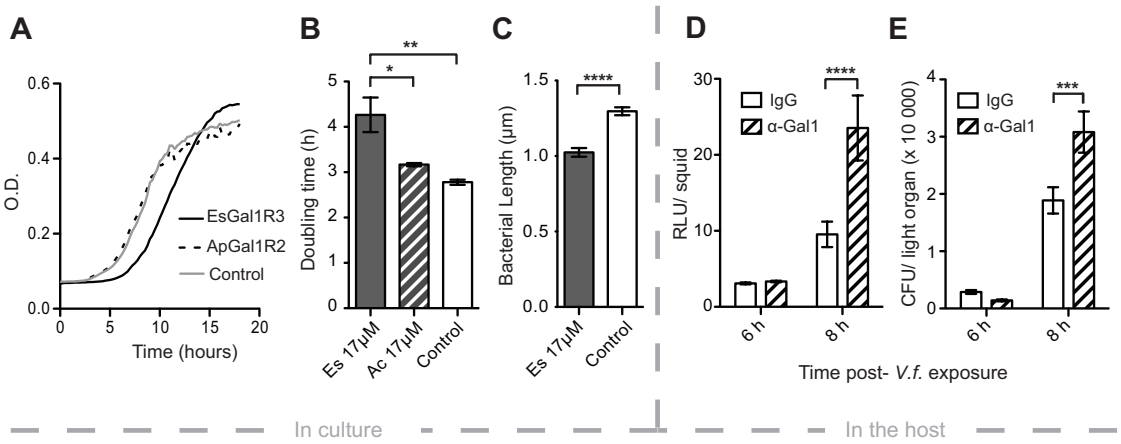

Fig. 3-10. The effect of EsGal1R3 on *V. fischeri* growth *in vitro* and *in vivo*. (A) Growth curve of *V. fischeri* cells exposed to 17.4 μM EsGal1R3 (solid line), 17.4 μM ApGal1R2 (dashed line), or to no peptide (gray line). (B) Quantification of *V. fischeri* doubling times in experiment shown in (A). Experiment in (A) and (B) was performed with three biological replicates and two technical replicates. (C) Length of *V. fischeri* cells exposed to 17.4 μM EsGal1R3 (gray bar) or no peptide (open bar). N= 117 and 124, respectively. (D) Effect of α-EsGal1 antibody or rabbit IgG exposure on animal luminescence at 6 or 8 h after exposure to bacteria. (E) Effect of α-EsGal1 antibody or rabbit IgG exposure on the number of colony-forming units (CFU) in the juvenile light organ at 6 and 8 h after exposure to *V. fischeri*. N= 23 to 27 for each condition. Error bars denote the standard error of the mean. * = $p< 0.05$, ** = $p<0.01$, *** = $p<0.001$, **** = $p<0.0001$ by an ANOVA with a post-hoc Tukey's pairwise comparison.

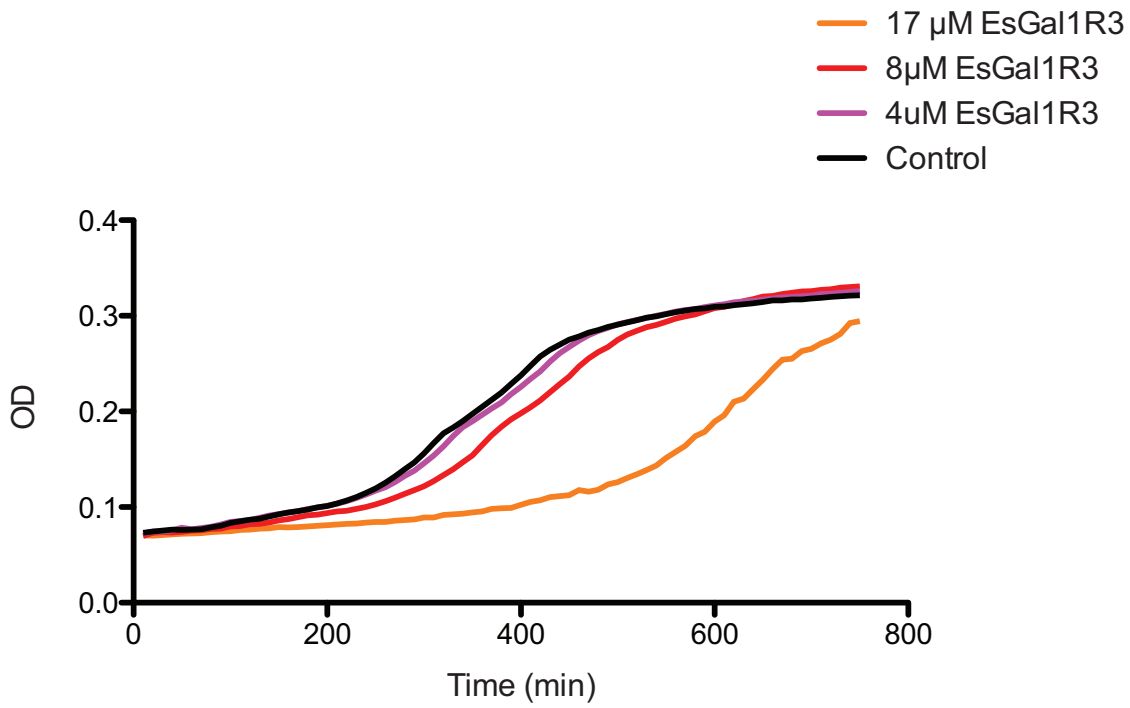

Fig. 3-11. Dose-response of *V. fischeri* growth to exposure to EsGal1R3. Growth curve of *V. fischeri* cells exposed to 17.4 µM EsGal1R3 (orange line), 8.2 µM EsGal1R3 (red line), 4.1 µM EsGal1R3 (pink line), or to no peptide (black line). The experiment was performed with 3 biological replicates (except for the 17.4 µM condition, which had 2) and 2 technical replicates.

DISCUSSION:

In this study, we investigated the role of a host protein, EsGal1, in the habitat transition of *Vibrio fischeri* from the seawater to the light organ of the squid *Euprymna scolopes.* We provide evidence for the activity of this protein in the selection of *V. fischeri* from the complex bacterioplankton, as well as in the long-term maintenance of this symbiont in a cooperative, binary association.

EsGal1 in *V. fischeri* habitat transition

In marine habitats, a given microbial species such as *V. fischeri* can be found in a wide variety of environments; for example, they can occur as members of the bacterioplankton and in marine snow, sediments, and symbiotic associations (Fuhrman, 2009; Stabb and Dr Karen L Visick, 2013). As such, habitat transitions are often a critical feature of their ecology. Because the association between *V. fischeri* and *E. scolopes* is a horizontally transmitted symbiosis (Bright and Bulgheresi, 2010), the microbial partner must be capable of a robust response both to environmental stressors in the planktonic environment and to the selective pressures imposed by the host niche (Wang *et al.*, 2010). The host, in turn, must provide conditions that: 1) promote selection of the coevolved symbiont from thousands of microbial species in the bacterioplankton during symbiosis onset; and, 2) once the symbiosis is established, maintain the association so that it persists throughout the life of the animal (Visick and Ruby, 1996; Nyholm *et al.*, 2002).

Over the 3-4 h following initial exposure to seawater with natural levels of environmental bacteria, *V. fischeri* cells outcompete other bacterial cells associating with the epithelial cell surface of the host's light organ. The first step in this process of 'winnowing' is the elimination of Gram-positive bacteria (for review, see (Nyholm and McFall-Ngai, 2004)). We found that the

host protein EsGal1 is produced on the surface of the epithelial field and secreted into the mucus (Fig. 3-6C), the environment where *V. fischeri* attaches and then aggregates (Altura *et al.*, 2013). The lack of symbiont-dependent regulation of *esgal1* transcription during time points coincident with aggregation demonstrates that provision of EsGal1 stores is "hard-wired" during embryogenesis to be in place, ready for secretion when the animal hatches from the egg (Fig. 3-4A). Further, a peptide predicted to occur on the protein surface, corresponding to a single repeat of EsGal1, was active against Gram-positive bacteria in *in vitro* assays. Earlier studies provided evidence for the involvement of other proteins that are active against Gram-positives, specifically the findings that a peptidoglycan-recognition protein (EsPGRP2,(Troll *et al.*, 2010)) is also secreted into the mucus and the gene encoding a lysozyme isoform is upregulated during initial interactions with *V. fischeri* (Kremer *et al.*, 2013). In addition, other antimicrobials, such as nitric oxide (Davidson *et al.*, 2004), occur in abundance in the mucus. From these studies, a scenario is emerging in which the host provides a selective environment that *V. fischeri* can withstand and to which it can adapt, and that the symbiont cells participate in the creation of this environment through signal exchange with the host.

Growth modulation by host molecules

Our data also provide evidence that EsGal1 modulates the growth of symbiont populations that have already colonized the host. An earlier study demonstrated that colonization of the crypts causes a significant increase in expression of the gene encoding EsGal1 (Chun *et al.*, 2008) at about 18 h following colonization. In the present study, we showed that this upregulation is detectable as early as 10 h, during the initial symbiont outgrowth to fill the crypt spaces. We confirmed that EsGal1 is secreted into the crypts, where it can act directly on

symbiont cells, and co-incubation of juvenile squid during initial colonization with the EsGal1 antibody increased the growth rate of *V. fischeri,* such that the crypts are colonized more quickly. Once the symbiosis is established, we show that EsGal1 gene expression changes over the day/night cycle, being highest during the rapid growth of *V. fischeri* following the daily venting of cells into the environment in response to the dawn light cue (Graf and Ruby, 1998). The upregulation of *esgal1* during bacterial growth in the light organ is reminiscent of the provision of the antimicrobial coleoptericin by weevils into regions where their intracellular symbionts occur. This protein controls the growth and limits the location of the symbionts to specific host cells, or bacteriocytes (Login *et al.*, 2011). Taken together, these data suggest that the symbiont participates in creating an environment that imposes a governor on symbiont population growth.

The precise mechanisms by which the symbiont signals the host are not fully understood. Although our data show that bacterial cell-envelope molecules may play a role (Fig. 3-5B), they could not induce the same responses as the presence of the symbiont, suggesting that they may work in synergy with other factors. For some squid-host responses, light works in synergy with these molecules (Heath-Heckman *et al.*, 2013). However, in this study, Δ*lux* mutants had no defect in inducing normal expression of *esgal1*, so the evidence suggests another factor. Alternatively, under normal conditions these molecules may induce these host responses, but the cell envelope molecules, when added as pharmacological agents, are not presented to host tissue in the same manner as the intact bacterial cell (e.g., concentration, configuration); or, direct interactions with the bacterial cell enable host responses, as has been noted before for other host responses (Chun *et al.*, 2008; Heath-Heckman *et al.*, 2013)

The selection of symbionts by host biomolecules in the squid-vibrio system has parallels in other mutualisms. For example, in *Hydra* spp., overexpression of periculin, a secreted

antimicrobial protein, changes the microbial community density along the host surface and the composition of the community in mature polyps (Fraune *et al.*, 2010). Additionally, *Hydra* spp. lacking the capability to express antimicrobial peptides, such as arminin, lose the capacity to select for a species-specific microbiota (Franzenburg *et al.*, 2013). In the mammalian gut, exposure of the host to gram-negative bacteria during initial gut colonization induces the secretion of RegIII-gamma, a lectin that is anti-gram-positive (Cash *et al.*, 2006). This protein alters microbial community structure in the gut by creating a zone of exclusion between host cells and the microbiota through its bacteriocidal activity. In so doing, it reduces potential symbiont-mediated inflammatory processes in the intestine (Cash *et al.*, 2006; Vaishnava *et al.*, 2011). The mammalian gut also expresses α-defensin, an antimicrobial peptide that has been shown to structure the microbial community to promote gut homeostasis (Salzman *et al.*, 2010). Collectively, these studies suggest that the bacteriostatic property of EsGal1 against *V. fischeri* may benefit the host by restricting symbionts to the light organ, and maintaining immune homeostasis. Taken together, these examples demonstrate that antimicrobial peptide expression by animal hosts perform a conserved function of population or community structuring across multiple stages of symbioses.

Galaxin structure and function

Our *in silico* analysis of galaxin sequences in available databases identifies proteins with sequence similarity to EsGal1 in all major groups of the animal kingdom, except the arthropods and vertebrates (Table 3-2). Selection and alignment of a subset of widely divergent representatives showed that certain conserved residues are maintained through evolution (Fig. 3-2B). The conserved residues may serve as a structural scaffold for the protein with the remaining

amino acids diverging to confer alternate functions within an animal or in different species. The wide range of sizes and isoelectric points of galaxin proteins supports the hypothesis of other functions for the various members of the protein family.

Few functional studies of galaxins are available. Although BLAST analysis revealed other family members, our study is only the second outside of the Cnidaria to report a sequence as belonging to the galaxin family of proteins, the first being the identification of a partial sequence in the vent tubeworm *Rifita pachyptila* (Sanchez *et al.*, 2007). Three in-depth studies of galaxins in corals (Phylum Cnidaria) have localized the proteins to the calcium carbonate exoskeleton, and larvae of the coral *Acropora millepora* express galaxins and galaxin-like transcripts in portions of the larva that secrete the exoskeleton during settlement (Reyes-Bermudez *et al.*, 2009). The close association of the galaxins to the coral exoskeleton, their high abundance, as well as the timing of their production, has led researchers to link the proteins with biomineralization of the exoskeleton. However, galaxins were found not to bind calcium, and direct involvement of galaxins with production of the coral exoskeleton has not been demonstrated. Interestingly, galaxin proteins were not found in the exoskeleton of sun corals (*Tubastrea* spp.), which coincidentally lack the photosynthetic partner of most corals, the zooxanthellae (Watanabe *et al.*, 2003). These data do not preclude the involvement of galaxins in exoskeletal formation in some corals, but do suggest alternative functions. The pattern of expression in coral larvae mirrors the symbiont-dependent developmental upregulation and pan-epithelial localization we observed in the juvenile squid, and suggests that coral galaxins may be involved in the first contact between host and microbe, as corals associate with both algal and

bacterial symbionts (Krediet *et al.*, 2013). Although the peptide derived from *Acropora palmata* was not antimicrobial under the conditions of our experiments, the protein in its native conformation, or with the addition or subtraction of additional amino acids on either end, may be active or may serve another function in this species. Alternatively, these data suggest that the ability to modulate bacterial growth through potent antimicrobial activity is not conserved among all galaxin proteins; rather it is a character restricted to particular animals or galaxin types. The various roles of galaxins in other animal species present a fruitful area of future research.

Finally, galaxins may also function as part of a general response to either biotic (e.g., symbiosis) or abiotic (e.g., temperature, heavy metals) stress. In a wide array of symbioses, including the squid-vibrio system, plant-legume associations, and coral-zooxanthellae partnership, various stress responses (e.g., oxidative, nitrosylative) are a part of the normal activity of the symbiotic state. In support of this possibility, transcription is downregulated by copper exposure in coral *Montastrea franksi*, and galaxin SNP variation is correlated with water temperature in *A. millepora* (Schwarz *et al.*, 2012; Lundgren *et al.*, 2013). Since corals also undergo profound biochemical and physiological changes due to their symbionts (Davy *et al.*, 2012), it is possible that galaxin transcription may instead be due to a stressor's effect on algal endosymbionts.

In conclusion, our study proposes a new function for galaxin proteins as antimicrobial agents used by the squid host to select and maintain a specific symbiont, and identifies a new taxonomic group in which galaxin proteins occur in abundance. Future studies will determine whether the biochemical role of galaxins in the squid-vibrio system is a widespread attribute of these proteins across animal taxa. In the greater context of host-microbe interactions, our data

support the growing paradigm that antimicrobial proteins do not serve to simply exclude bacteria from sites on an animal's body. Rather, they are selective forces imposed by hosts on microbial communities to favor the acquisition and maintenance of coevolved symbiotic partnerships.

ACKNOWLEDGEMENTS:

The authors would like to thank S. Mazzone, B. Rader, J. Schwartzman, and E. G. Ruby for assistance with data acquisition, figure development, and experimental design. This work was supported by grants from National Institutes of Health (NIH) R01-RR12294 (to EGR) and R01-AI50661 (to MM-N), and National Science Foundation IOS 0817232 (to MM-N & EGR). EACH-H was supported by NRSA T-32 GM07215.

REFERENCES:

Aeckersberg, F., Lupp, C., Feliciano, B., and Ruby, E.G. (2001) *Vibrio fischeri* outer membrane protein OmpU plays a role in normal symbiotic colonization. *J Bacteriol* **183**: 6590–6597.

Altura, M.A., Heath-Heckman, E.A., Gillette, A., Kremer, N., Krachler, A.M., Brennan, C., *et al.* (2013) The first engagement of partners in the *Euprymna scolopes*-*Vibrio fischeri* symbiosis is a two-step process initiated by a few environmental symbiont cells. *Environ Microbiol*. doi: 10.1111/1462-2920.12179

Blattner, F.R., Plunkett, G., Bloch, C.A., Perna, N.T., Burland, V., Riley, M., *et al.* (1997) The complete genome sequence of *Escherichia coli* K-12. *Science* **277**: 1453.

Boettcher, K.J., and Ruby, E.G. (1990) Depressed light emission by symbiotic *Vibrio fischeri* of the sepiolid squid *Euprymna scolopes*. *J Bacteriol* **172**: 3701–3706.

Bose, J.L., Rosenberg, C.S., and Stabb, E.V. (2008) Effects of *luxCDABEG* induction in *Vibrio fischeri*: enhancement of symbiotic colonization and conditional attenuation of growth in culture. *Arch Microbiol* **190**: 169–183.

Bright, M., and Bulgheresi, S. (2010) A complex journey: transmission of microbial symbionts. *Nat Rev Microbiol* **8**: 218–230.

Bulgarelli, D., Schlaeppi, K., Spaepen, S., Ver Loren van Themaat, E., and Schulze-Lefert, P. (2013) Structure and functions of the bacterial microbiota of plants. *Annu Rev Plant Biol* **64**: 807–838.

Bulgheresi, S., Gruber-Vodicka, H.R., Heindl, N.R., Dirks, U., Kostadinova, M., Breiteneder, H., and Ott, J.A. (2011) Sequence variability of the pattern recognition receptor Mermaid mediates specificity of marine nematode symbioses. *ISME J* **5**: 986–998.

Bustin, S.A., Benes, V., Garson, J.A., Hellemans, J., Huggett, J., Kubista, M., *et al.* (2009) The MIQE guidelines: minimum information for publication of quantitative real-time PCR experiments. *Clin Chem* **55**: 611–622.

Cash, H.L., Whitham, C.V., Behrendt, C.L., and Hooper, L.V. (2006) Symbiotic bacteria direct expression of an intestinal bactericidal lectin. *Science* **313**: 1126–1130.

Chun, C.K., Scheetz, T.E., Bonaldo Mde, F., Brown, B., Clemens, A., Crookes-Goodson, W.J., *et al.* (2006) An annotated cDNA library of juvenile *Euprymna scolopes* with and without colonization by the symbiont *Vibrio fischeri*. *BMC genomics* **7**: 154.

Chun, C.K., Troll, J.V., Koroleva, I., Brown, B., Manzella, L., Snir, E., *et al.* (2008) Effects of colonization, luminescence, and autoinducer on host transcription during development of the squid-vibrio association. *Proc Natl Acad Sci U.S.A.* **105**: 11323–11328.

Collins, A.J., LaBarre, B.A., Won, B.S., Shah, M.V., Heng, S., Choudhury, M.H., *et al.* (2012) Diversity and partitioning of bacterial populations within the accessory nidamental gland of the squid *Euprymna scolopes*. *Appl Environ Microbiol* **78**: 4200–4208.

Davidson, S.K., Koropatnick, T.A., Kossmehl, R., Sycuro, L., and McFall-Ngai, M.J. (2004) NO means "yes" in the squid-vibrio symbiosis: nitric oxide (NO) during the initial stages of a beneficial association. *Cell Microbiol* **6**: 1139–1151.

Davy, S.K., Allemand, D., and Weis, V.M. (2012) Cell biology of cnidarian-dinoflagellate symbiosis. *Microbiol Mol Biol Rev* **76**: 229–261.

de Oliveira, L.S., Gregoracci, G.B., Silva, G.G., Salgado, L.T., Filho, G.A., Alves-Ferreira, M., *et al.* (2012) Transcriptomic analysis of the red seaweed *Laurencia dendroidea* (Florideophyceae, Rhodophyta) and its microbiome. *BMC genomics* **13**: 487.

Doino, J.A., and McFall-Ngai, M.J. (1995) A transient exposure to symbiosis-competent bacteria induces light organ morphogenesis in the host squid. *Biol Bull* **189**: 347–355.

Dunlap, P.V. (1985) Osmotic control of luminescence and growth in *Photobacterium leiognathi* from ponyfish light organs. *Arch Microbiol* **141**: 44–50.

Dunn, A.K., Millikan, D.S., Adin, D.M., Bose, J.L., and Stabb, E.V. (2006) New rfp- and pES213-derived tools for analyzing symbiotic *Vibrio fischeri* reveal patterns of infection and lux expression in situ. *Appl Environ Microbiol* **72**: 802–810.

Edgar, R.C. (2004) MUSCLE: a multiple sequence alignment method with reduced time and space complexity. *BMC Bioinformatics* **5**: 113.

Fedders, H., and Leippe, M. (2008) A reverse search for antimicrobial peptides in *Ciona intestinalis*: identification of a gene family expressed in hemocytes and evaluation of activity. *Dev Comp Immunol* **32**: 286–298.

Foster, J.S., Apicella, M.A., and McFall-Ngai, M.J. (2000) *Vibrio fischeri* lipopolysaccharide induces developmental apoptosis, but not complete morphogenesis, of the *Euprymna scolopes* symbiotic light organ. *Dev Biol* **226**: 242–254.

Franzenburg, S., Walter, J., Kunzel, S., Wang, J., Baines, J.F., Bosch, T.C., and Fraune, S. (2013) Distinct antimicrobial peptide expression determines host species-specific bacterial associations. *Proc Natl Acad Sci U.S.A*. **110**: E3730-3738.

Fraune, S., Augustin, R., Anton-Erxleben, F., Wittlieb, J., Gelhaus, C., Klimovich, V.B., *et al.* (2010) In an early branching metazoan, bacterial colonization of the embryo is controlled by maternal antimicrobial peptides. *Proc Natl Acad Sci U.S.A* **107**: 18067–18072.

Fuhrman, J.A. (2009) Microbial community structure and its functional implications. *Nature* **459**: 193–199.

Fukuda, I., Ooki, S., Fujita, T., Murayama, E., Nagasawa, H., Isa, Y., and Watanabe, T. (2003)

Molecular cloning of a cDNA encoding a soluble protein in the coral exoskeleton. *Biochem Biophys Res Commun* **304**: 11–17.

Gallo, R.L., and Hooper, L.V. (2012) Epithelial antimicrobial defence of the skin and intestine. *Nat Rev Immunol* **12**: 503–516.

Gontang, E.A., Fenical, W., and Jensen, P.R. (2007) Phylogenetic diversity of gram-positive bacteria cultured from marine sediments. *Appl Environ Microbiol* **73**: 3272–3282.

Graf, J., and Ruby, E.G. (1998) Host-derived amino acids support the proliferation of symbiotic bacteria. *Proc Natl Acad Sci U.S.A.* **95**: 1818–1822.

Heath-Heckman, E.A.C., Peyer, S.M., Whistler, C.A., Apicella, M.A., Goldman, W.E., and McFall-Ngai, M.J. (2013) Bacterial bioluminescence regulates expression of a host cryptochrome gene in the Squid-Vibrio symbiosis. *MBio* **4**: e00167–13–e00167–13.

Koropatnick, T.A., Engle, J.T., Apicella, M.A., Stabb, E.V., Goldman, W.E., and McFall-Ngai, M.J. (2004) Microbial factor-mediated development in a host-bacterial mutualism. *Science* **306**: 1186–1188.

Krediet, C.J., Ritchie, K.B., Paul, V.J., and Teplitski, M. (2013) Coral-associated micro-organisms and their roles in promoting coral health and thwarting diseases. *Proc Biol Sci* **280**: 20122328–20122328.

Kremer, N., Philipp, E.E., Carpentier, M.C., Brennan, C.A., Kraemer, L., Altura, M.A., *et al.* (2013) Initial Symbiont Contact Orchestrates Host-Organ-wide Transcriptional Changes that Prime Tissue Colonization. *Cell Host Microbe* **14**: 183–194.

Lamarcq, L.H., and McFall-Ngai, M.J. (1998) Induction of a gradual, reversible morphogenesis of its host's epithelial brush border by *Vibrio fischeri*. *Infect Immun* **66**: 777–785.

Login, F.H., Balmand, S., Vallier, A., Vincent-Monegat, C., Vigneron, A., Weiss-Gayet, M., *et al.* (2011) Antimicrobial peptides keep insect endosymbionts under control. *Science* **334**: 362–365.

Lundgren, P., Vera, J.C., Peplow, L., Manel, S., and van Oppen, M.J. (2013) Genotype -- environment correlations in corals from the Great Barrier Reef. *BMC Genet* **14**: 9.

McFall-Ngai, M., Heath-Heckman, E.A., Gillette, A.A., Peyer, S.M., and Harvie, E.A. (2012) The secret languages of coevolved symbioses: insights from the *Euprymna scolopes-Vibrio fischeri* symbiosis. *Semin Immunol* **24**: 3–8.

McFall-Ngai, M., Nyholm, S.V., and Castillo, M.G. (2010) The role of the immune system in the initiation and persistence of the *Euprymna scolopes--Vibrio fischeri* symbiosis. *Semin Immunol* **22**: 48–53.

Needham, D.M., Chow, C.E., Cram, J.A., Sachdeva, R., Parada, A., and Fuhrman, J.A. (2013) Short-term observations of marine bacterial and viral communities: patterns, connections and

resilience. *ISME J* **7**: 1274–1285.

Nyholm, S.V., and McFall-Ngai, M.J. (1998) Sampling the light-organ microenvironment of *Euprymna scolopes*: description of a population of host cells in association with the bacterial symbiont *Vibrio fischeri. Biol Bull* **195**: 89–97.

Nyholm, S.V., and McFall-Ngai, M.J. (2003) Dominance of *Vibrio fischeri* in secreted mucus outside the light organ of *Euprymna scolopes*: the first site of symbiont specificity. *Appl Environ Microbiol* **69**: 3932–3937.

Nyholm, S.V., and McFall-Ngai, M.J. (2004) The winnowing: establishing the squid-vibrio symbiosis. *Nat Rev Microbiol* **2**: 632–642.

Nyholm, S.V., Deplancke, B., Gaskins, H.R., Apicella, M.A., and McFall-Ngai, M.J. (2002) Roles of *Vibrio fischeri* and nonsymbiotic bacteria in the dynamics of mucus secretion during symbiont colonization of the *Euprymna scolopes* light organ. *Appl Environ Microbiol* **68**: 5113–5122.

Nyholm, S.V., Stabb, E.V., Ruby, E.G., and McFall-Ngai, M.J. (2000) Establishment of an animal-bacterial association: recruiting symbiotic vibrios from the environment. *Proc Natl Acad Sci U.S.A* **97**: 10231–10235.

Pfaffl, M.W. (2001) A new mathematical model for relative quantification in real-time RT-PCR. *Nucleic Acids Res* **29**: e45.

Redmond, J.W., Batley, M., Djordjevic, M.A., Innes, R.W., Kuempel, P.L., and Rolfe, B.G. (1986) Flavones Induce Expression of Nodulation Genes in *Rhizobium*. *Nature* **323**: 632–635.

Reyes-Bermudez, A., Lin, Z., Hayward, D.C., Miller, D.J., and Ball, E.E. (2009) Differential expression of three galaxin-related genes during settlement and metamorphosis in the scleractinian coral *Acropora millepora*. *BMC Evol Biol* **9**: 178.

Ruby, E.G., and Asato, L.M. (1993) Growth and flagellation of *Vibrio fischeri* during initiation of the sepiolid squid light organ symbiosis. *Arch Microbiol* **159**: 160–167.

Salzman, N.H., Hung, K., Haribhai, D., Chu, H., Karlsson-Sjoberg, J., Amir, E., *et al.* (2010) Enteric defensins are essential regulators of intestinal microbial ecology. *Nat Immunol* **11**: 76–83.

Sanchez, S., Hourdez, S., and Lallier, F.H. (2007) Identification of proteins involved in the functioning of *Riftia pachyptila* symbiosis by Subtractive Suppression Hybridization. *BMC genomics* **8**: 337.

Schwarz, J.A., Mitchelmore, C.L., Jones, R., O'Dea, A., and Seymour, S. (2012) Exposure to copper induces oxidative and stress responses and DNA damage in the coral *Montastraea franksi*. *Comp Biochem Physiol C Toxicol Pharmacol* **157**: 272–279.

Shnit-Orland, M., Sivan, A., and Kushmaro, A. (2012) Antibacterial activity of *Pseudoalteromonas* in the coral holobiont. *Microb Ecol* **64**: 851–859.

Stabb, P.E.V., and Visick, D.K.L. (2013) *Vibrio fisheri:* Squid Symbiosis. *The Prokaryotes* 497–532.

Troll, J.V., Adin, D.M., Wier, A.M., Paquette, N., Silverman, N., Goldman, W.E., *et al.* (2009) Peptidoglycan induces loss of a nuclear peptidoglycan recognition protein during host tissue development in a beneficial animal-bacterial symbiosis. *Cell Microbiol* **11**: 1114–1127.

Troll, J.V., Bent, E.H., Pacquette, N., Wier, A.M., Goldman, W.E., Silverman, N., and McFall-Ngai, M.J. (2010) Taming the symbiont for coexistence: a host PGRP neutralizes a bacterial symbiont toxin. *Environ Microbiol* **12**: 2190–2203.

Vaishnava, S., Yamamoto, M., Severson, K.M., Ruhn, K.A., Yu, X., Koren, O., *et al.* (2011) The antibacterial lectin RegIIIgamma promotes the spatial segregation of microbiota and host in the intestine. *Science* **334**: 255–258.

Visick, K.G., and Ruby, E.G. (1996) Construction and symbiotic competence of a *luxA*-deletion mutant of *Vibrio fischeri*. *Gene* **175**: 89–94.

Wang, Y., Dunn, A.K., Wilneff, J., McFall-Ngai, M.J., Spiro, S., and Ruby, E.G. (2010) *Vibrio fischeri* flavohaemoglobin protects against nitric oxide during initiation of the squid-Vibrio symbiosis. *Mol Microbiol* **78**: 903–915.

Watanabe, T., Fukuda, I., China, K., and Isa, Y. (2003) Molecular analyses of protein components of the organic matrix in the exoskeleton of two scleractinian coral species. *Comp Biochem Physiol B Biochem Mol Biol* **136**: 767–774.

Wier, A.M., Nyholm, S.V., Mandel, M.J., Massengo-Tiasse, R.P., Schaefer, A.L., Koroleva, I., *et al.* (2010) Transcriptional patterns in both host and bacterium underlie a daily rhythm of anatomical and metabolic change in a beneficial symbiosis. *Proc Natl Acad Sci U.S.A.* **107**: 2259–2264.

Wollenberg, M.S., and Ruby, E.G. (2012) Phylogeny and fitness of *Vibrio fischeri* from the light organs of *Euprymna scolopes* in two Oahu, Hawaii populations. *ISME J* **6**: 352–362.

Chapter 4

Chitin as a Component of the Invertebrate Immune System

PREFACE:

Published in *Zoology* in September 2011 as:

Heath-Heckman, E.A.C. and McFall-Ngai, M.J. “Chitin as a component of the invertebrate immune system”

EACH and MJM formulated ideas and planned experiments. EACH performed experiments. EACH and MJM wrote and edited the chapter.

ABSTRACT:

The light-organ symbiosis of *Euprymna scolopes*, the Hawaiian bobtail squid, is a useful model for the study of animal-microbe interactions. Recent analyses have demonstrated that chitin breakdown products play a role in communication between *E. scolopes* and its bacterial symbiont *Vibrio fischeri*. In this study, we sought to determine the source of chitin in the symbiotic organ. We used a commercially available chitin-binding protein (CBP) conjugated to fluorescein to label the polymeric chitin in host tissues. Confocal microscopy revealed that the only cells in contact with the symbionts that labeled with the probe were the macrophage-like hemocytes, which traffic into the light-organ crypts where the bacteria reside. Labeling of extracted hemocytes by CBP was markedly decreased following treatment with purified chitinase, providing further evidence that the labeled molecule is polymeric chitin. Further, CBP-positive areas co-localized with both a halide peroxidase antibody and Lysotracker, a lysosomal marker, suggesting that the chitin-like biomolecule occurs in the lysosome or acidic vacuoles. Reverse transcriptase PCR of hemocytes revealed mRNA coding for a chitin synthase, suggesting that the hemocytes synthesize chitin *de novo*. Finally, upon surveying blood cells from other invertebrate species, we observed CBP-positive regions in all granular blood cells examined, suggesting that this feature is a shared character among the invertebrates; the vertebrate blood cells that we sampled did not label with CBP. Although the function of the chitin-like material remains undetermined, its presence and subcellular location in invertebrate hemocytes suggests a conserved role for this polysaccharide in the immune system of diverse animals.

INTRODUCTION:

Chitin, a polymer of β-linked n-acetylglucosamine molecules, is an abundant structural and nutritive polysaccharide. Its synthesis and use is a widespread trait among the invertebrates, from the sponges (Ehrlich *et al.*, 2007) through to the invertebrate chordates (Sannasi and Hermann, 1970). As a structural element, chitin is a principal component of invertebrate endo- and exoskeletons, such as the insect cuticle, and of the pens, beaks, and suckers of squid (Dilly and Nixon, 1976; Hunt and Sherief, 1990). Chitin-like substances have also been localized to hemocytes in three ecdysozoans (Baĭkova *et al.*, 1993; Martin *et al.*, 2003), although the precise biochemical identities and functions in the hemocytes are not yet known. In addition, the chitin produced by animals also serves as an important nutrient source for chitinolytic bacteria (Keyhani and Roseman, 1999). One such bacterium is *Vibrio fischeri*, a luminescent marine organism, specific strains of which form a mutualistic association with sepiolid squid species, including the Hawaiian squid *Euprymna scolopes*.

In the *E. scolopes*-*V. fischeri* light organ mutualism, the symbionts reside throughout the host's life in deep invaginations, or crypts, that occur within a bi-lobed organ in the center of the body cavity (for review, see (Nyholm and McFall-Ngai, 2004)). As extracellular partners, the symbionts communicate with the host across the apical surfaces of the crypt epithelial cells. The serum and blood cells, or hemocytes, of the highly vascularized light organ associate with both the host tissues and the symbiont population. The symbionts interact both directly and indirectly with the hemocytes, i.e., these cells not only move through the blood vessels of the organ but also exhibit 'diapedesis', a behavior in which they leave the vessels and move between the epithelial cells into the bacteria-filled crypts (Nyholm and McFall-Ngai, 1998).

A recent study of the squid-vibrio symbiosis suggested that the host provides chitin as a nutrient to the symbionts (Wier *et al.*, 2010). In this study, the transcriptomes of both the host and the symbiont population were analyzed at four times over the day-night cycle. These data demonstrated that the host upregulates the expression of one chitinase gene and one chitin synthase gene just before dawn. Simultaneously, the resident bacterial symbionts increase the transcription of genes that have been reported to be important for chitin recognition and breakdown in *Vibrio cholerae* (Meibom *et al.*, 2004; Li *et al.*, 2007). In addition, *V. fischeri* is genetically and physiologically capable of chitin breakdown and utilization (Ruby *et al.*, 2005; Sugita and Ito, 2006). The results of this transcriptional study provide evidence that a daily rhythm exists in the presentation of nutritive chitin by the squid host to symbiotic *V. fischeri*.

To determine whether chitin is provided to the symbiont by the host and to identify host cells responsible for this provision, we sought to define the site or sites of chitin production in the host light organ tissue. Our analyses provide evidence that all mature host hemocytes, both in the light organ and throughout the body, synthesize chitin-like material that localizes to acidic compartments of these cells. In addition, we analyzed the blood cells of various animal taxa to determine whether the presence of chitin in hemocytes is specific to *E. scolopes* or more widespread among animals.

MATERIALS AND METHODS:

General methods

Adult *E. scolopes* were collected from the wild in Oahu, Hawaii and then maintained in the lab as previously described (Montgomery and McFall-Ngai, 1993). Juvenile squid used in experiments were collected within 15 min of hatching and then washed three times in filter-sterilized Instant Ocean (FSIO, Aquarium Systems, Mentor, OH) to remove any external bacteria. The animals were then either colonized with *V. fischeri* by incubation with 5,000 colony-forming units per mL of FSIO overnight or left aposymbiotic by incubating with *V. fischeri*-free FSIO. Colonization states were confirmed by measuring luminescence levels of the animals in a TD-20/20 luminometer (Turner Designs, Sunnyvale, CA) (Ruby and Asato, 1993). Animal sources for taxonomic study : *A. forbesi*, *Arbacia* sp., C. *fornicata*, *M. mercenaria*, *M. edulis*, *N. viridans* specimens were purchased from Marine Biological Laboratories (Woods Hole, MA), and *S. pharaonis* specimens were purchased from the National Resource Center for Cephalopods (Galveston, TX). All confocal experiments were performed on a Zeiss LSM 510 confocal microscope, and all chemicals, except where specifically noted, were purchased from Sigma Aldrich (St. Louis, MO).

RT-PCR analysis

To determine the localization of chitin synthase transcript in *E. scolpes*, total RNA was isolated from extracted adult *E. scolopes* tissues (hemocytes, white body, hindgut, and eye). Single-stranded cDNA was then synthesized from the purified RNA using reverse transcriptase (Clontech, Mountain View, CA) and random primers. Using 500 ng of cDNA as a template for

each PCR reaction, single gene products were analyzed with specific primers subsequent to cDNA synthesis. All reactions were performed with a no-reverse-transcriptase control to confirm the lack of genomic DNA contamination in the reactions. Two chitin synthases were identified in a 3' expressed sequence tag database (Chun *et al.*, 2006), called chitin synthase 1 (similar to chitin synthase from nematode *Brugia malayi* by blast analysis with an E-value of 1e-9) and chitin synthase 2 (similar to chitin synthase from oyster *Pinctada fucata* by blast analysis with an E-value of 8e-36). Specific primers to the above transcripts used in this study were: CS1F: 5'-TTGGCGTGTTTGCACTCTCGGCCCT-3', CS1R: 5'-GACGTGCGTTCATTGCGTTGTTGA-3' to amplify chitin synthase 1, and CS2F: 5'-TGAATCTGCTGTGGAGTGTGGCTA-3', CS2R: 5'- AATGCGCCTCTTCTGTTCAACGTC-3' to amplify chitin synthase 2. As a loading control, we used the primers 40SF: 5'-AATCTCGGCGTCCTTGAGAA-3', 40SR: 5'- GCATCAATTGCACGACGAGT-3' to amplify RNA encoding the 40S ribosomal subunit.

Localization of putative chitin in *E. scolopes* tissues

To localize chitin-like biomolecules in tissues, whole juvenile *E. scolopes* and extracted light organs were prepared for immunocytochemistry as previously described (Kimbell and McFall-Ngai, 2004; Davidson *et al.*, 2004). Briefly, whole juvenile squid were anesthetized with 2% ethanol in filter-sterilized Instant Ocean and then fixed in 4% paraformaldehye in marine phosphate-buffered saline (mPBS – 50 mM sodium phosphate buffer with 0.45 M NaCl, pH 7.4) for 18 h at 4°C. The squid were then washed in mPBS, dissected, and permeabolized in permeabolization buffer (mPBS containing 1% Triton-X) overnight. Samples were then exposed to binding proteins at relevant concentrations: 167 nM for the fluorescein isothiocyanate

conjugated chitin-binding protein (FITC-CBP; New England Biolabs, Ipswich, MA), 0.25 μg/mL rhodamine phalloidin, 20 μg/mL rhodamine-conjugated succinylated wheat-germ agglutinin (Vector Labs, Burlingame, CA), all in permeabolization buffer, for 1-3 days. To visualize nuclei, samples were stained with TOTO-3 (Invitrogen, Carlsbad, CA), a nucleus-specific dye at a concentration of 1 μM. Squid tissues were mounted individually on slides in VectaShield (Vector Labs, Burlingame, CA), a mounting medium that reduces sample autofluorescence and bleaching. The samples were then analyzed by confocal microscopy to determine presence or absence of labeling by FITC-CBP, which only recognizes polymeric chitin (Hardt and Laine, 2004).

To characterize the CBP-labeling of hemocytes, blood cells were extracted from both adult and juvenile samples. Hemocytes were extracted from adult *E. scolopes* through the cephalic artery using a 1-ml syringe fitted with a 28-gauge needle. To release hemocytes from juvenile host tissues, ten *E. scolopes* juveniles were anesthetized with 2% ethanol in FSIO and then the entire cohort was homogenized manually in 1 mL Squid Ringer's solution (50 mM $MgCl_2$, 10 mM $CaCl_2$, 10 mM KCl, 530 mM NaCl, 10 mM HEPES). The homogenate was applied to coverslips in 12-well tissue culture plates and the hemocytes were allowed to adhere for 30 min. The coverslips were then washed three times for 5 min with Squid Ringer's solution to remove other tissues. In experiments designed to determine whether CBP labeling localized to acidic compartments, the hemocytes were exposed to a 1:1000 dilution of Lysotracker Red (Invitrogen, Carlsbad, CA) in Squid Ringer's solution to label the lysosomes, and then allowed to incubate in the stain for 15 min and rinsed with Squid Ringer's solution twice for 5 min. The cells were then fixed for 30 min in 4% paraformaldehyde in mPBS. Afterwards, samples were washed three times for 10 min in mPBS and exposed to permeabilization buffer for 1 h.

Following permeabilization, samples were washed three times for 10 min with permeabilization buffer and exposed to FITC-CBP for 3 h at room temperature. After another set of three 10-min washes, rhodamine phalloidin at a concentration of 20 μg/mL was added to the samples overnight at 4°C. After a final set of three 10-min washes with buffer, the coverslips were mounted onto glass slides and processed as for whole tissue mounts.

Chitinase treatment

To determine whether CBP-labeling of the hemocytes was affected by chitinase treatment, hemocytes were treated with a purified chitinase to disrupt the polymeric structure of any chitin that might have been present. Fixation and permeabolization were performed as described previously. Fixed hemocytes were exposed to three different conditions: (1) phosphate buffered saline (PBS; 50 mM sodium phosphate, 100 mM sodium chloride, pH 7.4) containing 1 mM sodium ethylenediaminetetraacetic acid, pH 6.0, and 40 units of purified *Brugia malayi* chitinase (New England BioLabs, Ipswich, MA); (2) buffer without chitinase; or, (3) as a control for the effects of the treatment conditions, 40 units of chitinase in the same buffer heated to 75°C for 20 min (heat-inactivated chitinase). Extracted hemocytes were exposed to each of the three treatments for 24 h at 37°C. The treated hemocytes were washed three times for 10 min with the above buffer and then exposed to CBP and rhodamine phalloidin as described above. The hemocytes were then visualized by confocal microscopy and the level of fluorescence in each cell was measured by Zeiss analysis software.

Assessment of possible protein association of CBP-positive biomolecules

Previous reports of the presence of chitin in invertebrate blood indicated that chitin can occur as a "chitinoprotein", i.e., with the chitin bound to a protein molecule (Kramerov *et al.*, 1990). Thus, we sought to determine whether the CBP-positive material in the *E. scolopes* hemocytes was protein associated. The chitin-like substance in *E. scolopes* hemocytes is bound by FITC-CBP (this study), so we used the New England BioLabs (Ipswich, MA) SNAP-Capture protein purification system to immobilize purified CBP bound to a SNAP tag as bait for the chitin-like substance contained in the squid hemocytes. To bind the SNAP magnetic beads to the purified CBP containing a SNAP-tag, the beads were first resuspended by gentle vortexing and then equilibrated in immobilization buffer (50 mM Tris-HCl pH 7.5, 100 mM NaCl, 1mM DTT and 0.1% Tween 20). Then, 100 μL of a solution of 1 mg/mL SNAP tag-CBP in immobilization buffer was added to the equilibrated SNAP-capture beads in a 1.5 mL Eppendorf tube and incubated with mixing overnight at 4º C. The beads were then washed four times by adding 500 μL immobilization buffer and vortexing for 1 min, then placed in a magnetic manifold for 10 sec and the supernatant was removed. Once the SNAP-CBP was bound to the magnetic SNAP-capture beads, 500 μL of a solution of 1 mg/mL *E. scolopes* hemocyte lysate in immobilization buffer containing an EDTA-free protease inhibitor cocktail was added to the washed beads and incubated for 3 h at room temperature. The beads were then washed an additional five times with 1 mL of immobilization buffer as described previously. To remove the bound proteins from the beads, 50 μL of SDS-PAGE loading buffer (Tris-SDS-BME) was added to the beads and heated at 95 degrees C for 5 min. All fractions were analyzed on SDS-PAGE gels.

Because we found no evidence for the binding of CBP-positive material to protein, we sought to determine the fraction of cell homogenate that contains the putative chitin biomolecules. Two whole gills from adult *E. scolopes* were homogenized in 1 mL of PBS

containing protease inhibitors (Sigma Aldrich protease inhibitor cocktail III). The homogenate was then centrifuged at 10,000 x g for 20 min at 4°C to separate the aqueous soluble (supernatant) and insoluble fractions (pellet). The pellet was washed twice with PBS, by resuspension in buffer followed by centrifugation for each wash, to remove residual soluble protein. To extract a subset of the membrane proteins, the pellet was resuspended in PBS containing 2% SDS and centrifuged at 10,000 x g for 20 min at room temperature. The supernatant was removed, and then the resulting pellet was washed twice, as described above, in PBS containing 2% SDS to remove residual membrane proteins soluble in 2% SDS. To solubilize the remainder of the integral membrane proteins and other SDS-soluble proteins, the pellet was resuspended in PBS containing 5% SDS and centrifuged as described above. The supernatant was removed from the sample, and the resulting pellet was washed twice with 5% SDS in PBS to remove any residual membrane-bound proteins. To bring proteins into solution that were insoluble in SDS, the remaining pellet was homogenized in 8 M urea, and then centrifuged as above. The supernatant was then removed and the resulting pellet was retained for subsequent analysis.

To visualize the proteins and determine which fractions contained chitin, 5 μL of each fraction was spotted onto Whatman-1 filter paper in duplicate and allowed to dry and then incubated in ProtoBlue Safe coomassie blue stain (National Diagnostics, Atlanta, GA) for 15 min and destained in deionized water for 30 min and allowed to dry. On a separate piece of filter paper, the same fractions were spotted and allowed to dry, and then the paper was incubated in 0.01% calcofluor white in water for 15 min and then visualized under UV light. Calcofluor white is a dye that binds with polymeric chitin and cellulose.

Hemocyte preparations for taxonomic survey

Hemolymph containing hemocyte populations was drawn from individuals of other aquatic animals using a 1- mL syringe fitted with a 28-gauge needle as follows: *S. pharaonis*, from the cephalic artery; *Mytilus edulis* and *Mercenaria mercenaria*, from the main hemolymph sinus of the foot; *Crepidula fornicata*, from the hemocoel of the foot; *Eisenia foetida* and *Nereis viridans*, from the dorsal blood vessel; *Arbacia* sp., through the periosomal membrane; *Asterias forbesi*, from the tip of an arm; and *Ciona intestinalis,* from the heart and associated tissues. After extraction, the hemolymph was spotted onto glass coverslips in tissue culture plate wells containing 500 µL of Squid Ringer's solution for 10 min to allow the hemocytes to adhere to the coverslips. The coverslips were then washed twice for 5 min in Squid Ringer's solution at room temperature, except for *E. foetida* samples, which were washed in PBS diluted 1:2 in water. The cells were then fixed on the coverslips by incubation for 30 min at room temperature in mPBS containing 4% paraformaldehyde, except for *E. foetida* hemocytes, which were fixed in 0.5% PBS containing 4% paraformaldehyde. The fixed cells were then washed three times for 10 min in mPBS and incubated in permabolization buffer for 1 h at room temperature. The buffer was then removed and replaced with permeabolization buffer containing 167 nM FITC-CBP, and then incubated with the samples for 3 h at room temperature. The samples were then washed with permeabolization buffer three times for 5 min at room temperature and then incubated with rhodamine phalloidin in permeabolization buffer for 1 h at room temperature or overnight at 4ºC. The coverslips were then washed three times for 5 min in mPBS and then mounted onto glass slides containing VectaShield and visualized by confocal microscopy.

Additional animals used in the taxonomic survey were sampled as follows:

Biomphalaria glabrata: Hemolymph was collected as described previously (SMINIA and BARENDSEN, 1980), then hemocytes were allowed to adhere to a coverslip and processed as described for *E. foetida*.

Atta colombica and *Drosophila melanogaster*: Whole animals (three *A. colombica* or 10 *D. melanogaster*) were homogenized as a single cohort manually in 500 μL 0.5x PBS. The homogenate was then applied to coverslips and the hemocytes were allowed to adhere for 30 min. The samples were then processed as described above for *E. foetida*.

Danio rerio: 48-h juvenile transgenic animals carrying a GFP-tagged myeloperoxidase gene (*GFP:MPO)*, which allows for visualization of neutrophils, were anesthetized in 2% tricaine methanesulfonate and then fixed in 4% paraformaldehyde in 0.5% PBS and processed as whole *E. scolopes* specimens, except that staining was performed with TRITC-labeled CBP instead of FITC-labeled CBP.

Mus musculus: A whole blood smear was fixed to a microscope slide with methanol and then permeabolized and stained as described above for *E. foetida*; in addition, the blood sample was stained with 1 μM TOTO-3 in PBS to identify neutrophils. The slides were then analyzed by confocal microscopy for CBP staining.

RESULTS:

Localization of chitin to *E. scolopes* hemocytes

In juvenile *E. scolopes* (Fig. 4-1A), the suckers and the surface of the beak, structures that are known to contain chitin (Dilly and Nixon, 1976) labeled strongly with CBP (Fig. 4-1B). In addition, we observed strong staining in cells inside the body of the light organ, including within appendages of the juvenile-specific ciliated surface (Fig. 4-1C). These appendages, which comprise a ciliated epithelium overlying a blood sinus, have a population of hemocytes within the sinus (Koropatnick *et al.*, 2007). The CBP staining appeared to localize to the hemocytes. To confirm that *E. scolopes* hemocytes label with the CBP, we extracted hemocytes, which can be identified by their u-shaped nuclei and adherence to coverslips (Nyholm *et al.*, 2009), from both juvenile (Fig. 4-1D) and adult (Fig. 4-1E) animals and incubated them with CBP. The probe bound to vesicle-like areas in all hemocytes that we stained and visualized, ($n > 50$ for each condition) suggesting that circulating hemocytes contain a molecule recognized by CBP.

Specificity of the chitin-binding probe

Chitin-binding probes, such as the one used in this study, are widely known to have a high affinity for chains of more than six n-acetyl glucosamine (GlcNAc) residues, generally referred to as polymeric chitin (Hardt and Laine, 2004). To confirm that the substance being stained by the probe is polymeric chitin and not shorter GlcNAc residues, which may theoretically bind the probe in the absence of larger chitin oligomers, we employed two approaches: 1) characterization of the specificity of CBP binding; and 2)

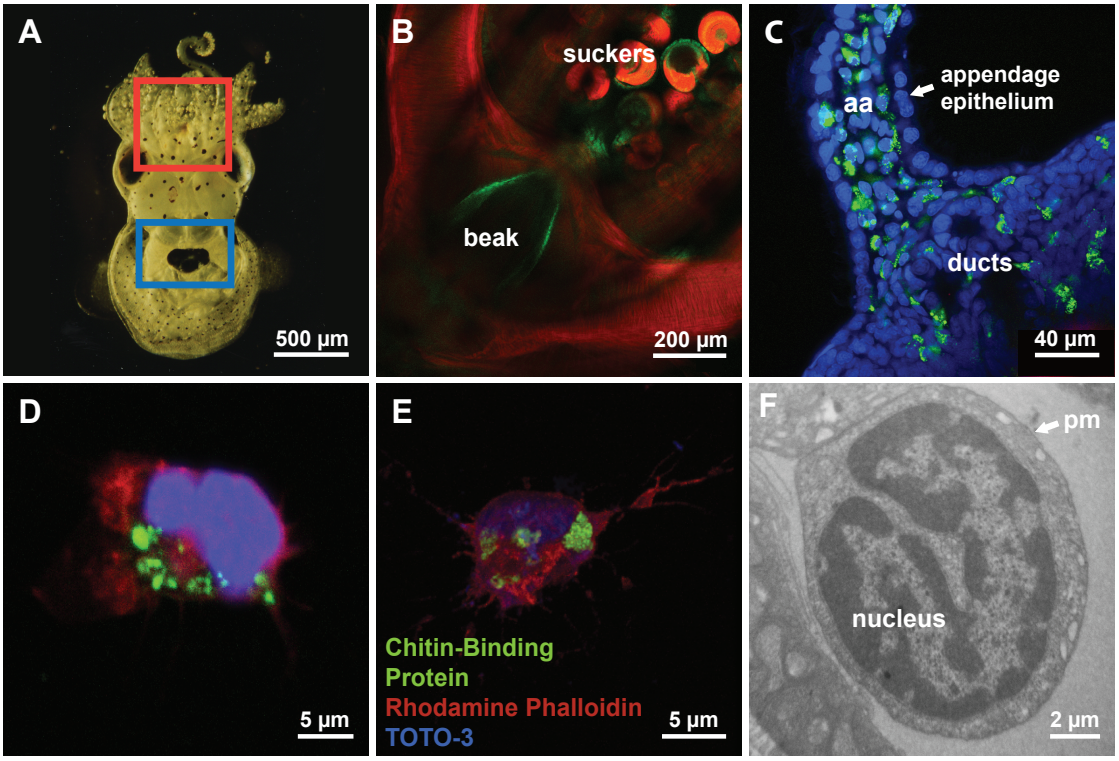

Fig. 4-1. Localization of chitin in the *E. scolopes* light organ: (A) Ventral surface of a juvenile *E. scolopes* resting on the substrate. Boxes represent the position of the buccal area (red) and light organ (blue). (B) Laser-scanning confocal micrograph of the buccal mass (red box in (A)), containing the beak and adjacent suckers, which show chitin-positive regions (green). (C) Confocal micrograph of a portion of one lobe of a juvenile light organ. Chitin-positive labeling (green) occurs in regions near the ducts, as well as in cells in the blood sinus of the anterior appendage (aa). CBP labeling is undetectable in the appendage epithelium that surrounds the blood sinus. (D) Confocal image of a single hemocyte extracted from a juvenile animal. Chitin labeling (green) is localized to intracellular granules surrounding the nucleus (blue). (E) Single confocal image of a three-dimensional reconstruction of a hemocyte from an adult *E. scolopes*. Green: FITC-Chitin-Binding Protein (CBP; chitin-positive areas); red: Phalloidin (filamentous actin); blue: TOTO-3 (nuclei).

determination of the susceptibility of the CBP-positive material to chitinase degradation. For approach (1), we stained whole juvenile animals with both the CBP and succinylated wheat germ agglutinin (sWGA), a lectin that specifically binds GlcNac residues. If CBP stains polymeric chitin to the exclusion of shorter GlcNac oligomers, we would expect that the CBP would only stain a subset of the areas that sWGA binds. Upon staining of the *E. scolopes* hemocytes in the gills, only a subset of the areas stained (Fig. 4-2A), suggesting that the CBP only stains particular types of GlcNac residues, most likely those containing larger numbers of GlcNac groups.

To determine whether the substance being stained by the probe has properties consistent with polymeric chitin, we applied purified chitinase to extracted hemocytes that had been permeabolized and measured the amount of probe binding in comparison with buffer or heat-killed chitinase controls. Active chitinase significantly reduced the fluorescence of CBP-exposed hemocytes (Fig. 4-2B). In addition, the chitinase treatment did not *increase* the amount of CBP staining providing further evidence that CBP does not stain breakdown products of chitin that were produced by the purified chitinase. Taken together, these data suggest that chitinase breaks down polymeric chitin within the hemocytes.

Expression of chitin synthase mRNA in *E. scolopes* hemocytes

The 3' EST library (Chun *et al.*, 2006) of the *E. scolopes* light organ contains two putative chitin synthases identified by sequence similarity to other known chitin synthase transcripts, which we have named EsCS1 and EsCS2. To determine whether *E. scolopes* hemocytes expressed either chitin synthase, we performed semi-quantitative reverse

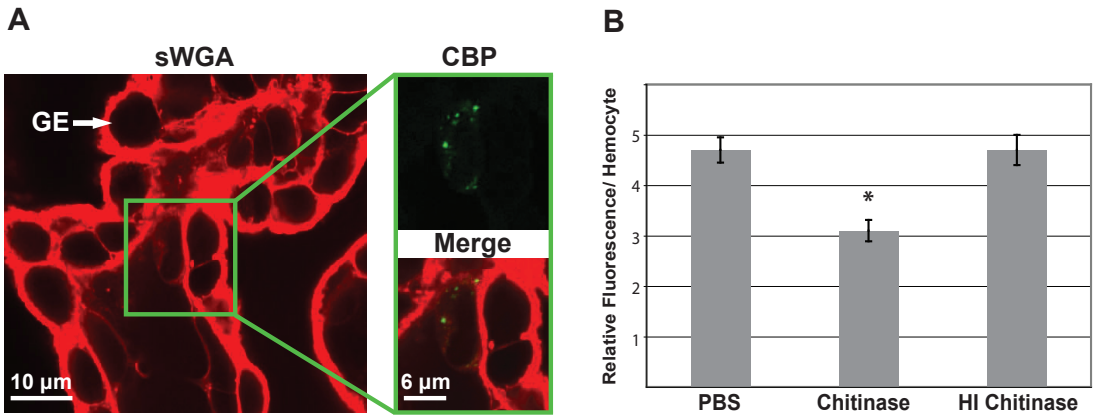

Fig. 4-2. Specificity of Chitin-Binding Protein (CBP) labeling: (A) Confocal micrograph of a juvenile *E. scolopes* gill labeled with succinylated wheat germ agglutinin (sWGA, red) and FITC-CBP (green). A single hemocyte within the gill tissue is shown in the CBP and merged images (right panels). GE = gill epithelium (B) The effect of chitinase application on the level of fluorescence attributed to FITC-CBP. Fixed *E. scolopes* were treated with a PBS only control (PBS), active chitinase (Chitinase), or heat-killed chitinase (HK Chitinase). Asterisk = significant difference from the PBS control at a p-value of <0.01 as determined by a student's t-test with a Bonferroni correction for multiple comparisons.

transcriptase PCR on cDNA prepared from various *E. scolopes* tissues, including hemocytes, the hematopoietic gland (white body), hindgut, and eye using primers specific to either chitin synthase or the 40S ribosomal subunit RNA as a control for equal loading (Figure 4-3). We found that the hemocytes produce transcripts for both chitin synthases. However, the white body, where hemocytes are produced, does not appear to express both chitin synthases to the same degree as the hemocytes did when we carried out end-point PCR using the same amount of cDNA template, suggesting that chitin synthesis only occurs in mature hemocytes. Upon staining the white body with FITC-CBP, we did not detect any staining of immature hemocytes with the CBP, further supporting this hypothesis. The hindgut sample was included as a positive control because it contains high levels of both transcripts, a finding which is consistent with the reported ability of the hindgut to secrete a chitinous layer (Harrison and Kohn, 1997). These data suggest that *E. scolopes* hemocytes are capable of producing enzymes that synthesize chitin.

Biochemical characteristics of chitin-containing compartments

The punctate labeling of the CBP in the hemocytes suggested that the chitin-like molecule localizes to specific subcellular compartments. Extracted hemocytes co-stained with FITC-CBP and Lysotracker Red revealed co-localization of these fluorochromes to intracellular acidic compartments (Fig 4-4A). The CBP staining also co-localized with an antibody specific to *E. scolopes* halide peroxidase (data not shown; (Weis *et al.*, 1996; Small and McFall-Ngai, 1999)), a protein that typically localizes to lysosomes (Baggiolini *et al.*, 1969; Nauseef, 1998). Taken together, these data suggest that the intracellular chitin occurs in or is associated with the lysosomes of *E. scolopes* hemocytes.

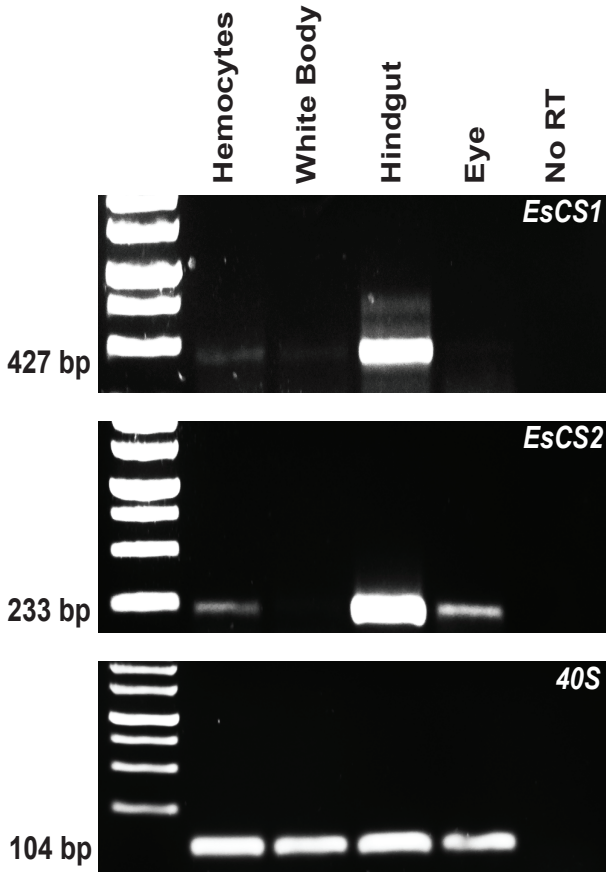

Fig. 4-3. Production of chitin synthase transcript in *E. scolopes* hemocytes: cDNA was prepared from RNA that had been extracted from four adult squid cell types or tissues (hemocytes, white body, hindgut, and eye). 500 ng of cDNA was used as a template for end-point PCR. CS1 = *E. scolopes* chitin synthase 1; CS2 = *E. scolopes* chitin synthase 2, 40S = 40S subunit ribosomal RNA, used as a loading control. Numbers to the left of the gel show the size of each gene product.

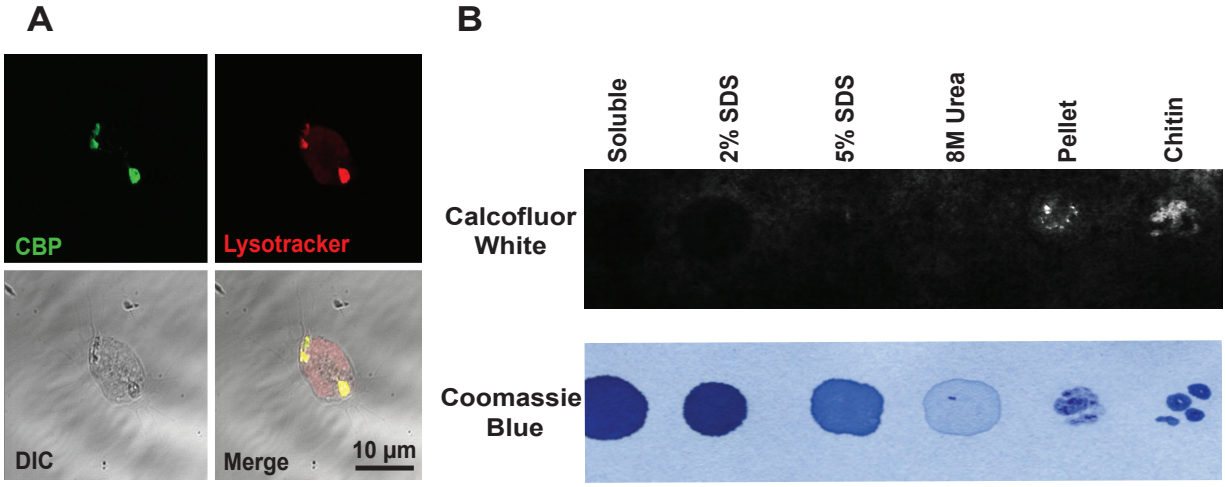

Fig. 4-4. Biochemical characterization of CBP-positive compartments: (A) Confocal micrograph of a single *E. scolopes* hemocyte co-stained with FITC-CBP (green) and Lysotracker Red (red). DIC = image of the same cell by differential interference contrast. (B) Images of protein extracts from adult *E. scolopes* gill tissue probed with calcofluor white and imaged under UV light (top), or stained with ProtoBlue coomassie blue stain and imaged under visible light (bottom).

Calcofluor-positive labeling was only present in material pelleted after extraction of hemocyte-rich tissues with aqueous solvents, SDS and urea (Fig. 4-4B), in which the majority of proteins should be soluble, but chitin is not. A coomassie stain was used as the counterstain for all fractions due to its binding to proteins and chitin (Liau and Lin, 2008). These data, coupled with our inability to capture any material with the CBP fused to a SNAP tag as bait, provide evidence that the chitinous material in *E. scolopes* hemocytes is not a chitinoprotein.

Survey of animal hemocytes for CBP labeling

To determine whether the presence of chitin in hemocytes is specific to *E. scolopes*, we examined circulating blood cells in other animal taxa for CBP-positive labeling. Blood cells from 15 species in five phyla, either from a hemocyte extraction or tissue whole-mount, were labeled with FITC-conjugated CBP and analyzed. Between 15 and 40 cells per preparation were viewed by confocal microscopy (Fig. 4-5A). Invertebrate granulocytes we surveyed labeled with CBP, regardless of phylum. However, neither of the vertebrates that we sampled (*Mus musculus* and *Danio rerio*) had any blood cells that stained positively for chitin, which is consistent with the absence of any known chitin synthetic enzymes in either species.

Blood cell extractions from five species (*M. edulis*, *M. mercenaria*, *C. fornicata*, *B. glabrata*, and *N. viridans*) produced the two known distinct blood cell types, identified as granulocytes and hyalinocytes by both size and morphology (Kuchel *et al.*, 2010). In species that produced both of these types of hemocytes, such as *Biomphalaria glabrata*, we only found CBP staining in the granulocytes (Fig. 4-5B), a feature that may provide insight into the function of CBP-reactive substances in blood cells.

A

Phylum	Species	Presence of Chitin in Blood Cell Sample
Mollusca	*Euprymna scolopes*	Yes
	Sepia pharaonis	Yes
	Mytilus edulis	Yes
	Mercenaria mercenaria	Yes
	Crepidula fornicata	Yes
	Biomphalaria glabrata	Yes
Annelida	*Nereis viridans*	Yes
	Eisenia foetida	Yes
Arthropoda	*Atta colombica*	Yes
	Drosophila melanogaster	Yes
Echinodermata	*Arbacia sp.*	Yes
	Asterias forbesi	Yes
Chordata	*Ciona intestinalis*	Yes
	Danio rerio	No
	Mus musculus	No

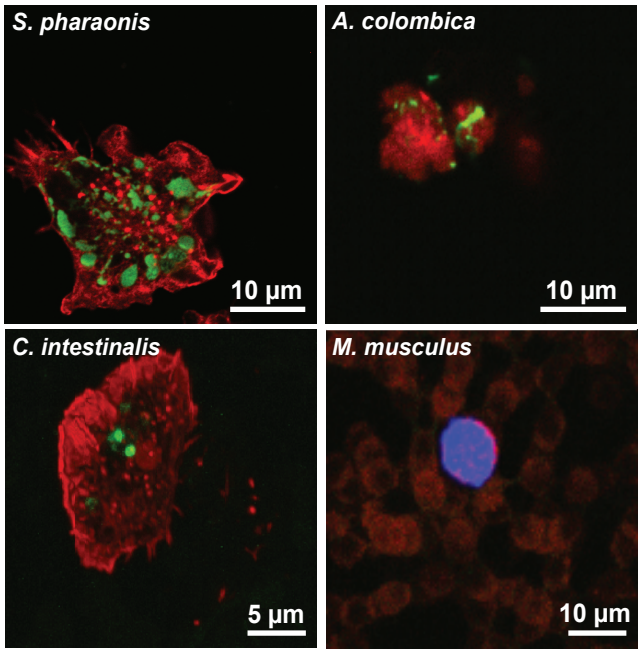

B

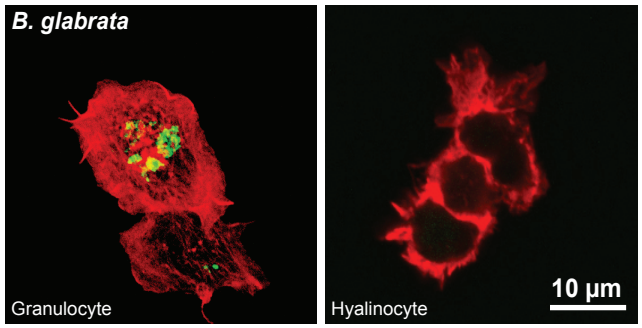

Fig. 4-5. Taxonomic survey of chitin carriage in hemocytes: (A) All organisms surveyed with the presence or absence of chitin as detected by FITC-CBP labeling (green) noted in each sample. Included are confocal micrographs of representative samples from four phyla. (B) Confocal micrographs of a granulocyte (left) and a hyalinocyte (right) from *B. glabrata*. Counterstains: red = rhodamine phalloidin (filamentous actin), blue = TOTO-3 (nuclei).

DISCUSSION:

The results of this study provide evidence that all mature *E. scolopes* hemocytes contain endogenously produced chitin in lysosomal compartments. In addition, we demonstrate that the presence of chitin-like molecules in granulocytes is a widespread character among the invertebrates.

The chitin in *E. scolopes* hemocytes may be important in the *E. scolopes – V. fischeri* symbiosis in immune surveillance of the light organ. Hemocytes are known to infiltrate the light organ early in the initiation of the symbiosis, eventually potentiating the development of the light organ into a mature symbiotic structure (Nyholm and McFall-Ngai, 1998; Kimbell *et al.*, 2006; Koropatnick *et al.*, 2007). In addition, studies of the behavior of these cells have demonstrated that the hemocytes sample the crypt spaces and communicate the status of these symbiont-containing regions to the rest of the body of the animal (Nyholm and McFall-Ngai, 1998; Nyholm *et al.*, 2009). As such, they behave similarly to mammalian dendrocytes that sample the gut. To determine whether chitin is important for such immune activity will require further study.

Abundant evidence exists that the symbionts ferment host chitin, which may be provided to the bacteria as a nutrient source (Wier *et al.*, 2010). However, whether this nutrient is provided by chitin synthesized in the abundant population of hemocytes within the bacteria-containing tissue of the light organ, in the crypt epithelial cells themselves, or in both cell types remains to be determined. As the epithelium of the molluscan gut is often lined by chitin (Berkeley, 1935; Moueza and Frenkiel, 1979; Harrison and Kohn, 1997), and the light organ is embryologically derived from the *E. scolopes* hindgut/ink-sac complex, it would not be

surprising to find that the crypt epithelium synthesizes chitin. We did not observe labeling of the crypt epithelium with CBP, but if this tissue synthesizes chitin, the chitin may be produced, transported and consumed immediately by the symbionts, so that any chitin present would be undetectable. This question could be answered in future studies in which the major sites of *EsCS1* transcription would be identified using *in situ* hybridization with probes specific to *EsCS1*.

The position and size of CBP-positive compartments in *E. scolopes* hemocytes were consistent with their co-localization within acidic and halide-peroxidase positive lysosomes of these cells (Nyholm and McFall-Ngai, 1998). Although their function is unknown, other polysaccharides have been reported to be present in lysosomes in other systems. Abundant polysaccharides, produced in the endoplasmic reticulum of certain mammalian cells, can be targeted to the lysosome. In certain lysosomal storage disorders, the polysaccharides that have been targeted to lysosomes for recycling are not broken down, a condition that can impede normal lysosomal function (Meikle *et al.*, 2003). While lysosomal storage disorders have been best characterized in muscle tissue, these defects can also be evident in macrophages(Kieseier *et al.*, 1997). The widespread presence of a chitin-like molecule in invertebrate blood cells is unlikely to be due to a defect in metabolism. However, the presence of polysaccharides in mammalian lysosomes does suggest a possible function for these molecules in the lysosomes of invertebrate granulocytes, i.e., for the storage and recycling of polysaccharides. Since the chitin only localizes to invertebrate granulocytes, it is likely that the compound plays a role that is specific to this cell type. For example, as a nonreactive molecule, chitin may serve as a scaffolding or matrix for the proteins and other biomolecules in the lysosome.

Like other cephalopods, *Euprymna scolopes* has only been shown to produce one type of hemocyte, which is most similar to invertebrate granulocytes (Cowden and Curtis, 1981; Nyholm and McFall-Ngai, 1998). However, other molluscs surveyed in this study produce both of the major molluscan blood cell types, i.e., granulocytes and hyalinocytes, and only granulocytes stained with the CBP. The presence of chitin in granulocytes but not hyalinocytes may be due to the different functions of these cells; granulocytes are primarily phagocytic and involved in respiratory burst, while the role of hyalinocytes is not yet well defined (Goedken and De Guise, 2004). As such, if the chitin-like molecule is restricted to the lysosome, as suggested in *E. scolopes* hemocytes, the undetectable labeling of CBP in hyalinocytes may be due to the presence of fewer lysosomes, which is characteristic of this cell type (Mateo *et al.*, 2009).

While ours is the first study to be done on this scale, several previous studies have shown that circulating immune cells in invertebrates may contain chitin-like substances. *Drosophila melanogaster* cell lines produce a heavily sulfated chitin-like molecule, possibly composed of chitin linked to a protein (Kramerov *et al.*, 1986). An antibody to this molecule labels granules in cell lines of *D. melanogaster* and other insect species and is present in regions of the imaginal discs of developing *D. melanogaster* larvae (Kramerov *et al.*, 1990). This same antibody binds to granules in *D. melanogaster* hemocytes in whole-animal analyses (Baĭkova *et al.*, 1993). These studies suggested that the chitin-like polysaccharide molecules in *Drosophila melanogaster* hemocytes are linked to a protein, although the sequence of the hypothetical protein was not determined (Kramerov *et al.*, 1986; Kramerov *et al.*, 1990; Baĭkova *et al.*, 1993). In contrast, our analyses suggested that the chitin-like molecules in *E. scolopes* hemocytes are not linked to protein; specifically, the chitin-positive compound was not soluble in water, SDS, or urea (Fig. 4-4), and could not be isolated by a CBP-based protein purification protocol. Taken

together, the data on chitin-like substances in invertebrate hemocytes suggest that the chitin may occur in different forms in these cells.

Other evidence for possible chitin carriage in invertebrate hemocytes has been suggested by the presence of specific sugar residues. Wheat germ agglutinin, a lectin that binds specifically to n-acetyl-glucosamine and sialic acid residues, recognizes materials in the large granulocytes of *Sicyonia ingentis* and *Homarus americanus* (Martin *et al.*, 2003). Our study, probing with fluorescently labeled CBP, suggests that these lectins are labeling chitin within these cells and that this character is common to many invertebrate phyla, not just ecdysozoans (Fig. 4-5).

While this study provides evidence for the presence of chitin in invertebrate granulocytes, we have not yet determined its function in the immune system. One possible approach would be the study of this chitin-like compound in cell culture of invertebrate granulocytes, where the cells are more easily manipulated directly and can be isolated in higher numbers. Although not present in all blood cells sampled in this study, the conspicuous nature of the chitin in invertebrate hemocytes may help to elucidate the role of polysaccharides in immune cells in general, which is an understudied area. The lack of chitin in vertebrate immune cells, though anticipated due to the lack of chitin synthetic enzymes in most vertebrates, may point to an invertebrate-specific function, and may be tied to the differences between the invertebrate and vertebrate immune systems. Finally, one practical outcome of this research is the development of a tool for the study of invertebrate granulocytes, specifically an easily used, relatively inexpensive, and reliable marker for these cells, i.e., CBP.

ACKNOWLEDGMENTS:

We thank Dr. G. Boekhoff-Falk, Dr. C. Currie, Dr. A. Huttenlocher, Dr. L. Knoll, Dr. B. Rader, and Dr. T. Yoshino for generously providing blood cell samples. In addition we thank all members of the McFall-Ngai and EG Ruby laboratories for discussion and critique of the manuscript. This work was supported by NSF (IOS 0817232) to MMN, by NIH (RO1-AI50661) to MMN and NIH (RR R01-12294) to EG Ruby and MMN, and NIH Molecular Biosciences Training Grant through UW-Madison to E. Heath-Heckman.

REFERENCES

Baggiolini, M., Hirsch, J.G., and deDuve, C. (1969) Resolution of Granules From Rabbit Heterophil Leukocytes Into Distinct Populations by Zonal Sedimentation. *J Cell Biol* **40**: 529–41.

Baĭkova, N.A., Gvozdev, V.A., and Kramerov, A.A. (1993) [The tissue localization of "chitinoprotein," detectable by using specific antibodies, in the development of *Drosophila melanogaster*]. *Ontogenez* **24**: 33–42.

Berkeley, C. (1935) The chemical composition of the crystalline style and of the gastric shield: with some new observations on the occurrence of the style oxidase. *Biol Bull* **68**: 107-114.

Chun, C.K., Scheetz, T.E., Bonaldo Mde, F., Brown, B., Clemens, A., Crookes-Goodson, W.J., *et al.* (2006) An annotated cDNA library of juvenile *Euprymna scolopes* with and without colonization by the symbiont *Vibrio fischeri*. *BMC genomics* **7**: 154.

Cowden, R.R., and Curtis, S.K. (1981) *Invertebrate blood cells*.

Davidson, S.K., Koropatnick, T.A., Kossmehl, R., Sycuro, L., and McFall-Ngai, M.J. (2004) NO means "yes" in the squid-vibrio symbiosis: nitric oxide (NO) during the initial stages of a beneficial association. *Cell Microbiol* **6**: 1139–1151.

Dilly, P.N., and Nixon, M. (1976) Cells That Secrete Beaks in Octopods and Squids (Mollusca, Cephalopoda). *Cell Tissue Res* **167**: 229–241.

Ehrlich, H., Maldonado, M., Spindler, K.-D., Eckert, C., Hanke, T., Born, R., *et al.* (2007) First evidence of chitin as a component of the skeletal fibers of marine sponges. Part I. *Verongidae* (Demospongia : Porifera). *J Exp Zool B Mol Dev Evol* **308B**: 347–356.

Goedken, M., and De Guise, S. (2004) Flow cytometry as a tool to quantify oyster defence mechanisms. *Fish Shellfish Immunol* **16**: 539–552.

Hardt, M., and Laine, R.A. (2004) Mutation of active site residues in the chitin-binding domain ChBD(ChiAl) from chitinase A1 of *Bacillus circulans* alters substrate specificity: Use of a green fluorescent protein binding assay. *Arch Biochem Biophys* **426**: 286–297.

Harrison, F.W., and Kohn, A.J. (1997) Mollusca II.

Hunt, S., and Sherief, El, A. (1990) A periodic structure in the "pen" chitin of the squid *Loligo vulgaris*. *Tissue Cell* **22**: 191–197.

Keyhani, N.O., and Roseman, S. (1999) Physiological aspects of chitin catabolism in marine bacteria. *Biochim Biophys Acta* **1473**: 108–122.

Kieseier, B.C., Wisniewski, K.E., and Goebel, H.H. (1997) The monocyte-macrophage system is affected in lysosomal storage diseases: an immunoelectron microscopic study. *Acta Neuropathol*

94: 359–362.

Kimbell, J.R., and McFall-Ngai, M.J. (2004) Symbiont-induced changes in host actin during the onset of a beneficial animal-bacterial association. *Appl Environ Microbiol* **70**: 1434–1441.

Kimbell, J.R., Koropatnick, T.A., and McFall-Ngai, M.J. (2006) Evidence for the participation of the proteasome in symbiont-induced tissue morphogenesis. *Biol Bull* **211**: 1–6.

Koropatnick, T.A., Kimbell, J.R., and McFall-Ngai, M.J. (2007) Responses of host hemocytes during the initiation of the squid-Vibrio symbiosis. *Biol Bull* **212**: 29–39.

Kramerov, A.A., Mukha, D.V., Metakovsky, E.V., and Gvozdev, V.A. (1986) Glycoproteins Containing Sulfated Chitin-Like Carbohydrate Moiety Are Synthesized in an Established *Drosophila melanogaster* Cell Line. *Insect Biochem* **16**: 417–&.

Kramerov, A.A., Rozovsky, Y.M., Baĭkova, N.A., and Gvozdev, V.A. (1990) Cognate Chitinoproteins Are Detected During *Drosophila melanogaster* Development and in Cell Cultures From Different Insect Species. *Insect Biochem* **20**: 769–&.

Kuchel, R.P., Raftos, D.A., Birch, D., and Vella, N. (2010) Haemocyte morphology and function in the Akoya Pearl Oyster, *Pinctada imbricata*. *J Invertebr Pathol* **105**: 36-48.

Li, X., Wang, L.-X., Wang, X., and Roseman, S. (2007) The chitin catabolic cascade in the marine bacterium *Vibrio cholerae*: Characterization of a unique chitin oligosaccharide deacetylase. *Glycobiology* **17**: 1377–1387.

Liau, C.Y., and Lin, C.-S. (2008) A modified Coomassie Brilliant Blue G 250 staining method for the detection of chitinase activity and molecular weight after polyacrylamide gel electrophoresis. *J Biosci Bioeng* **106**: 111–113.

Martin, G.G., Castro, C., Moy, N., and Rubin, N. (2003) N-acetyl-D-glucosamine in crustacean hemocytes; possible functions and usefulness in hemocyte classification. *Invertebrate Biology* **122**: 265–270.

Mateo, D.R., Spurmanis, A., Siah, A., Araya, M.T., Kulka, M., Berthe, F.C.J., *et al.* (2009) Changes induced by two strains of *Vibrio splendidus* in haemocyte subpopulations of *Mya arenaria*, detected by flow cytometry with LysoTracker. *Dis Aquat Org* **86**: 253–262.

Meibom, K.L., Li, X., Nielsen, A.T., Wu, C.Y., Roseman, S., and Schoolnik, G.K. (2004) The *Vibrio cholerae* chitin utilization program. *Proc Natl Acad Sci U.S.A* **101**: 2524–2529.

Meikle, P.J., Fuller, M., and Hopwood, J.J. (2003) Mass spectrometry in the study of lysosomal storage disorders. *Cell Mol Biol (Noisy-le-grand)* **49**: 769–777.

Montgomery, M.K., and McFall-Ngai, M.J. (1993) Embryonic development of the light organ of the sepiloid squid *Euprymna scolopes* Berry. *Biol Bull* **184**: 296–308.

Moueza, M., and Frenkiel, L. (1979) Fine-Structure and Histochemistry of the Gastric Shield in

the Lamellibranch *Donax trunculus* L. *Z Mikrosk Anat Forsch* **93**: 169–181.

Nauseef, W.M. (1998) Insights into myeloperoxidase biosynthesis from its inherited deficiency. *J Mol Med* **76**: 661–668.

Nyholm, S.V., and McFall-Ngai, M.J. (1998) Sampling the light-organ microenvironment of *Euprymna scolopes*: description of a population of host cells in association with the bacterial symbiont *Vibrio fischeri*. *Biol Bull* **195**: 89–97.

Nyholm, S.V., and McFall-Ngai, M.J. (2004) The winnowing: establishing the squid-vibrio symbiosis. *Nat Rev Microbiol* **2**: 632–642.

Nyholm, S.V., Stewart, J.J., Ruby, E.G., and McFall-Ngai, M.J. (2009) Recognition between symbiotic *Vibrio fischeri* and the haemocytes of *Euprymna scolopes*. *Environ Microbiol* **11**: 483–493.

Ruby, E.G., and Asato, L.M. (1993) Growth and flagellation of *Vibrio fischeri* during initiation of the sepiolid squid light organ symbiosis. *Arch Microbiol* **159**: 160–167.

Ruby, E.G., Urbanowski, M., Campbell, J., Dunn, A., Faini, M., Gunsalus, R., *et al.* (2005) Complete genome sequence of *Vibrio fischeri*: A symbiotic bacterium with pathogenic congeners. *Proc Natl Acad Sci U.S.A.* **102**: 3004–3009.

Sannasi, A., and Hermann, H.R. (1970) Chitin in the cephalochordata, *Branchisotoma floridae*. *Experientia* **26**: 351–352.

Small, A.L., and McFall-Ngai, M.J. (1999) Halide peroxidase in tissues that interact with bacteria in the host squid *Euprymna scolopes*. *J Cell Biochem* **72**: 445–457.

Sminia, T., and Barendsen, L. (1980) A Comparative Morphological and Enzyme Histochemical-Study on Blood-Cells of the Fresh-Water Snails *Lymnaea stagnalis*, *Biomphalaria glabrata*, and *Bulinus truncatus*. *J Morphol* **165**: 31–39.

Sugita, H., and Ito, Y. (2006) Identification of intestinal bacteria from Japanese flounder (*Paralichthys olivaceus*) and their ability to digest chitin. *Lett Appl Microbiol* **43**: 336–342.

Weis, V.M., Small, A.L., and McFall-Ngai, M.J. (1996) A peroxidase related to the mammalian antimicrobial protein myeloperoxidase in the *Euprymna-Vibrio* mutualism. *Proc Natl Acad Sci U.S.A.* **93**: 13683–13688.

Wier, A.M., Nyholm, S.V., Mandel, M.J., Massengo-Tiasse, R.P., Schaefer, A.L., Koroleva, I., *et al.* (2010) Transcriptional patterns in both host and bacterium underlie a daily rhythm of anatomical and metabolic change in a beneficial symbiosis. *Proc Natl Acad Sci U.S.A.* **107**: 2259–2264.

Chapter 5

Exogenous light and bacterial LPS influence host-cell microvillar dynamics in the *Euprymna scolopes* symbiotic organ

PREFACE:

In preparation for submission to *Cellular Microbiology* as:

Heath-Heckman, E.A.C., Foster, J., Goldman, W.E., Apicella, M.A., and McFall-Ngai, M.J. "Exogenous light and bacterial LPS control host-cell microvillar dynamics in the *Euprymna scolopes* symbiotic organ"

EACH and MJM formulated ideas and planned experiments. WEG and MAA contributed reagents. EACH and JF performed experiments. EACH and MJM wrote and edited the chapter.

ABSTRACT:

Recent studies of microbe-associated molecular patterns (MAMPs) suggest that they play critical roles in the development, maturation and maintenance of mutualisms. In the light-organ symbiosis between the squid *Euprymna scolopes* and the bacterium *Vibrio fischeri,* derivatives of the MAMPs lipopolysaccharide (LPS) and peptidoglycan (PGN) regulate many host responses. In early development, MAMPs induce apoptosis of, and attenuate nitric oxide production within, a superficial epithelium of the juvenile light organ that functions in initial symbiont harvesting. Once within host tissues, the symbionts proliferate to fill internal crypts, which are lined with microvillous epithelia. Colonization there induces swelling of the epithelial cells and an increase in microvillar density. Studies of both juvenile and adult animals have revealed that at dawn each day the host vents ~90% of its symbionts. In adults, this venting is correlated with the effacement of microvilli of the crypt epithelia. The purpose of this study was to characterize the timing of effacement and regrowth, and to determine whether MAMPs might be involved in this process. Analysis by transmission electron microscopy revealed that effacement occurs in the juvenile squid at dawn, but studies of non-symbiotic squid revealed that this behavior is not dependent upon symbiosis. We determined that the cue is light exposure itself by manipulating exposure to 'dawn', with early, normal, or late light cues. Symbiosis did, however, increase microvillar density during regrowth. As MAMPs play multiple roles in the symbiosis, we sought to determine their possible involvement in the formation of microvilli. We exposed animals to LPS and PGN derivatives and found that exposure to LPS led to an increase in the density of microvilli and, as opposed to MAMP-driven apoptosis, does not appear to act in synergy with PGN. In addition, treatment with alkaline phosphatase abrogated the ability of LPS

to induce microvillar elaboration, suggesting that the phosphorylation state of LPS is important for signaling to the host. These data provide the first evidence for MAMPs regulating the elaboration of microvilli, and provide evidence that LPS is a signal for two disparate modes of development in the same organ.

INTRODUCTION:

Perhaps the most common type of symbiosis found in nature is that in which bacteria directly interface with host epithelia (McFall-Ngai *et al.*, 2010). This arrangement is not surprising, since epithelia form the layers between the animal proper and luminal spaces or the outside world and, as such, would be the most likely to contact extracellular bacteria (McCaffrey and Macara, 2011). A defining characteristic of epithelia is cell polarity, or the distinction between the apical (lumen-facing) and basal (basement membrane-facing) sides of the cells forming epithelial sheets (McCaffrey and Macara, 2011). Because the apical ends of cells interact with the luminal spaces, they often develop specialized structures that allow the cells to both sense extracellular stimuli and react to those same stimuli. One such reaction is the development of microvilli, projections of the plasma membrane that increase the cellular surface area, giving the cell extra absorptive and excretory capabilities. Since microvilli are always produced on the apical ends of cells, they are often in contact with bacterial species. In fact, many symbionts have direct contact with or intercalate between host microvilli (e.g. Wang *et al.*, 2004; Durand *et al.*, 2010; Duperron *et al.*, 2008). Previous studies showed that microvillus-derived vesicles help to communicate with and control bacterial populations in the mammalian gut (Shifrin *et al.*, 2012). Reciprocally, recent studies have shown that the application of probiotics can affect the morphology of these same microvilli (Ringø *et al.*, 2007; Chichlowski *et al.*, 2007; Shukla *et al.*, 2012; Cerezuela *et al.*, 2012). However, as of yet no studies have determined what effect native symbionts have on host microvilli or how these features might change over time.

The *Euprymna scolopes* crypt epithelium begins as a simple, columnar epithelial layer. Upon colonization by *Vibrio fischeri,* however, the epithelial cells double in width to become

cuboidal, and the number of microvilli per unit area increase significantly (Lamarcq and McFall-Ngai, 1998; Montgomery and McFall-Ngai, 1998). The exact mechanisms by which these morphological transitions are signaled are not known. In addition, it was shown that in adult squid, crypt epithelial cells undergo a cycle of microvillus release and regrowth, with a correlated change in the expression of certain cytoskeletal genes (Wier *et al.*, 2010); however, the timing and stimulus of this phenomenon was not determined.

The release of membranes from microvilli is important for host-microbe interactions in other systems. For example, in both mice and zebrafish, microvillus-derived vesicles contain the enzyme alkaline phosphatase (AP), which is necessary for the control of luminal microbial populations and the detoxification of microbial products (Bates *et al.*, 2007; Shifrin *et al.*, 2012). In zebrafish, AP removes phosphate groups from the lipid A moiety of bacterial lipopolysaccharide (LPS), rendering the molecule non-immunogenic (Bates *et al.*, 2007). In the squid-vibrio system, LPS does not appear to have detrimental effects on the host; rather, it is one of a suite of microbe-associated molecular patterns (MAMPs) which, in addition to the peptidoglycan monomer (TCT), is presented by symbionts and induces normal host development through apoptosis of epithelial fields outside of the light organ (Foster *et al.*, 2000; Koropatnick *et al.*, 2004). However, if LPS is treated with AP, it can no longer induce apoptosis in the light organ, suggesting that one or more phosphate groups are important for signaling (Rader *et al.*, 2012). Later in the symbiosis, experimental inhibition of native host AP activity leads to the inappropriate loss of symbionts from the light organ, suggesting that after apoptosis has begun AP activity (which may be microvillus-derived) is important for the continuation of the symbiosis (Rader *et al.*, 2012). These data have led to the model that AP activity is detrimental early in the symbiosis, where it may prevent signal transduction necessary for normal host

development, but is necessary later in the mature association. While the roles of LPS and TCT in the development of the external light-organ epithelia have been well-documented (Foster *et al.*, 2000; Koropatnick *et al.*, 2004; Troll *et al.*, 2010), as of yet the effect of these MAMPs on the epithelial cells that directly interact with symbionts throughout the life of the host has yet to be examined.

The current study was conducted to test the model that the host crypt-cell microvilli go through a cycle of release and renewal, and that the density of these microvilli is dependent upon the presence of symbionts. We characterized the timecourse of and stimulus for microvillar rearrangement in the squid light organ, as well as determined the bacterial features necessary for microvillar regrowth.

Materials and Methods:

General Methods

Adult *Euprymna scolopes* were collected and maintained as previously described (Wollenberg and Ruby, 2012). Juveniles from the breeding colony were collected within 15 min of hatching. Aposymbiotic (Apo) animals were maintained in *V. fischeri*-free, unfiltered seawater, while juveniles were exposed to ~5,000 colony-forming units (CFU) /mL of the *V. fischeri* strain ES114 (see Table 1) overnight to produce the symbiotic (Sym) condition. Colonization of the symbiotic juvenile squid was determined by measuring luminescence output of the symbionts with a TD 20/20 luminometer (Turner Designs, Sunnyvale, CA); aposymbiotic squid were also analyzed to ensure that their light organs had not been colonized. In experiments with *V. fischeri* surface molecules, the LPS and the peptidoglycan monomer (also called tracheal cytotoxin, or TCT) were prepared as previously described (Foster *et al.*, 2000; Koropatnick *et al.*, 2004) and exposed to animals at 10 μg/mL and 10 μM, respectively. For experiments in which venting behavior was experimentally manipulated, animals were placed in a darkroom with constant dim red light, a wavelength that is not perceived by the squid rhodopsin. Venting was assayed by removing the squid from its seawater-containing vial, measuring the luminescence of the squid-free seawater, and then placing the squid back into its original vial. All reagents were obtained from Sigma-Aldrich (St. Louis, MO) unless otherwise noted. All animal experiments conform to the relevant regulatory standards established by the University of Wisconsin – Madison.

TUNEL Assay

The DeadEnd Fluorometric TUNEL System (Promega, Madison WI) assay was

Table 5-1: *V. fischeri* strains used in this study

Strain	**Relevant genotype**	**Source**
ES114 (WT)	Wild-type *V. fischeri*	(Boettcher and Ruby, 1990)
EVS102 (*Δlux*)	ES114 *ΔluxCDABEG*	(Bose *et al.*, 2008)
VCW3F6 (*lysA-)*	ES114 *lysA*::EZ::Tn*kan*R	(Whistler *et al.*, 2007)
MB06859 (*waaL*-)	ES114 *waaL*::Tn5*erm*R,	(Post *et al.*, 2012)
CAB1532 (*Δmam7*)	ES114 *Δmam7*	(Altura *et al.*, 2013)

performed as previously described (Troll *et al.*, 2009). Briefly, juvenile animals were fixed overnight in 4% paraformaldehyde in marine PBS (mPBS; 0.05M sodium phosphate buffer with 0.45M NaCl, pH 7.4), washed in mPBS, and then stained with rhodamine phalloidin overnight. The light organs were then washed 4 x 30 min in mPBS and taken through the TUNEL kit procedure per the manufacturer's instructions and then washed and counterstained with TOTO-3 to visualize light-organ nuclei. The samples were then mounted and visualized with a Zeiss LSM510 confocal microscope (Carl Zeiss Inc., Thornwood, NY).

Electron Microscopy

Juvenile animals were dropped directly into fixative (2% glutaraldehyde and 2% paraformaldehyde in mPBS) and incubated at RT for 5 min. The animals were then removed from the fixative, their mantles were dissected open and the funnels removed to allow for penetration of the fixative into the light organ. The samples were then placed back into fixative and incubated at RT for 12 h, after which they were washed 2 x 10 min in mPBS and post-fixed in 1% osmium tetroxide (Ted Pella) in mPBS for 1 h at RT. The samples were then washed 2 x 10 min in mPBS to remove any excess osmium and dehydrated using a graded ethanol series (30-100%) in 10-min washes, and then using 100% propylene oxide for 3 x 10 min. The animals were then incubated in 50% propylene oxide and 50% unaccelerated Spurr's resin (Ted Pella Inc., Redding CA) for 2 h at RT, and then in unaccelerated Spurr's resin only for 1 week at RT. The samples were then incubated in accelerated Spurr's resin for 24 h at RT, and then were placed into molds with fresh accelerated Spurr's resin for 24 h at 60°C to polymerize the blocks. The blocks were then sectioned on a Leica EM UC6 ultramicrotome (Leica Microsystems Inc., Buffalo Grove IL), mounted on 300 mesh copper grids (Electron Microscopy Sciences, Hatfield

PA), stained with 8% uranyl acetate in 50% ethanol and Reynold's lead citrate sequentially, and visualized on a Phillips CM120 STEM (Philips, Eindhoven Netherlands).

Quantification of Microvillar Density and Cellular Swelling

Quantification of microvillar density was performed as previously described (Lamarcq and McFall-Ngai, 1998). Briefly, after visualization by TEM, 7 5μm fields within crypt 1 of the light organ were identified per juvenile squid, and within each field all of the microvilli attached to epithelial cells in the field were counted to give the linear density of microvilli. Three squid light organs were analyzed for each condition. The data are extrapolated to the microvillar density per unit area, as examined features of the epithelial cells are uniform across their entire apical surfaces (Montgomery and McFall-Ngai, 1994). Swelling of the crypt epithelial cells was determined by measuring the width, at their widest point, of epithelial cells of crypt 1. As above, 7 cells were measured per light organ and 3 light organs were measured per condition. All statistical comparisons were performed on the linear density using Graphpad Prism software (GraphPad Software Inc., La Jolla CA).

Immunocytochemistry

Juvenile squid were anesthetized in a 1:1 solution of 0.37M $MgCl_2$ and filtered natural seawater for 5 min. The animals were then fixed for 1 h, while rotating, in a solution containing 1% glutaraldehyde, 1% paraformaldehyde in mPBS. The fixed samples were rinsed three times for 10 min each in mPBS buffer and dehydrated using a graded methanol series (15 – 100%). The samples were then infiltrated in a 1:1 mix of 100% methanol and LR White (Ted Pella Inc., Redding, CA) at 4°C for 12 h, then incubated in 100% LR White for 72 h while rotating. The

samples were then embedded in fresh LR White and cured overnight at 52°C. Ultrathin sections of the juvenile light organ were placed on slotted nickel grids and incubated in a blocking solution containing mPBS, 0.5% bovine serum albumin (BSA), and 1% goat serum for 1 h in a humid chamber. The sections were then incubated in blocking solution containing the primary polyclonal LPS antibody, or for control purposes, pre-immune serum at a dilution of 1:100 for 7 h in a humid chamber. The sections were rinsed twice in mPBS for 5 min each rinse and then incubated with goat polyclonal secondary antibody to rabbit conjugated to 15 nm gold spheres at a 1:50 dilution for 1 h. The unstained sections were rinsed twice for 5 min each in mPBS, dried, and examined with a Zeiss LEO 912 Omega transmission electron microscope.

LPS de-phosphorylation

V. fischeri LPS was dephosphorylated using a protocol adapted from (Bates *et al.*, 2007). Briefly, 5 units of alkaline phosphatase-conjugated agarose beads were resuspended in phosphate-buffered saline (PBS; 50 mM sodium phosphate with 0.1 M NaCl, pH 7.4), and then exposed to 100 µg *V. fischeri* LPS in PBS were added. The mixture was then incubated at 37°C for 4 h to allow for dephosphorylation of the LPS. The sample was then spun to remove the alkaline phosphatase-conjugated beads from the mixture and the supernatant containing the de-phosphorylated LPS was removed for squid experiments. As a negative control, the same procedure was followed with alkaline phosphatase-conjugated beads that had been heat-inactivated at 70°C for 10 min to stop any enzymatic activity. Both samples of LPS were then exposed to the squid at a final concentration of 10 µg/mL of seawater for 48 h with a water change every 24 h.

RESULTS:

Effect of light cue manipulation on venting behavior

The venting behavior of *Euprymna scolopes* is dependent upon an exogenous light cue, presented in nature by sunlight at dawn (Nyholm and McFall-Ngai, 1998). However, the approaches used to observe venting in earlier studies were restricted to observation in adult animals. In order to observe and manipulate the venting of juvenile squid, we developed an assay in which juvenile animals were placed into seawater in individual scintillation vials, and then removed from the vials at time points before and after they were given a light cue. Once the animals were removed from the vials, we measured the amount of luminescence in the seawater that previously held the squid to determine whether luminescent symbionts had been expelled into the seawater. Like previous studies in adults (Nyholm and McFall-Ngai, 1998), our results showed that symbiont venting occurs in response to a light cue in the juvenile animals. Once the symbionts were vented into the surrounding seawater (First Luminescence, Fig. 5-1A), bacterial luminescence increased until peak seawater luminescence occurred, usually by 2 h after the light cue (Peak Luminescence). This peak was followed by a decline in the amount of seawater luminescence, usually resulting in a loss of seawater luminescence by 6 h post light exposure (Fig. 5-1A).

To characterize the extent of the light-induced venting behavior, we manipulated the dawn light cue in order to determine whether venting is purely dependent upon exogenous light or, instead, that the expelling of symbionts, as measured by seawater luminescence, can occur in absence of an external light cue. We performed the above assay with animals that were exposed

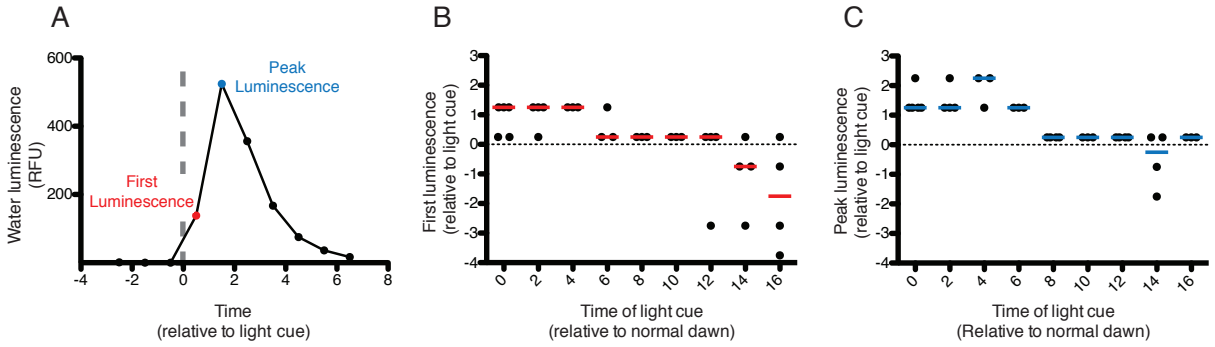

Fig. 5-1. The effect of delayed light presentation on symbiont venting behaviors.

A. Luminescence of symbionts in seawater squid over time. Data shown are from the water surrounding one host animal measured every 2 h over a period of 12 h, with the light cue given at 0 h (gray dotted line). First seawater luminescence is shown in red, and the peak luminescence is shown in blue. B and C. The effect of delayed light cues on the time of first luminescence (B) and peak luminescence (C) in the seawater. Each data point represents one animal, with 3-5 animals in each treatment group. Solid lines represent the median of each group, and the horizontal dotted lines denote the time at which the light cue was given.

to a normal light cue (time 0), or to a light cue from 2 to 16 hours past the normal dawn (Fig. 5-1B and C).

Within a 10-h time period the animals only vented symbionts into the surrounding seawater in response to the dawn light cue (Figure 5-1B). However, if not given a light cue until between 10 and 16 h past normal dawn, animals began to "leak" symbionts into the surrounding seawater in the absence of exogenous light, as shown by first luminescence occurring before the light cue is given (Figure 5-1B).

We also found that delaying the light cue influenced how long it took for juvenile squid to expel the majority of their symbionts into the seawater, as measured by how long after the light cue peak seawater luminescence occurred. If given a light cue at 6 h after normal dawn, peak seawater luminescence occurred between 1.25 to 2.25 h after the light cue. However, if the animals were denied a light cue for more than 6 h, peak luminescence occurred within 0.25 h after the light cue (Figure 5-1C). Thus, these data suggest that the venting process is strongly influenced by, but is not completely dependent upon, the presentation of exogenous light.

Timing of crypt cell microvillar effacement

We examined whether microvillar effacement occurs in the juvenile light-organ crypt cells (Figure 5-2A-C) and, if so, whether the process is affected by the time of day and symbiotic state of the animal. Effacement started as soon as 5 min after the dawn cue (*i.e.*, just after 36 h post-hatching), when microvillar density was 55 – 65% of that observed at 24 h post-hatching (*i.e.*, sundown; control condition) (Figure 5-2D). By 38 h post-hatching the microvillar density had decreased to 25 – 35% of the control condition (Figure 5-2D). Both symbiotic and

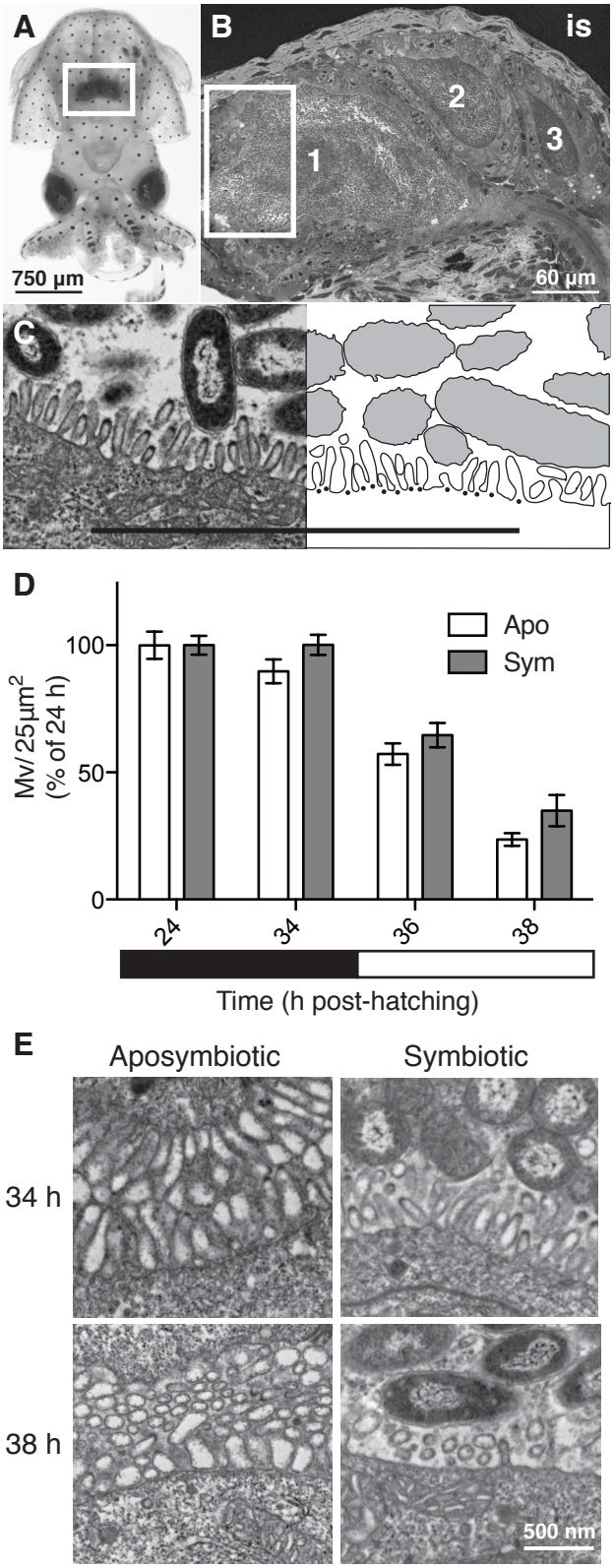
A
750 µm
B
is
1
2
3
60 µm
C
D
Mv/25µm² (% of 24 h)
100
50
0
Apo
Sym
24
34
36
38
Time (h post-hatching)
E
Aposymbiotic
Symbiotic
34 h
38 h
500 nm

Fig. 5-2. Measurement of crypt-cell microvillar effacement in juvenile squid.

Juvenile *E. scolopes* (A) hatch with a nascent light organ located ventral to the ink sac (white box). Soon after hatching, the light organ becomes colonized with *V. fischeri*, which localize to and grow to fill the three crypt spaces (B; 1, 2, and 3), that are lined with microvillous epithelial cells, in each half of the light organ (is, ink sac). All measurements of microvillar density were performed in the medial portions of crypt 1 (white box). C. An example image of crypt epithelial cells. Left, a TEM image of the apical portions of crypt 1 epithelial cells reveals a field of microvilli in contact with bacterial symbionts. In a diagram overlay of the same image (right), the microvilli attached to the crypt-cell body are indicated with black dots, with the bacterial cells shown in gray. Scale bar, 5 μm. D. Quantification of microvillar density in aposymbiotic (Apo, white columns) and symbiotic (Sym, gray columns) juvenile squid at 24, 34, 36, and 38 h after hatching. The external light regimen is shown in black and white bars below the graph. Microvillar density is normalized to the 24 h time point for both the Apo and Sym conditions. N = three biological replicates and seven technical replicates per condition. Error bars represent the standard error of the mean. E. Representative images of the fields measured for the 34 and 38 h conditions in (D).

aposymbiotic animals showed a similar, significant decrease in microvillar density in response to the dawn cue, indicating that the effacement was not dependent upon colonization state. In addition, the effacement was localized to the microvilli and did not extend into the crypt epithelial cells (Figure 5-2E), as was seen previously in adult squid (Wier *et al.*, 2010). These data suggest that effacement occurs in both juvenile and adult animals.

Effect of light cue manipulation on microvillar effacement

Because we found the effacement began soon after the dawn light cue, we tested if a dawn cue could serve as a stimulus for the effacement of crypt-cell microvilli. To this end, we presented juvenile animals with a light cue 6 h before their anticipated dawn, at normal dawn, or 6 h after their normal dawn, and then measured the microvillar density 2 h before the light cue, 5 min after the light cue, and 2 h after the light cue in all three conditions. The crypt-cell microvilli significantly decreased in number beginning 5 min after the light cue whether the cue was given early, at normal dawn, or after normal dawn (Figure 5-3), suggesting that effacement is triggered by exogenous light. However, the decrease occurred more slowly in animals presented an early light cue as shown by a significant decrease in microvillar density between 0 and 2 h after the light cue in the animals given an early light cue ($p<0.05$), but not in those given light cues at normal dawn or after normal dawn (Figure 5-3, 6 h early).

Evidence for light-cue dependent apoptosis in the light-organ appendages

Apoptosis and regression of the ciliated epithelial fields is dependent upon an irreversible signal consisting of *V. fischeri* - derived peptidoglycan monomer (tracheal cytotoxin, or TCT) and lipopolysaccharide (LPS) given at 12 h post- hatching

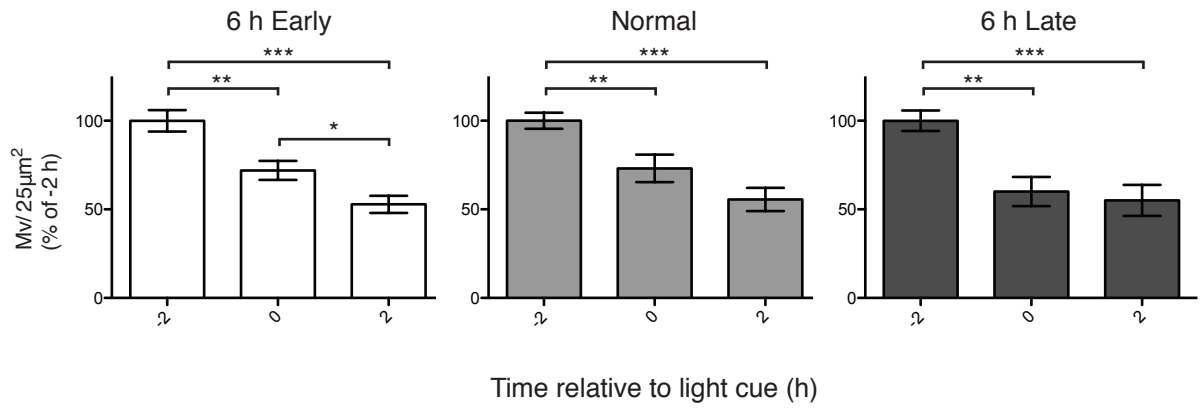

Fig. 5-3. The effect of light-cue manipulation on crypt-cell microvillar density.

Light cues were given to cohorts of animals 6 h before normal dawn (left, white bars), at normal dawn (middle, gray bars), or 6 h after normal dawn (right, dark gray bars). Within each cohort, microvillar density was measured 2 h before (-2), at (0), or 2 h after (2) the light cue. Within each graph, the data were normalized to the -2 h condition. N = three biological replicates and seven technical replicates per condition. Error bars represent the standard error of the mean. * = $p < 0.05$, ** = $p < 0.01$, *** = $p < 0.001$ by an ANOVA with a Tukey's pairwise comparison.

(Doino and McFall-Ngai, 1995; Koropatnick *et al.*, 2004). As the first venting event of the symbiosis also occurs at 12 h (typically the first dawn light cue of the animal's life), we hypothesized that the TCT and LPS signal might be given in the ducts during the first venting of resident symbionts as high numbers of bacteria pass through these regions. Due to the finding that venting can be delayed for at least 8 h by denying the animal a light cue (Figure 5-1B), we compared levels of late-stage apoptosis at 24 h in animals given a normal first light cue to those given a light cue 7 hours after the animals' normal dawn. The number of apoptotic cells in the anterior appendage of symbiotic animals was significantly higher in animals exposed to a normal light cue relative to those exposed to a light cue 7 hours late ($p<0.001$). Animals exposed to a normal light cue had 60% more apoptotic cells in the anterior appendage than those exposed to a late light cue and, therefore, a delayed symbiont venting (Figure 5-4A). By contrast, changing the timing of the dawn light cue did not affect the number of apoptotic cells in the anterior appendages of aposymbiotic animals ($p = 0.93$) (Figure 5-4B). These data suggest that manipulating the first venting of symbionts affects the presentation of the irreversible morphogenic signal in this symbiosis.

Symbiosis-dependent regrowth of crypt microvilli and its uncoupling from epithelial cell swelling

While effacement of the crypt-cell microvilli was not symbiosis dependent, previous data showed that microvillar density in the crypts is increased by symbiosis in a reversible manner (Lamarcq and McFall-Ngai, 1998). Following effacement, regrowth of the microvilli occured ~3x faster in symbiotic animals than in aposymbiotic animals (86 mv/μm^2/h vs. 31 mv/μm^2/h). As shown previously (Lamarcq and McFall-Ngai, 1998),

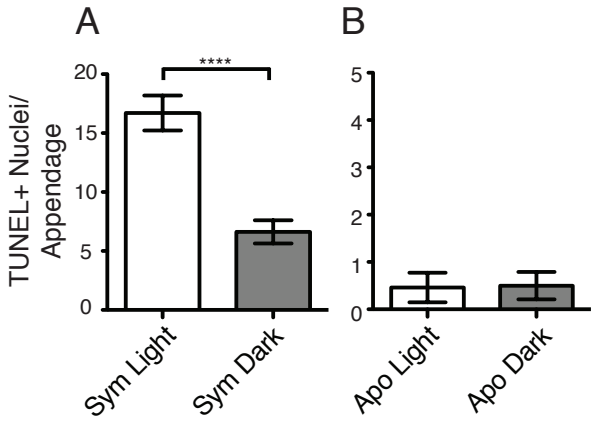

Fig. 5-4. The influence of light-cue manipulation on late-stage apoptosis

Symbiotic (Sym, A) and aposymbiotic (Apo, B) squid were given either a normal first light cue at 12 h post-hatching (white, Light), or were denied a light cue until 19 h post-hatching (gray, Dark). TUNEL+ nuclei per anterior appendage were quantified at 24 h post-hatching. N = 12-16 animals per condition. Bars denote the standard error of the mean. **** = $p < 0.0001$ by an unpaired, 2-tailed t-test.

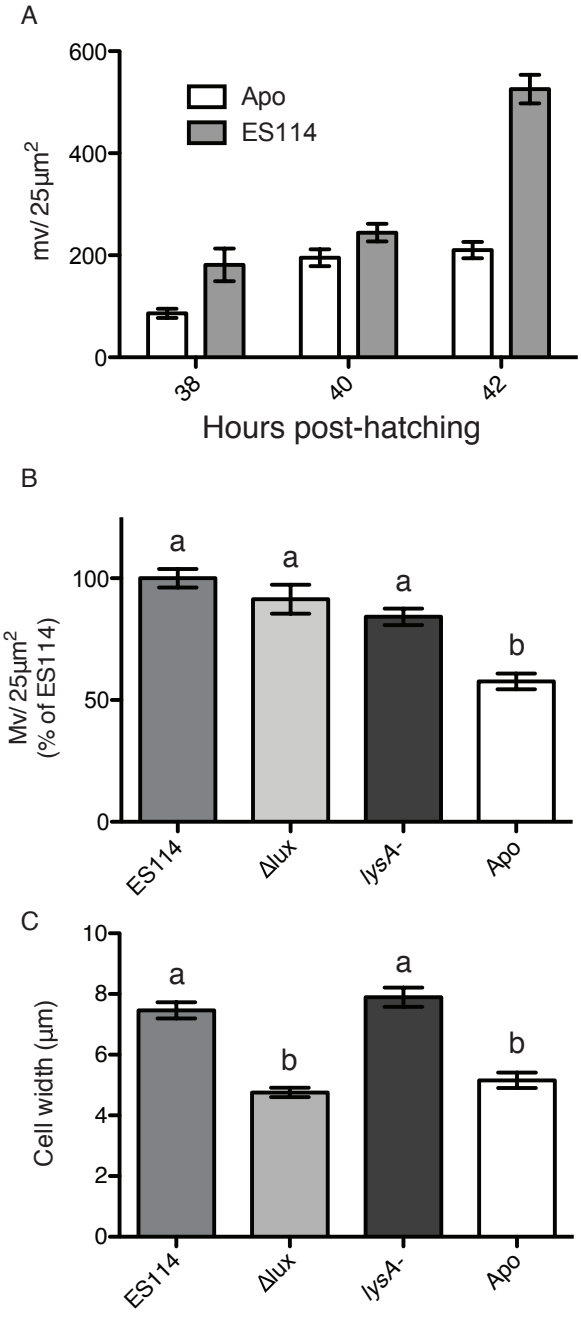
A
600
400
200
0
mv/ 25µm2
Apo
ES114
38
40
42
Hours post-hatching
B
100
50
0
Mv/ 25µm2
(% of ES114)
a
a
a
b
ES114
Δlux
lysA-
Apo
C
10
8
6
4
2
0
Cell width (µm)
a
b
a
b
ES114
Δlux
lysA-
Apo

Fig. 5-5. The influence of symbiosis on microvillar regrowth.

A. Quantification of microvillar density in aposymbiotic (Apo, white columns) and wild-type colonized (ES114, gray columns) juvenile squid at 38, 40, and 42 h after hatching. Microvillar density (B) and cellular width (C) of the crypt epithelium in animals at 48 h post-hatching colonized with wild-type (ES114), light-deficient (Δ*lux*), or lysine auxotroph (*lysA*-) symbionts, or left uncolonized (Apo). Lettering (a, b) denotes groups of statistically similar means using a significance level of $p < 0.05$ by an ANOVA followed by a Tukey's pairwise comparison. Error bars denote the standard error of the mean. N = three biological replicates and seven technical replicates per condition.

symbiotic animals reached a microvillar density more than twice that of their aposymbiotic counterparts (Figure 5-5A). Animals colonized with *V. fischeri* strain ES114, the non-luminescent strain *Δlux,* and the lysine auxotroph *lysA*- exhibited microvillar densities that were statistically indistinguishable from each other (Figure 5-5C), and that were all 50-75% higher than the level found in aposymbiotic animals (Fig. 5B, $p<0.001$). Both the *lysA*- and *Δlux* strains exhibit a bacterial colonization level approximately 10% of ES114 (Whistler *et al.*, 2007; Bose *et al.*, 2008). Therefore, the induction of symbiont-mediated microvillar growth was not dependent upon bacterial density or bacterial light. However, as was shown previously, both the *Δlux*-colonized and the aposymbiotic animals showed a significant 30% decrease in cell width as compared to ES114- and *lysA*- colonized animals (Figure 5-5C), suggesting that the symbiosis-mediated increase in microvillar density was not coupled to cell swelling.

Effect of bacterial products on microvillar regrowth

We tested whether the bacterial products TCT and LPS are necessary for stimulation of microvillar elaboration. Either LPS alone or LPS and TCT combined induced microvillar densities that were statistically indistinguishable from symbiotic animals. However, TCT-treated animals exhibited a microvillar density about 75% of ES114-colonized animals ($p<0.05$), suggesting that LPS induces microvillar elaboration in the juvenile squid (Figure 5-6A).

To determine whether the crypt epithelial cells come into direct contact with LPS, we performed immuno-electron microscopy using a polycolonal antibody generated to *V. fischeri* LPS to localize the molecule. LPS localized to the outer envelope of colonized *V. fischeri* cells, the host crypt lumen, and inside of the epithelial cells themselves (Figure 5-6B). These results suggest that *V. fischeri* sheds LPS in the crypts that can then be recognized by the host cells.

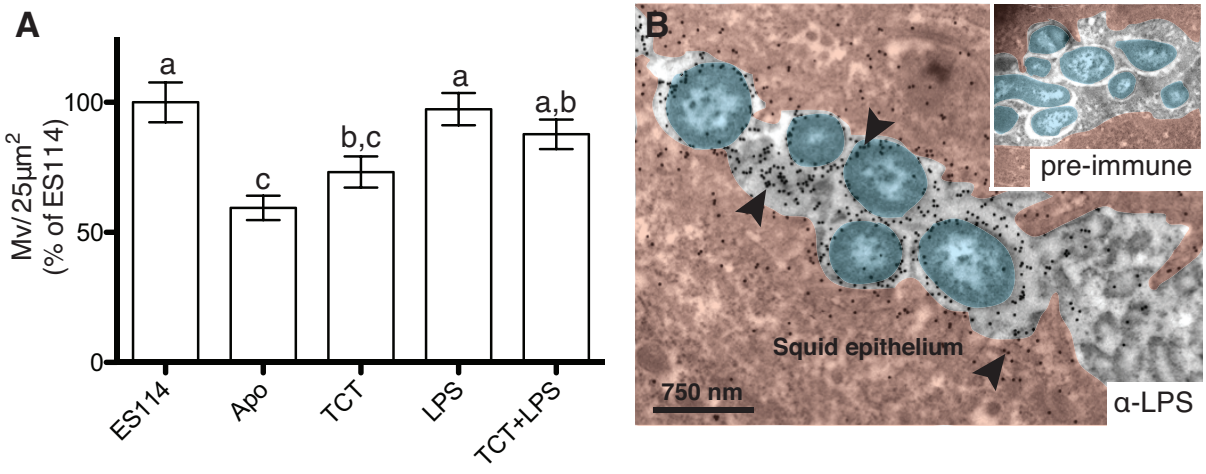

Fig. 5-6. Location and consequences of *V. fischeri* LPS presentation in the host crypts. A. Juvenile animals were colonized with wild-type *V. fischeri* (ES114), left uncolonized (Apo), or exposed to *V.fischeri* lipopolysaccharide (LPS) and peptidoglycan monomer (TCT) individually, or in combination (TCT+LPS). The graph shows the microvillar density of crypt epithelial cells at 48 h post-hatching. Lettering (a, b, c) denotes groups of statistically similar means using a significance level of $p < 0.05$ by an ANOVA followed by a Tukey's pairwise comparison. Error bars denote the standard error of the mean. N = three biological replicates and seven technical replicates per condition. B. Localization of *V. fischeri* LPS in juvenile crypt spaces. Anti-LPS antibody staining is visualized by 15 nm gold particles, seen as black puncta on the image (black arrowheads), which are absent from the pre-immune control (inset). False coloring denotes bacterial (blue) and host (pink) cells, with the crypt lumen remaining uncolored.

Thus LPS exposure alone might induce symbiotic-like microvillar elaboration in the host crypt cells. In addition, the animal is exposed to free LPS under normal symbiotic conditions.

Regrowth of the microvillar border in response to phosphorylated symbiont lipid A

Several symbiotic phenomena, such as early-stage apoptosis and nitric oxide attenuation, are affected by different portions of *V. fischeri* LPS, namely the phosphate groups, acyl chains, and the O-antigen (Altura *et al.*, 2011; Rader *et al.*, 2012; Post *et al.*, 2012) (Figure 5-7A). To determine if the O-antigen moiety of *V. fischeri* LPS is necessary for microvillar elaboration, we colonized juvenile squid with a mutant that does not elaborate an O-antigen (*waaL*-) and compared the microvillar density in those animals at 48 hours to animals colonized with wild-type *V. fischeri* (ES114), and animals left uncolonized (Apo). Microvillar density did not differ significantly between the ES114- and *waaL*- colonized animals. Both colonization conditions produced microvillar densities significantly larger than that found in aposymbiotic animals ($p<0.001$, Figure 5-7B), suggesting that the O-antigen is not necessary for the induction of microvillar elaboration.

A previous study in the squid-vibrio symbiosis showed that the presence of one or more of the phosphate groups in the *V. fischeri* lipid A moiety is necessary for the induction of early-stage apoptosis in the ciliated epithelium on the surface of the light organ (Rader *et al.*, 2012). To test whether this phosphorylation is necessary for the induction of microvillar growth in the light organ, we treated LPS with alkaline phosphatase (AP), or with heat-inactivated AP as a control. We then exposed juvenile animals to both LPS preparations and compared the microvillar densities of treated animals to those of animals colonized with ES114 or left aposymbiotic. Microvillar density was significantly lower in aposymbiotic animals and those

exposed to AP-treated LPS relative to animals treated with heat-inactivated AP or colonized with ES114 (60-70% of ES114, $p<0.001$, Figure 5-7C). However, the microvillar density of animals treated with AP-LPS was slightly but significantly higher than that of aposymbiotic animals ($p<0.05$, Figure 5-7C), suggesting that either not all of the phosphate groups were cleaved from the LPS molecule during AP treatment, or that another portion of the *V. fischeri* lipid A moiety has an effect on host crypt-cell microvillar density. Taken together, these data suggest that phosphate groups present on the *V. fischeri* lipid A molecule are necessary for typical levels of host-cell microvillar elaboration.

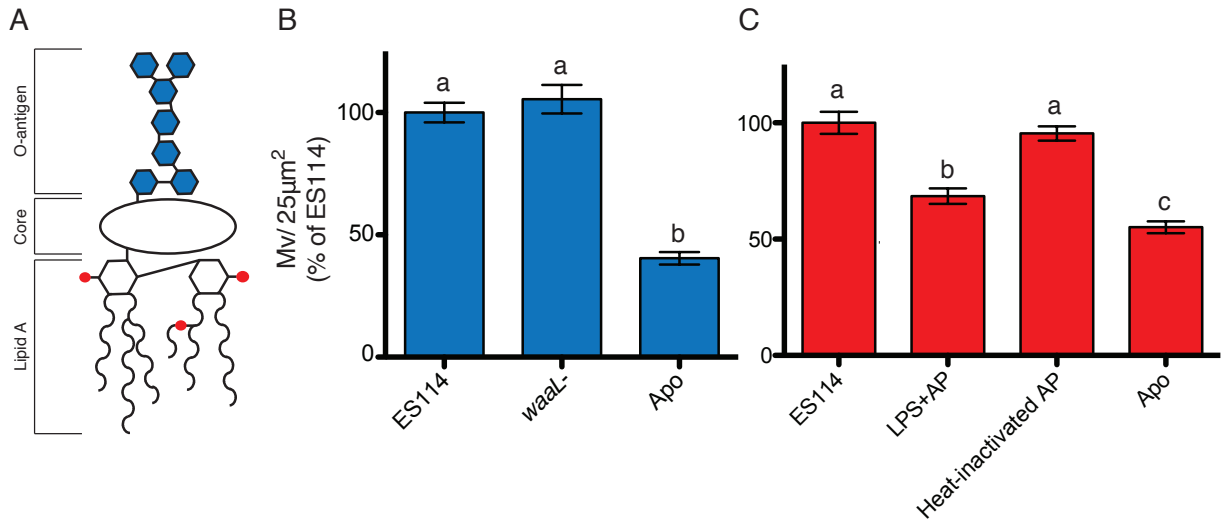

Fig. 5-7. The effect of LPS structure modifications on microvillar density.

A. Diagram of *V. fischeri* LPS, showing the lipid A, core oligosaccharide, and O-antigen (blue). The phosphate groups attached to the lipid A moiety are shown in red. B. The effect of O-antigen elaboration on microvillar density. Animals were colonized with wild-type *V. fischeri* (ES114), a mutant incapable of attaching the O-antigen to LPS (*waaL*-), or were left uncolonized (Apo). C. Influence of LPS de-phosphorylation on microvillar density. Animals were colonized with wild-type *V. fischeri* (ES114), exposed to LPS that had been de-phosphorylated with alkaline phosphatase (LPS+AP), LPS exposed to heat-inactivated alkaline phosphatase (Heat-inactivated AP), or left uncolonized (Apo). Microvillar densities are shown as the proportion relative to the wild-type colonized condition within each graph. Lettering (a, b, c) denotes groups with statistically similar means using a significance level of $p < 0.05$ by an ANOVA followed by a Tukey's pairwise comparison. Error bars denote the standard error of the mean. N = three biological replicates and seven technical replicates per condition.

DISCUSSION:

In this study, we characterized the behavior of light organ crypt-cell microvilli over the day/night cycle in the squid/vibrio symbiosis. We provide evidence for a daily light-induced, but symbiosis-independent, effacement of crypt-cell microvilli, which is followed by a symbiosis-dependent regrowth of the brush border. Specifically, the increased regrowth seen in symbiotic animals appears to be due to the presentation of phosphorylated lipid A by *V. fischeri* to the host. These data represent the first example of bacterial products regulating the normal elaboration of host microvilli.

Microvillar shedding as a trait of photoreceptive tissues

Light-induced microvillar effacement has not been shown previously in gut-derived epithelia such as the light organ (Montgomery and McFall-Ngai, 1993). However, shedding of entire or portions of microvilli in response to light is common in invertebrate rhabdomeric photoreceptors, which are composed of highly specialized cells containing photoreceptive pigment in their microvilli (Stark *et al.*, 1988; Gray *et al.*, 2008; Battelle, 2013). The cells of the squid light organ crypts have several characters that suggest that they are physiologically and developmentally convergent upon photoreceptor tissue, including the production of photoreceptive proteins (Tong *et al.*, 2009) and the expression of so-called "eye specification" genes during early development (Peyer *et al.*, 2014). One of the most well-documented examples is the photoreceptor shedding seen in *Limulus polyphemus*, the American horseshoe crab (Battelle, 2013). Horseshoe crab photoreceptors undergo two types of photoreceptor shedding: transient shedding, a large-scale but temporary disorganization of the microvillar border which is

stimulated by even dim dawn light cues and requires circadian input, and light-driven shedding, which is stimulated by bright light and continues for hours after the light cue, but requires no circadian input (Sacunas *et al.*, 2002). The microvillar shedding seen in the squid light organ appears to have more in common with *Limulus* transient shedding, as the shedding begins very soon after dawn, includes a disorganization of the microvillar border, and appears to complete quickly, as opposed to continuing for several hours after the light cue (Fig. 5-2), (Sacunas *et al.*, 2002). In addition, although our study did not investigate circadian inputs to the light organ, a previous study that was the first to document microvillar effacement in the light organ showed that a large-scale upregulation of actin-related genes preceded microvillar effacement by about two hours, suggesting that the regrowth following effacement, which would require actin and actin-related proteins, may have circadian underpinnings (Wier *et al.*, 2010). In addition, it was shown previously that the light organ expresses transcripts involved in circadian input regulated by bacterial light, suggesting that the light organ has the capability for circadian entrainment (Heath-Heckman *et al.*, 2013). These data lead to the question of whether the underpinnings of effacement are indeed circadian in nature and, if they are, the nature of the circadian input.

One major difference between microvillar shedding in the horseshoe crab and other animals and what we observed in the squid light organ is that in *Limulus* photoreceptors the microvillar membranes are shed by a mass endocytosis event and therefore are taken *into* the cell and recycled (Sacunas *et al.*, 2002; Battelle, 2013), whereas in the squid light organ the microvillar membranes are released *out* into the crypt lumen. In photoreceptor renewal this process is thought to allow the cell to degrade proteins damaged by exposure to light and recycle other components, such as membranes, for use by the cell (Boesze-Battaglia and Goldberg, 2002). In the squid light organ, it is possible that these released membranes are of more use to

the symbiosis as nutirents for the bacterial symbionts in the crypts, a hypothesis supported by the expression of symbiont glycerol utilization genes four hours after dawn in the mature symbiosis (Wier *et al.*, 2010). It appears that the release and renewal of microvilli containing photoreceptive proteins may be a common trait of photoreceptive tissue, no matter the embryonic provenance of the epithelial layer.

Bacterial symbionts and their effect on the host cytoskeleton

While the release of microvilli in the light organ appears to be regulated in a symbiosis-independent manner, microvillar regrowth is dependent upon the presence of symbiont products, suggesting that *V. fischeri* is able to manipulate host microvilli. The effect of bacteria on host microvilli has been studied primarily in pathogenic associations, the most prominent of which is the association of enteropathogenic and enterohemorrhagic *E. coli* (EPEC and EHEC) with epithelial layers in the mammalian gut. Both of these bacteria cause attaching and effacing (A/E) lesions in the host, which are caused by the effacement of microvilli through the cleavage of anchoring proteins in the host cell (Lai *et al.*, 2011), followed by the production of actin-rich "pedestals" at the site of bacterial attachment. Both of these pathogens cause these cytoskeletal phenotypes by producing secreted effectors, including the translocated intimin receptor (Tir) protein, which is inserted into the host cell membrane (DeVinney *et al.*, 2001; Gruber and Sperandio, 2014). Afterwards, intimin proteins in the bacterial outer membrane bind to the Tir protein in the host membrane, leading to a dramatic rearrangement of the underlying host actin network to form the characteristic pedestals through recruitment of host actin nucleation proteins (specifically N-WASP and Arp2/3) (Gruenheid *et al.*, 2001). It has also been shown that both *Vibrio cholerae* and *Vibrio parahaemolyticus* have the capacity to modify the host actin

cytoskeleton through secreted effectors (Liverman *et al.*, 2007; Kudryashov *et al.*, 2008; Yarbrough *et al.*, 2009; Broberg *et al.*, 2010). However, in these *Vibrio* species, the capacity to alter the actin cytoskeleton typically leads to the death of the affected host cell, not simply the loss of its microvilli.

Perhaps more relevant to the squid system is the interaction that *Neisseria meningitidis* has with host cells. Upon binding to host cells through the production of type IV pili, *N. meningitidis* causes the elaboration of host microvilli, which the bacterium then uses to invade the cell. This increased microvillar elaboration and length are dependent upon the production of, and ability to retract, the type IV pilus (Higashi *et al.*, 2009). While Higashi *et al*. postulated that the microvillar elaboration may be due to the application of force to the cortical cell membrane by retraction of the pilus, the exact mechanism of signaling was not shown. Because our study showed that the application of exogenous lipid A could cause an increase in microvillar density (Fig. 5-6), it is possible that the retraction of a type IV pilus instead allows the cell to get close enough to the host membrane to present LPS or another effector to the host. While electron microscopy observations in the squid did not show any evidence for the elaboration of pili in the light organ (Fig. 5-2), a previous study in the squid/vibrio system provided evidence for a competitive advantage in colonization to those *V. fischeri* cells that produce a pilin subunit (Stabb and Ruby, 2003), and another showed that the *V. fischeri* genome encodes over 4 different Type IV pilin subunits (Ruby *et al.*, 2005), suggesting that pili may be important to the symbiosis as a whole. Further studies are needed to define what bacterial genes are needed for the effective presentation of LPS in the light-organ crypts.

The effect of MAMPs on the eukaryotic cytoskeleton

While most mechanistic studies of the effect of symbiosis on the host apical cytoskeleton have focused on bacterial effectors that directly manipulate the host actin network, several systems have found evidence for the manipulation of host cytoskeletal aspects by MAMPs. The largest body of literature on this topic involves the effect of LPS on the host's actin cytoskeleton. LPS effects seem to be specific to cell type, *i.e.*, LPS can lead to both assembly (abd-el-Basset and Fedoroff, 1995; Gutiérrez-Venegas *et al.*, 2008; Kleveta *et al.*, 2012) and disassembly (Isowa *et al.*, 1999) of the cortical actin array depending on the host cell. However, because all four studies were performed with purified LPS, it is not necessary for the whole bacterial cell to be present to induce this phenotype. The potential role of these actin rearrangements also appears to differ by cell type. In macrophages, the increase in actin filament formation contributes to cell motility (Kleveta *et al.*, 2012) while in microglia it is thought that the same filament formation instead leads to increased phagocytic activity (abd-el-Basset and Fedoroff, 1995). Because the elaboration of microvilli also requires the production of short actin filaments, it is possible that these studies represent a common response to LPS that can result in different uses depending on the cell type and role in the organism. It is also important to note that LPS is not the only conserved bacterial product that can modify the eukaryotic cytoskeleton. In addition to the potential role of pilins described above, secreted *Pseudomonas* flagellins, whether presented pharmacologically or by the bacterium, have the capacity to increase actin filament density in *Arabidopis thaliana* cells (Henty-Ridilla *et al.*, 2013), suggesting that the capacity of host cells to respond to pathogens with modification of the cytoskeleton may be a characteristic shared by many host-microbe associations. Because MAMPs are required for the normal development of large host structures such as gut-associated lymphoid tissue (Bouskra *et al.*, 2008), our work suggests that mutualists also signal the normal development of subcellular

structures such as microvilli. Future work in other systems will be needed to determine whether this trait is widespread, although the finding that probiotics can alter the number and morphology of host microvilli (Ringø *et al.*, 2007; Shukla *et al.*, 2012; Cerezuela *et al.*, 2012) suggests that it is.

Microvillar dynamics in the squid/vibrio association

This work further refines the model of the cycle of microvillar release and regrowth in the squid/vibrio association. Previously, it had been shown that symbiosis increases the microvillar density of cells in the light organ crypts in a reversible manner *i.e.*, upon symbiont depletion the microvillar density decreases back to aposymbiotic levels (Lamarcq and McFall-Ngai, 1998). In addition, symbionts modify the organization of the actin cytoskeleton in the ducts of the light organ upon symbiosis onset (Kimbell and McFall-Ngai, 2004). However, because microvillar density was measured at the same time every day, no influence of the day/night cycle could be measured. A different publication showed that in adult squid the crypt-cell microvilli and apical portions of the epithelial cells appeared to undergo a cycle of effacement around dawn, but a detailed timecourse was not defined at that time (Wier *et al.*, 2010). Our study merges both of these findings by showing that effacement occurs every day, even in juvenile animals, but is not dependent upon symbiosis. Rather, like microvillar renewal in photoreceptive tissue, the release of microvilli is caused by the dawn light cue (Fig. 5-8). However, regrowth of the microvillar border *is* dependent upon symbiosis, as aposymbiotic animals regrow the microvillar border to the same density as the previous morning every day, while symbiotic animals increase the maximum microvillar density each morning, at least in the first few days of symbiosis (Fig. 5-8). The fact that this increase in microvillar density can be

recapitulated with phosphorylated symbiont lipid A suggests that the previously seen daily cycle of alkaline phosphatase activity in the light organ (Rader *et al.*, 2012) may affect the ability of the symbiont cells to signal for microvillar elaboration in the light organ. Further studies into whether and how this interplay occurs are required to determine exactly how and when this signaling occurs.

This study proposes a new model for the cycle of microvillar release and regrowth in the squid light organ, as well as defining the squid as a new system in which to study the effect of MAMPs on the eukaryotic cytoskeleton. Future investigations will determine the signaling pathways activated by symbiont lipid A that participate in the increased elaboration of crypt-cell microvilli and the participation of circadian rhythms in allowing for microvillar renewal to occur. In the greater context of host-microbe interactions, our data provide further evidence that symbionts and symbiont-derived products are potent signals for the modification of the host actin cytoskeleton in both pathogenic and mutualistic associations.

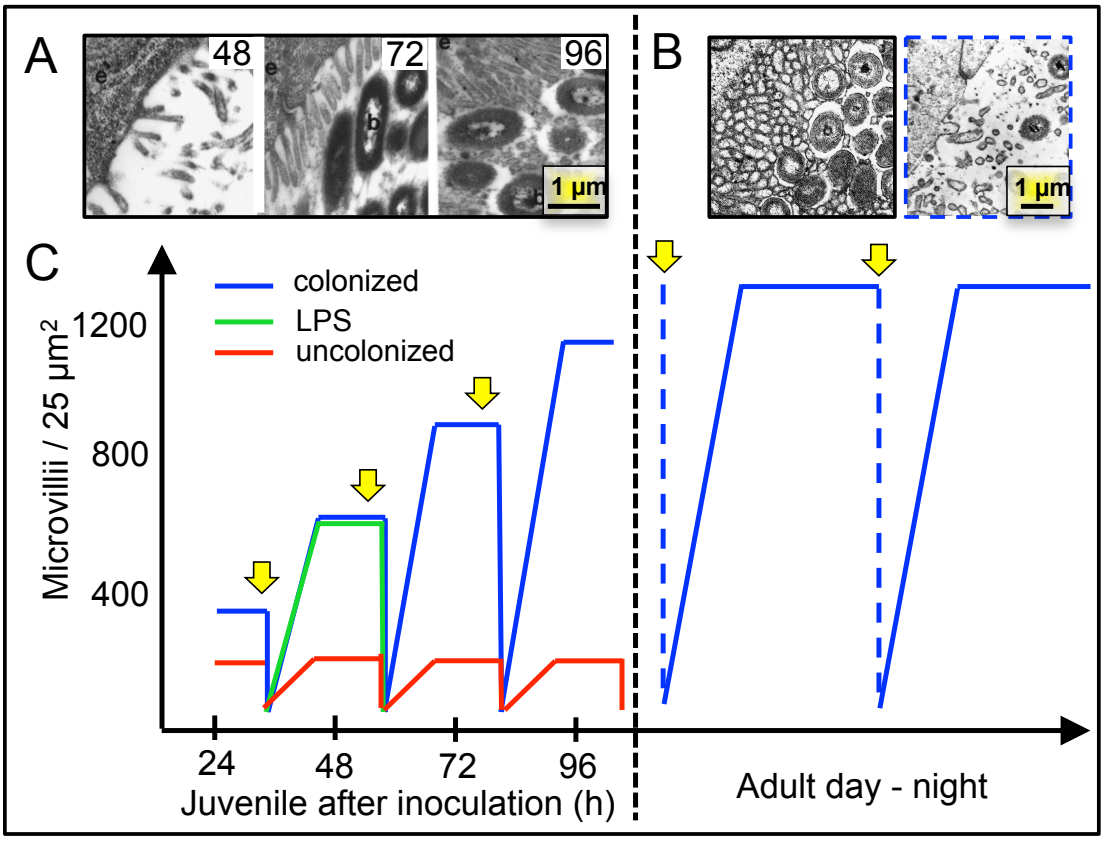

Figure 5-8: Model of microvillar dynamics in the squid/vibrio association.

(A and B): Example TEM images of juvenile (A) and adult (B) squid crypt microvillar borders.

(C): Model of microvillar dynamics in the crypt spaces of juvenile and adult animals. Yellow arrows denote the dawn light cue. Blue denotes animals colonized with wild-type bacteria, green denotes animals treated with LPS, and red denotes aposymbiotic animals.

ACKNOWLEDGEMENTS:

The authors would like to thank B. August and R. Massey for their assistance with TEM and E. Ruby for discussion of the manuscript. This work was supported by grants from National Institutes of Health (NIH) R01-RR12294 (to EGR) and R01-AI50661 (to MM-N), and National Science Foundation IOS 0817232 (to MM-N & EGR). EACH-H was supported by NRSA T-32 GM07215.

REFERENCES:

abd-el-Basset, E., and Fedoroff, S. (1995) Effect of bacterial wall lipopolysaccharide (LPS) on morphology, motility, and cytoskeletal organization of microglia in cultures. *J Neurosci Res* **41**: 222–237.

Altura, M.A., Heath-Heckman, E.A., Gillette, A., Kremer, N., Krachler, A.M., Brennan, C., *et al.* (2013) The first engagement of partners in the Euprymna scolopes-Vibrio fischeri symbiosis is a two-step process initiated by a few environmental symbiont cells. *Environ Microbiol* doi: 10.1111/1462-2920.12179

Altura, M.A., Stabb, E., Goldman, W., Apicella, M., and McFall-Ngai, M.J. (2011) Attenuation of host NO production by MAMPs potentiates development of the host in the squid-vibrio symbiosis. *Cell Microbiol* **13**: 527–537.

Bates, J.M., Akerlund, J., Mittge, E., and Guillemin, K. (2007) Intestinal alkaline phosphatase detoxifies lipopolysaccharide and prevents inflammation in zebrafish in response to the gut microbiota. *Cell Host Microbe* **2**: 371–382.

Battelle, B.-A. (2013) What the clock tells the eye: lessons from an ancient arthropod. *Integr Comp Biol* **53**: 144–153.

Boesze-Battaglia, K., and Goldberg, A.F.X. (2002) Photoreceptor renewal: a role for peripherin/rds. *Int Rev Cytol* **217**: 183–225.

Boettcher, K.J., and Ruby, E.G. (1990) Depressed light emission by symbiotic *Vibrio fischeri* of the sepiolid squid *Euprymna scolopes*. *J Bacteriol* **172**: 3701–3706.

Bose, J.L., Rosenberg, C.S., and Stabb, E.V. (2008) Effects of *luxCDABEG* induction in *Vibrio fischeri*: enhancement of symbiotic colonization and conditional attenuation of growth in culture. *Arch Microbiol* **190**: 169–183.

Bouskra, D., Brézillon, C., Bérard, M., Werts, C., Varona, R., Boneca, I.G., and Eberl, G. (2008) Lymphoid tissue genesis induced by commensals through NOD1 regulates intestinal homeostasis. *Nature* **456**: 507–510.

Broberg, C.A., Zhang, L., Gonzalez, H., Laskowski-Arce, M.A., and Orth, K. (2010) A Vibrio effector protein is an inositol phosphatase and disrupts host cell membrane integrity. *Science* **329**: 1660–1662.

Cerezuela, R., Fumanal, M., Tapia-Paniagua, S.T., Meseguer, J., Moriñigo, M.A., and Esteban, M.A. (2012) Histological alterations and microbial ecology of the intestine in gilthead seabream (*Sparus aurata* L.) fed dietary probiotics and microalgae. *Cell Tissue Res* **350**: 477–489.

Chichlowski, M., Croom, W.J., Edens, F.W., McBride, B.W., Qiu, R., Chiang, C.C., *et al.* (2007) Microarchitecture and spatial relationship between bacteria and ileal, cecal, and colonic epithelium in chicks fed a direct-fed microbial, PrimaLac, and salinomycin. *Poult Sci* **86**: 1121–1132.

DeVinney, R., Puente, J.L., Gauthier, A., Goosney, D., and Finlay, B.B. (2001) Enterohaemorrhagic and enteropathogenic Escherichia coli use a different Tir-based mechanism for pedestal formation. *Mol Microbiol* **41**: 1445–1458.

Doino, J.A., and McFall-Ngai, M.J. (1995) A transient exposure to symbiosis-competent bacteria induces light organ morphogenesis in the host squid. *Biol Bull* **189**: 347–355.

Duperron, S., Laurent, M.C.Z., Gaill, F., and Gros, O. (2008) Sulphur-oxidizing extracellular bacteria in the gills of *Mytilidae* associated with wood falls. *FEMS Microbiol Ecol* **63**: 338–349.

Durand, L., Zbinden, M., Cueff-Gauchard, V., Duperron, S., Roussel, E.G., Shillito, B., and Cambon-Bonavita, M.-A. (2010) Microbial diversity associated with the hydrothermal shrimp *Rimicaris exoculata* gut and occurrence of a resident microbial community. *FEMS Microbiol Ecol* **71**: 291–303.

Foster, J.S., Apicella, M.A., and McFall-Ngai, M.J. (2000) *Vibrio fischeri* lipopolysaccharide induces developmental apoptosis, but not complete morphogenesis, of the *Euprymna scolopes* symbiotic light organ. *Dev Biol* **226**: 242–254.

Gray, S.M., Kelly, S., and Robles, L.J. (2008) Rho signaling mediates cytoskeletal re-arrangements in octopus photoreceptors. *Am Malacol Bull* **26**: 19–26.

Gruber, C.C., and Sperandio, V. (2014) Posttranscriptional control of microbe-induced rearrangement of host cell actin. *MBio* **5**: e01025–13–e01025–13.

Gruenheid, S., DeVinney, R., Bladt, F., Goosney, D., Gelkop, S., Gish, G.D., *et al.* (2001) Enteropathogenic *E. coli* Tir binds Nck to initiate actin pedestal formation in host cells. *Nat Cell Biol* **3**: 856–859.

Gutiérrez-Venegas, G., Contreras-Marmolejo, L.A., Román-Alvárez, P., and Barajas-Torres, C. (2008) *Aggregatibacter actinomycetemcomitans* lipopolysaccharide affects human gingival fibroblast cytoskeletal organization. *Cell Biol Int* **32**: 417–426.

Heath-Heckman, E.A.C., Peyer, S.M., Whistler, C.A., Apicella, M.A., Goldman, W.E., and McFall-Ngai, M.J. (2013) Bacterial bioluminescence regulates expression of a host cryptochrome gene in the squid-Vibrio symbiosis. *MBio* **4**: e00167–13–e00167–13.

Henty-Ridilla, J.L., Shimono, M., Li, J., Chang, J.H., Day, B., and Staiger, C.J. (2013) The plant actin cytoskeleton responds to signals from microbe-associated molecular patterns. *PLoS Pathog* **9**: e1003290.

Higashi, D.L., Zhang, G.H., Biais, N., Myers, L.R., Weyand, N.J., Elliott, D.A., and So, M. (2009) Influence of type IV pilus retraction on the architecture of the *Neisseria gonorrhoeae*-infected cell cortex. *Microbiology* **155**: 4084–4092.

Isowa, N., Xavier, A.M., Dziak, E., Opas, M., McRitchie, D.I., Slutsky, A.S., *et al.* (1999) LPS-induced depolymerization of cytoskeleton and its role in TNF-alpha production by rat pneumocytes. *Am J Physiol* **277**: L606–15.

Kimbell, J.R., and McFall-Ngai, M.J. (2004) Symbiont-induced changes in host actin during the onset of a beneficial animal-bacterial association. *Appl Environ Microbiol* **70**: 1434–1441.

Kleveta, G., Borzęcka, K., Zdioruk, M., Czerkies, M., Kuberczyk, H., Sybirna, N., Sobota, A., and Kwiatkowska, K. (2012) LPS induces phosphorylation of actin‐regulatory proteins leading to actin reassembly and macrophage motility. *J Cell Biochem* **113**: 80-92

Koropatnick, T.A., Engle, J.T., Apicella, M.A., Stabb, E.V., Goldman, W.E., and McFall-Ngai, M.J. (2004) Microbial factor-mediated development in a host-bacterial mutualism. *Science* **306**: 1186–1188.

Kudryashov, D.S., Durer, Z.A.O., Ytterberg, A.J., Sawaya, M.R., Pashkov, I., Prochazkova, K., *et al.* (2008) Connecting actin monomers by iso-peptide bond is a toxicity mechanism of the Vibrio cholerae MARTX toxin. *Proc Natl Acad Sci U.S.A.* **105**: 18537–18542.

Lai, Y., Riley, K., Cai, A., Leong, J.M., and Herman, I.M. (2011) Calpain mediates epithelial cell microvillar effacement by enterohemorrhagic *Escherichia coli*. *Front Microbiol* **2**: 222.

Lamarcq, L.H., and McFall-Ngai, M.J. (1998) Induction of a gradual, reversible morphogenesis of its host's epithelial brush border by *Vibrio fischeri*. *Infect Immun* **66**: 777–785.

Liverman, A.D.B., Cheng, H.-C., Trosky, J.E., Leung, D.W., Yarbrough, M.L., Burdette, D.L., *et al.* (2007) Arp2/3-independent assembly of actin by Vibrio type III effector VopL. *Proc Natl Acad Sci U.S.A.* **104**: 17117–17122.

McCaffrey, L.M., and Macara, I.G. (2011) Epithelial organization, cell polarity and tumorigenesis. *Trends Cell Biol* **21**: 727–735.

McFall-Ngai, M., Nyholm, S.V., and Castillo, M.G. (2010) The role of the immune system in the initiation and persistence of the *Euprymna scolopes*--*Vibrio fischeri* symbiosis. *Semin Immunol* **22**: 48–53.

Montgomery, M.K., and McFall-Ngai, M. (1994) Bacterial symbionts induce host organ morphogenesis during early postembryonic development of the squid *Euprymna scolopes*. *Development* **120**: 1719–1729.

Montgomery, M.K., and McFall-Ngai, M.J. (1993) Embryonic development of the light organ of the sepiloid squid *Euprymna scolopes* Berry. *Biol Bull* **184**: 296–308.

Montgomery, M.K., and McFall-Ngai, M.J. (1998) Late postembryonic development of the symbiotic light organ of *Euprymna scolopes* (Cephalopoda: Sepiolidae). *Biol Bull* **195**: 326–336.

Nyholm, S.V., and McFall-Ngai, M.J. (1998) Sampling the light-organ microenvironment of *Euprymna scolopes*: description of a population of host cells in association with the bacterial symbiont *Vibrio fischeri*. *Biol Bull* **195**: 89–97.

Peyer, S.M., Pankey, M.S., Oakley, T.H., and McFall-Ngai, M.J. (2014) Eye-specification genes in the bacterial light organ of the bobtail squid *Euprymna scolopes*, and their expression in

response to symbiont cues. *Mech Dev* **131**: 111–126.

Post, D.M., Yu, L., Krasity, B.C., Choudhury, B., Mandel, M.J., Brennan, C.A., *et al.* (2012) O-antigen and core carbohydrate of *Vibrio fischeri* lipopolysaccharide: composition and analysis of their role in *Euprymna scolopes* light organ colonization. *J Biol Chem* **287**: 8515–8530.

Rader, B.A., Kremer, N., Apicella, M.A., Goldman, W.E., and McFall-Ngai, M.J. (2012) Modulation of symbiont lipid A signaling by host alkaline phosphatases in the squid-vibrio symbiosis. *MBio* **3**.

Ringø, E., Salinas, I., Olsen, R.E., Nyhaug, A., Myklebust, R., and Mayhew, T.M. (2007) Histological changes in intestine of Atlantic salmon (*Salmo salar* L.) following in vitro exposure to pathogenic and probiotic bacterial strains. *Cell Tissue Res* **328**: 109–116.

Ruby, E.G., Urbanowski, M., Campbell, J., Dunn, A., Faini, M., Gunsalus, R., *et al.* (2005) Complete genome sequence of *Vibrio fischeri:* A symbiotic bacterium with pathogenic congeners. *Proc Natl Acad Sci U.S.A.* **102**: 3004–3009.

Sacunas, R.B., Papuga, M.O., Malone, M.A., Pearson, A.C., Marjanovic, M., Stroope, D.G., *et al.* (2002) Multiple mechanisms of rhabdom shedding in the lateral eye of *Limulus polyphemus*. *J Comp Neurol* **449**: 26–42.

Shifrin, D.A., McConnell, R.E., Nambiar, R., Higginbotham, J.N., Coffey, R.J., and Tyska, M.J. (2012) Enterocyte microvillus-derived vesicles detoxify bacterial products and regulate epithelial-microbial interactions. *Curr Biol* **22**: 627–631.

Shukla, G., Sidhu, R.K., and Verma, A. (2012) Restoration of anthropometric, biochemical and histopathological alterations by *Lactobacillus casei* supplementation in *Giardia intestinalis* infected renourished BALB/c mice. *Antonie Van Leeuwenhoek* **102**: 61–72.

Stabb, E.V., and Ruby, E.G. (2003) Contribution of pilA to competitive colonization of the squid Euprymna scolopes by Vibrio fischeri. *Appl Environ Microbiol* **69**: 820–826.

Stark, W.S., Sapp, R., and Schilly, D. (1988) Rhabdomere turnover and rhodopsin cycle: maintenance of retinula cells in *Drosophila melanogaster*. *J Neurocytol* **17**: 499–509.

Tong, D., Rozas, N.S., Oakley, T.H., Mitchell, J., Colley, N.J., and McFall-Ngai, M.J. (2009) Evidence for light perception in a bioluminescent organ. *Proc Natl Acad Sci U.S.A.* **106**: 9836–9841.

Troll, J.V., Adin, D.M., Wier, A.M., Paquette, N., Silverman, N., Goldman, W.E., *et al.* (2009) Peptidoglycan induces loss of a nuclear peptidoglycan recognition protein during host tissue development in a beneficial animal-bacterial symbiosis. *Cell Microbiol* **11**: 1114–1127.

Troll, J.V., Bent, E.H., Pacquette, N., Wier, A.M., Goldman, W.E., Silverman, N., and McFall-Ngai, M.J. (2010) Taming the symbiont for coexistence: a host PGRP neutralizes a bacterial symbiont toxin. *Environ Microbiol* **12**: 2190–2203.

Wang, Y., Stingl, U., Anton-Erxleben, F., Geisler, S., Brune, A., and Zimmer, M. (2004) "*Candidatus hepatoplasma crinochetorum*," a new, stalk-forming lineage of Mollicutes colonizing the midgut glands of a terrestrial isopod. *Appl Environ Microbiol* **70**: 6166–6172.

Whistler, C.A., Koropatnick, T.A., Pollack, A., McFall-Ngai, M.J., and Ruby, E.G. (2007) The GacA global regulator of *Vibrio fischeri* is required for normal host tissue responses that limit subsequent bacterial colonization. *Cell Microbiol* **9**: 766–778.

Wier, A.M., Nyholm, S.V., Mandel, M.J., Massengo-Tiasse, R.P., Schaefer, A.L., Koroleva, I., *et al.* (2010) Transcriptional patterns in both host and bacterium underlie a daily rhythm of anatomical and metabolic change in a beneficial symbiosis. *Proc Natl Acad Sci U.S.A.* **107**: 2259–2264.

Wollenberg, M.S., and Ruby, E.G. (2012) Phylogeny and fitness of *Vibrio fischeri* from the light organs of *Euprymna scolopes* in two Oahu, Hawaii populations. *ISME J* **6**: 352–362.

Yarbrough, M.L., Li, Y., Kinch, L.N., Grishin, N.V., Ball, H.L., and Orth, K. (2009) AMPylation of Rho GTPases by Vibrio VopS disrupts effector binding and downstream signaling. *Science* **323**: 269–272.

Chapter 6

Synthesis and Future Directions

PREFACE:

EACH formulated ideas and wrote the chapter.

CRYPTOCHROME REGULATION BY SYMBIOSIS:

My thesis provides a foundation for the study of the effect of symbiosis on circadian rhythms and our knoepenswledge of day/night cycles in the squid/vibrio association. Using qRT-PCR and bacterial mutants defective in both light production and colonization level, I have shown that symbiont-derived light affects transcription of a host cryptochrome gene (Chapter 2). In addition, my study was the first to characterize cryptochrome genes in a mollusc, a major phylum whose circadian underpinnings are understudied. My study was the first to show that a symbiosis could entrain a circadian effector in the host, but was quickly followed by a publication from another group showing that the presence of gut symbionts in mice drastically affected the transcription of host circadian rhythm-associated genes (Mukherji *et al.*, 2013), suggesting that the regulation of circadian rhythms by symbionts may occur in many different associations.

Future Directions:

1. How is the circadian circuitry organized in *E. scolopes?*

   In my dissertation work, I sequenced and characterized the transcription of two cryptochrome genes in the *E. scolopes* light organ. Cryptochrome proteins are known blue-light sensors that act as inputs to the proteins that allow for free-running cycles to continue, called clock proteins. While there is one study detailing the sequence

and transcription of a molluscan clock gene called *period* (Constance *et al.*, 2002), the mechanisms underpinning circadian rhythms in molluscs have not been widely studied. However, physiological circadian rhythms have been well studied in several molluscan systems, specifically *Bulla gouldiana* and *Mytilus edulis*, to name two. However, as the constiuents and modes of interaction of clock proteins can differ greatly even within single Orders of animals (Tomioka and Matsumoto, 2010), it is important to define the circadian circuitry of molluscan systems to understand the breadth of mechanisms that exist in nature. To this end, I have identified two potential clock genes in *E. scolopes* transcriptional databases and determined that transcription of at least one (*timeless*) is regulated over the day/night cycle (Appendix B). Future experiments would include creating transcriptional libraries of the head and/or eyes, where circadian pacemakers usually reside, and determining what canonical components of circadian circuitry are expressed. Then through the production of antibodies one could determine which proteins interact with each other, and eventually, if reverse genetics became available, to determine which components are necessary for circadian entrainment.

2. Does symbiont activity affect other circadian rhythms in the symbiosis?

While transcriptional oscillators are the most well-known regulators of circadian rhythms, recent data have shown that a post-translational rhythm of the oxidation state of peroxiredoxin proteins may be the most evolutionary widespread circadian rhythm (Edgar *et al.*, 2012). Since it is likely that both the host and symbionts can

drive changes in the oxygen availability in the light organ (Boettcher *et al.*, 1996), it is possible that the symbiosis can affect this circadian cycle as well. Future experiments to address this possibility include: Using western blotting with an antibody specific to oxidized peroxiredoxin (from both the host and symbiont) to determine if the host and/or symbiont shows rhythmicity on the oxidation state of the protein; performing qRT-PCR analyses to determine if transcription of these genes is also regulated, as was suggested in Wier *et al*.; and deleting the protein from *V. fischeri* (if possible) to determine function or producing a transcriptional or translational fusion to see when and where the symbiont protein is produced.

DAY/NIGHT CYCLES IN THE SYMBIOSIS:

I have sought in this work to characterize three day/night cycles that were first suggested in a previous microarray study from the McFall-Ngai lab (Wier *et al.*, 2010). The first was a cycle of transcription of a gene of unknown function called galaxin. Using qRT-PCR, I determined that the cycle of high transcription during periods of symbiont growth occurred in both adult and juvenile squid and, using bacterial growth inhibition assays and a galaxin-specific antibody, I showed that the protein likely acts as a governor on symbiont growth during cell division. In addition to acting as a bacterial growth modulator during the maintenance of the symbiosis, I showed by immunocytochemistry that the protein may also act a selective force outside of the light organ during symbiosis initiation. While galaxins are expressed in many invertebrate animals, our study was the first to provide evidence for a function for a galaxin

protein. As this family of proteins is prominent in several host-microbe associations, our work may act as a jumping-off point for the study of galaxins as modulators of symbiotic systems.

Another major rhythm found in the Wier *et al.* microarray was a potential cycle of chitin production by the host and chitin breakdown on the part of the symbiont. While my work on the host genes that were regulated in the Wier *et al.* microarray were included in publications on which I am a junior author (Appendix A), Chapter 4 details my work on determining the source of chitin in the squid light organ. Using a fluorescent chitin-binding probe, I showed that in the juvenile squid light organ chitin localizes to the circulating immune cells, or hemocytes, to lysosomes or lysosome-like compartments. In addition, I showed that this character is not specific to the squid, and that staining for chitin granules may be a useful tool for the identification of invertebrate granulocytes in systems that do not yet have known granulocyte markers.

Finally, I characterized the daily cycle of microvillar release and regrowth in the light-organ crypt epithelial cells which interact with the symbiont population, the foundation for which was presented in two previous publications from the McFall-Ngai lab (Lamarcq and McFall-Ngai, 1998; Wier *et al.*, 2010). Using TEM, I showed that each day the light organ crypt cells undergo a process of light-induced microvillar release followed by a symbiont-induced increase in microvillar density. Using purified bacterial products and *V. fischeri* mutants defective in various cellular characters, I showed that the bacterial product necessary for microvillar regrowth is the lipid A portion of *V. fischeri* lipopolysaccharide and that treatment with alkaline phosphatase abolishes the capability of LPS to increase microvillar density in the light organ. To my knowledge, this study is the first to show that LPS can induce microvillar elaboration and also the first work to show conclusively that mutualists can induce the growth of microvilli. My

work also adds to the growing body of literature showing that the light organ crypt epithelium is physiologically convergent upon the eye, and suggests that microvillar renewal is a common trait of all photoreceptive tissue, not just of those photoreceptors that are located in the eye.

Development of new tools:

1. Fluorescent chitin-binding protein (CBP) as a marker for invertebrate granulocytes

   In chapter 4, I developed protocols for extracting and subsequently staining the immune cells of over eight invertebrate species for the presence of chitin-positive granules. By doing so I showed that fluorescent CBP can be used a marker for granulocytes in invertebrate species for which markers for these immune cells do not yet exist.

2. Juvenile *E. scolopes* hemocyte extraction and staining protocols

   With Bethany Rader, I developed a protocol for the extraction of hemocytes from juvenile animals (found in Chapter 4). In addition, we modified the existing ICC protocol from the McFall-Ngai lab for use on the extracted hemocytes to allow for localization of proteins and sugars using antibodies and labeled lectins.

Future Directions:

1. What is the sequence and function of EsGalaxin2?

   While in Chapter 3 I characterized the expression and production patterns of EsGalaxin1, I was not able to determine the full-length sequence of EsGalaxin2. However, the expression pattern of *esgalaxin2* suggests that it may be integral to the accessory nidamental gland symbiosis in adult female animals, and the idea that the galaxin transcripts may be symbiosis-specific is exciting. The first steps in determining function for EsGalaxin2 would be to determine the full-length coding sequence, and then to generate an antibody to allow for localization and inactivation of the EsGalaxin2 protein.

2. What is the mechanism by which LPS leads to an increase in microvillar density in light-organ crypt cells?

   In Chapter 5, I determined that LPS (specifically, lipid A) signals an increase in microvillar density in the light organ crypts. The signaling pathways by which the animal perceives this MAMP, however, remain unknown. There are known LPS-binding proteins (LBPs) in the light organ (Krasity *et al.*, 2011), which are theorized to interact with the Nf-κB pathway (Goodson *et al.*, 2005). The first set of experiments to explore whether the LPS-induced microvillar elaboration is through Nf-κB signaling would be to determine if LBP proteins are expressed in the light organ during the early morning hours, when elaboration is occurring, and if so, whether Nf-κB has been activated as measured by translocation to the nucleus.

Further experiments using Nf-κB pathway inhibitors would determine whether microvillar elaboration could be repressed if the pathway were inactivated.

SYNTHESIS:

"It's a cruel season that makes you get ready for bed while it's light out."

- Bill Watterson, *Calvin and Hobbes*

Although several associations show signs of circadian rhythmicity in transcription or behavior, the direct effect of symbionts on circadian circuitry is only beginning to be explored. In our recent study described in chapter 3, we proved that symbiont-provided light can directly influence the transcription of a host cryptochrome gene, the product of which is used to integrate light cues into the core circadian machinery in other invertebrates and plants (Heath-Heckman *et al.*, 2013). Our study represented the first instance of a mutualist directly affecting the transcription of a circadian effector in its host. Soon afterwards, however, Mukherji *et al.* demonstrated that in mice that had been treated with antibiotics the cycle of clock gene transcription in the gut was all but abolished (Mukherji *et al.*, 2013), showing that the phenomenon of symbiont-induced clock gene modulation is common to at least two model experimental animals. These studies represent the beginning of a new and exciting line of research into yet another way that symbionts are integrated into host physiology and shine new light on the importance of day/night cycles in symbiosis.

The understanding of the integration of symbiosis and circadian rhythms has profound implications for how scientific research should be conducted. Because the time of day can profoundly influence the outcome of both pathogenic and beneficial host-symbiont associations, researchers should be mindful of the time of day at which experiments are performed, and be sure to accurately record and report the timing of experiments. In this vein, animal facilities should also be maintained under day/night conditions as close to natural as possible in order to minimize the disruption of subject circadian behaviors. It is entirely possible that there are discrepancies in the literature due to the fact that different animal facilities are sometimes on different day/night cycle and irradiance regimes and that researchers will perturb the animals at different times of day to perform experiments.

One final important aspect of our increasing knowledge of the integration of circadian and immune functions is the potential that it has to improve our approach to human health. For example, transcription of the murine Toll-like receptor 9 gene is circadian and in a recent study this was shown to result in a diurnal fluctuation in vaccine efficacy (Silver *et al.*, 2012), introducing the idea that tuning vaccine delivery to a certain time of day may improve immunization outcome in humans. With the development of new treatments and technologies that can impact our microbial communities, such as fecal transplants and probiotics, it would behoove us as a community to understand and respect the interplay between symbiosis and our body's internal clock to ensure that these treatments are implemented as effectively as possible.

REFERENCES:

Boettcher, K.J., Ruby, E.G., and McFall-Ngai, M.J. (1996) Bioluminescence in the symbiotic squid *Euprymna scolopes* is controlled by a daily biological rhythm. *J Comp Physiol A* **179**: 65–73.

Constance, C.M., Green, C.B., Tei, H., and Block, G.D. (2002) *Bulla gouldiana* period exhibits unique regulation at the mRNA and protein levels. *J Biol Rhythms* **17**: 413–427.

Edgar, R.S., Green, E.W., Zhao, Y., van Ooijen, G., Olmedo, M., Qin, X., *et al.* (2012) Peroxiredoxins are conserved markers of circadian rhythms. *Nature* **485**: 459–464.

Goodson, M.S., Kojadinovic, M., Troll, J.V., Scheetz, T.E., Casavant, T.L., Soares, M.B., and McFall-Ngai, M.J. (2005) Identifying components of the NF-kappaB pathway in the beneficial *Euprymna scolopes*-*Vibrio fischeri* light organ symbiosis. *Appl Environ Microbiol* **71**: 6934–6946.

Heath-Heckman, E.A.C., Peyer, S.M., Whistler, C.A., Apicella, M.A., Goldman, W.E., and McFall-Ngai, M.J. (2013) Bacterial bioluminescence regulates expression of a host cryptochrome gene in the squid-Vibrio symbiosis. *MBio* **4**: e00167–13–e00167–13.

Krasity, B.C., Troll, J.V., Weiss, J.P., and McFall-Ngai, M.J. (2011) LBP/BPI proteins and their relatives: conservation over evolution and roles in mutualism. *Biochem Soc Trans* **39**: 1039–1044.

Lamarcq, L.H., and McFall-Ngai, M.J. (1998) Induction of a gradual, reversible morphogenesis of its host's epithelial brush border by *Vibrio fischeri*. *Infect Immun* **66**: 777–785.

Mukherji, A., Kobiita, A., Ye, T., and Chambon, P. (2013) Homeostasis in intestinal epithelium is orchestrated by the circadian clock and microbiota cues transduced by TLRs. *Cell* **153**: 812–827.

Silver, A.C., Arjona, A., Walker, W.E., and Fikrig, E. (2012) The Circadian Clock Controls Toll-like Receptor 9-Mediated Innate and Adaptive Immunity. *Immunity* **36**: 251–261.

Tomioka, K., and Matsumoto, A. (2010) A comparative view of insect circadian clock systems. *Cell Mol Life Sci* **67**: 1397–1406.

Wier, A.M., Nyholm, S.V., Mandel, M.J., Massengo-Tiasse, R.P., Schaefer, A.L., Koroleva, I., *et al.* (2010) Transcriptional patterns in both host and bacterium underlie a daily rhythm of anatomical and metabolic change in a beneficial symbiosis. *Proce Natl Acad Sci of U.S.A.* **107**: 2259–2264.

Appendix A

Additional Scientific Contributions

In addition to the work described within this thesis, I performed research that was incorporated into the following eight publications:

1. McFall-Ngai M., **Heath-Heckman E.A.**, Gillette, A.A., Peyer, S.M., and Harvie E.A. (2012) The secret languages of coevolved symbioses: insights from the *Euprymna scolopes – Vibrio fischeri* symbiosis. *Semin Immunol*, **24** (1):p. 3-8.

   Contribution: I performed the quantitative immunofluorescence using the EsPGRP2 antibody confirming that animals colonized with the Δ*lux* strain of *V. fischeri* were deficient in PGRP2 secretion into the crypt spaces. In addition, I supervised and performed the data analysis for hemocyte counting experiments performed by A. Gillette, a high school student in the lab, showing that Δ*lux* and TCT secretion mutants (strain DMA388) were deficient in hemocyte traficking through independent pathways.

2. Mandel M.J., Schaefer A.L., Brennan C.A., **Heath-Heckman E.A.**, Deloney-Marino C.R., McFall-Ngai M.J., and Ruby E.G. (2012) Squid-derived chitin oligosaccharides are a chemotactic signal during colonization by *Vibrio fischeri*. *Appl Environ Microbiol*, **78** (13): p. 4620-6.

   Contribution: Using the chitin-binding probe and protocols from Chapter 4, I localized chitin in the juvenile light organ to regions near the light-organ ducts,

showing that the localization is consistent with the chitobiose gradient implied in the rest of the paper.

3. Chaston J.M., Murfin K.E., **Heath-Heckman E.A**., and Goodrich-Blair H. (2013) Previously unrecognized stages of species-specific colonization in the mutualism between *Xenorhabdus* bacteria and *Steinernema* nematodes. *Cell Microbiol*, **15** (9): p. 1545-59.

   Contribution: I assisted K. Murfin in the acquisition of confocal micrographs documenting new stages in the progression of the *S. carpocapsae – X. nematophila* symbiosis.

4. Altura M.A., **Heath-Heckman E.A.C**., Gillette A., Kremer N., Krachler A.-M., Brennan C.A., Ruby E.G., Orth K., and McFall-Ngai M.J.. (2013) The first engagement of partners in the *Euprymna scolopes – Vibrio fischeri* symbiosis is a two-step process initiated by a few environmental symbiont cells. *Environ Microbiol* Epub ahead of print doi: 10.1111/1462-2920.12179.

   Contribution: I performed experiments showing that the Δ*mam7* mutant does not exhibit a defect in binding to the light-organ cilia as compared to wild-type *V. fischeri*. In addition, I supervised and performed the statistical analysis for the hemocyte counting experiments performed by A. Gillette.

5. Kremer N., Philipp E., Carpentier M.-C., Brennan C.A., Kraemer L., Altura M.A., Augustin R., Haesler R., **Heath-Heckman E.A.C.**, Peyer S.M., Schwartzman J., Rader B., Ruby E.G., Rosenstiel P., and McFall-Ngai M.J. (2013) Initial symbiont contact orchestrates host-organ-wide transcriptional changes that prime tissue colonization. *Cell Host Microbe* **14** (2): p. 183-194

   Contribution: I generated and validated the *E. scolopes* chitin synthase (EsCS1) antibody used in the study, as well as assisting with sample collection and preparation for the RNASeq experiment in the manuscript.

6. Koropatnick T., Goodson M., **Heath-Heckman E.A**., and McFall-Ngai M.J. (2013) Identifying the cellular mechanisms of symbiont-induced epithelial morphogenesis in the squid-vibrio association. Accepted to *Biol Bull*

   Contribution: Using an antibody to *E. scolopes* Chitotriosidase 1 (EsChit1) that I generated, I performed immunocytochemistry on juvenile light organs, showing that the protein localizes preferentially to one side of the anterior appendage.

7. Altura M.A., Kremer N., **Heath-Heckman E.A.C.**, Gillette A.A., and McFall-Ngai M.J. (Expected 2014) Soluble guanylate cyclase-like proteins are expressed in the

Euprymna scolopes light organ and play a role in MAMP-induced apoptosis. Submitted to *Biol Bull.*

Contribution: With Amani Gillette, I performed RACE on the guanylate cyclase-like proteins to confirm spice variants and also performed sequence analysis for the paper. I also re-formatted the figures to better conform to the journal style after submission.

8. Schwartzman J., **Heath-Heckman E.A.**, Zhou L., Koch E., Kremer N., McFall-Ngai M., and Ruby E. (Expected 2014) Provision of nutrients by host immune cells drives symbiont metabolic and physiological rhythms over development and time in a model mutualism. In preparation for submission to *PNAS*

Contribution: I assisted J. Schwartzman with experimental design for the manuscript. I also generated and validated (through western blotting and ICC) the EsCS1 and EsChit1 antibodies and designed the qRT-PCR primers for all host genes probed in the study. I also determined the sequence of *eschit1* and annotated its putative domain structure and phylogenetic position within the family of proteins.

Appendix B

Identification of Period and Timeless in the *E. scolopes* Light Organ

PREFACE:

EACH and MMN formulated ideas and planned the experiments. EACH performed all experiments and writing.

Cryptochromes are blue-light receptors that serve to entrain the core clock circuitry to the cycle of exogenous light, usually sunlight. While our study of cryptochromes in the *E. scolopes* light organ showed that transcription of at least one of the cryptochromes expressed in the light organ could also be altered by the presentation of bacterial blue light. However, no investigation of the so-called "core" clock genes (those making up the central oscillator which cryptochromes can entrain) has been made in the squid system. Cryptochrome proteins directly interact with the period-timeless heterodimer in systems such as *D. melanogaster* (Fig. B-1), making these proteins a logical starting point. In addition, only one of these proteins (Period) has been characterized in a mollusc (Constance *et al.*, 2002), suggesting that characterization of these core clock components in the Mollusca is important for understanding the various roles of the proteins in the invertebrates.

EsPeriod

To identify Period in the light organ, we searched a recent RNASeq database (Natacha Kremer, unpublished) for transcripts annotated as Period or Period-like. Once we identified a potential transcript (Figure B-2) we determined the open reading frame using the ExPASy Translate tool (Figure B-3) and then used the NCBI BLAST utility to determine that the proteins with the highest BLAST hits were also confirmed period proteins. The top BLAST hit was *Crassostrea gigas* (oyster) period, with an E-value of $5e^{-103}$. Using InterProScan 4 (http://www.ebi.ac.uk/Tools/pfa/iprscan/), we identified several functional domains conserved in period proteins, including two PAS (Per/Arnt/Sim) domains, a PAS C-terminal domain, and two period domains. In addition, we identified a putative nuclear localization signal using cNLS Mapper (http://nls-mapper.iab.keio.ac.jp/cgi-bin/NLS_Mapper_form.cgi), suggesting that the

protein can localize to the nucleus, which is essential for function in other systems (Chang and Reppert, 2003). However, due to the fact that the transcript shown here has not been verified by PCR or RACE, one or more of these steps will be necessary to validate the transcript sequence.

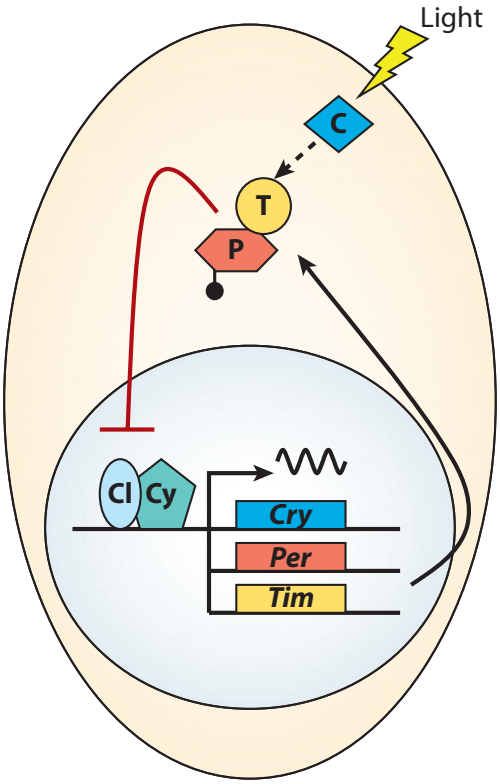

Figure B-1: Cryptochrome interactions with Period and Timeless in *D. melanogaster*. Beige denotes the cell cytoplasm, with the nucleus in gray. Cryptochrome (C or Cry) is shown in blue, Period (P or Per) is shown in red, and Timeless (T or Tim) is in yellow. The transcriptional activators Clock (Cl) and Cycle (Cy) are also pictured. Upon exposure to light Cryptochrome can bind Timeless, leading to its degradation and allowing Clock and Cycle to induce transcription of the three genes pictured. However, in the absence of light, the Timeless-Period heterodimer can bind Clock and Cycle, leading to the inhibition of transcription of *cry*, *per,* and *tim*. Figure adapted from Chaves et al. 2011.

ATGACCACCCATCGACAAGCGGATGCAGTAGCATGCATCTTACTGGTCACGAAGTTA
AGAAACTCAAGAAAGAGAAAGTGAAGGCCTACATTCAGCAAATCAAATCTATGGTG
CCGCCGTCCAAGGAGCGTGGCAAAAAAAACTGGCACATTAAAAGCATTACAGCATG
TCATTGATAAGCTAAAAAATTTGAAAGAAAGCAAGAATGAATCTAAATTCAATTCC
GGTGACGATAGTGCCGCCGGAAGTGTCAGCCAGTACAGTGGCAGTAGTCTTGCACA
AAGTACAGAAATCGAAAGGAAACCACAAAAGGAATCCTTCCAGGTTGCTGTTACAC
TGGACTGTCGGGTGGAATCGGTTGACTCTGCCTTGCTAGAATATCTTGGCTATCCTA
AAGATAGCTGGCATGGACATCTGCTGACGAGTTTCACATCCCGAAAGGACATCATA
ACGGTAAACAATCTGTCAAAGAATGAAAGTGTCTTCAAAAGATTTACCGATCCTGG
AGGAACAGCAAACCAAAAGGAAAAAGTGATTTATTTCCGACTACGGTATTACAAAC
ATTTGAACGAAGGCTACGGTCTAAAACGGCCAGACAGGTTCTGTGCACTACAAGCA
TCTGTCACGACACAAGTCATCGACACACCTCCATCTGAGAAAGATCGAGGTGATGC
CTCAGGCATGAAAAAGACAAAACATTTTATCCTAAAATGCGTCCCTCTTCATTCCGC
TTATATTGTCGGTTCCTTGCCCAAAAATTTTTCATTTTCAACAACACATACACTTTAC
TGCAACCTTAATTATGTCAGTAACAGTTCTATCGCGCTGCTGGGTTTCCTGCCACAA
GATTTGATCGGGCTTTCTGTATTTGACTTGTACCACCCAGATGACTTGCCGTACCTCT
ACACGGCTTATCAGCGAATTGTCTCTTCAAAAGGCAAAGCGTTTAAGAGTGAGCCTT
ACAGAATGCGCACACGGAATCAGAACTGGGTCTATGTTGAGACTGAATTTTCCGGCT
CAGTCAATCATTGGTCCAAGTGGTTTGAACATATCAGTGGGCAACACACCGTTGTCA
GAGTGCCCGAAAATCCTAATGTCTTCGACGAAGAGAACAGCAAAGCGAGCCCAATC
TTGTCGGATGAAACTCAACTTCAACAACAGAAACTTCAAAGGAGGATTCAGGATCTT
TTACTGCAACAGACGACGAGTGATGACTCTGCTATCATCACGCTGCCATCAAAACCA
TCCACGTCCTTCGATGTTGCAACCACTGCTGTCATGTCAGCTAAAGAAACCGACGCT
ACACCTAATCTAGGCAAAAAATGTGAGGGTAAATCGAAAGAAGCACTAATGACTGC
TGGCAGTTTTGTTGAAGAAGTCATTCGCTGTCAGAATGATGGTAATATCAGCCCTGC
AGTGTCTCATTCCAGTTCTCCTCAAATTATCTTCGACTCAGACACTTCCATTACGTAC
GAGCAACTCAACTATTCTTATAATATCAAAAGGTTTTTGCTGAGCCAACCGAAAACT
TATCACTCGGATAACTCTGACCAAGAAGATGCAAAACTCACCAGTCTGAAAGATGT
GAAAGAAGTTCTGGATGCAAAACACCCAAAACTGTTTAGCAATAGTGATGTCTGCG
GAGATGCTGATTTTGCTTCAGTGGATATTCCAATCCTTAATCCTCCAAGTTTTGGTAG
CAGTACAAAGGTTTTAGTGTCTGACCAAGAACCAAGAGAAACTACCAGCCCACCAG
CCGACGAGTATTTTGAAGACTTCATTATCCACAAAGAACTCTCCCAACCAAACCAGG
TCTTTTCTGACGGACAGAATCTGTACCAACCCGTTGCTCTCACACCAGAAGTGCTAC
GAATGCACACCAAGTTCCAAGAACGTTTATACGTCCAACAGGCCACAAGTGATTCC
AGTTTATTCGAGCTCGACCGTGGTAACAGCTCGGACAATAGTGGCAATAGCAACGT
GAAACGTTCAAAGCGGCACTTGCCCAATAGCGGTGAGCCAGACACTTATTCGCATC
AGCTGAAAGTGCCCCGCTTCGAGGATCCTTACATGTCAGCCAGCAATTTACAGCAAC
AGCAGCAGCAAAATACAATGTCGAGCTCCCAGACGAAACCTGGGTCATACTTTAAC
AAGCAACAATCATTCTTTCGTCCTTCCATCCCCGTTAGCATGTCCTATCCCAAGTTTT
CACCGCAGCCCAATTTCCAAAACATTCATAATACATTTCAACAATACCAACAGCCAA
AACTAGGACTGTATTCACAGGCAATTCCGATGTTGTCGTACGATACAACAATTCACA
TGACCACAAACACGACAACGTCAACAACCACACAAAAGAACTATTCTTCCAATACA
ACTGCTAACTCACTATCAAACACCTACTGGCCTTGTTATACCCAAACAGGAATGTCA
TTCATGCCGACTCAACTCGTAGGAGGCACTCAGTTGATGGGAGGTTTTTATCAACCA
ATGCCCGGAATGTTCCAGACGTTTGCCACACCGATTCCTTACCCCACAAATTTACCC
AGTATGGCAAATAAAACACCAGGCCCAGTACAAAATTCGACGACCCCTCCATCAGC

AATGCATCTGAAGACCTCGATTTCTTCCAATTTGAATAAACACGAATCACTGAAACA
ACCATCCAAAATCTCTGAAAGTACCGGCAGCACCTCATCACAAGAAGAGACCAGTT
CATCATTATTATATCTATTAGAGACTGGAAGCTACAACACAACCCCCTCTCCACCAC
CTGATGATATTGAAAAACTGAGGGGGAGCAGACGACTTCCACGCGATCCATTCTGG
CTCCAGAGTACAAACTGGTCGTCCAATATCCGCATGAAGTACACGGTGCCACAAAA
GTCGATGAAGCGTGTCCTTAAAGAGGATAACGAGAAACTGAATTCCCTTTATCAGCC
GAAACCGCTGCTGGAACAGCTGAAAGATCTCAAAACACGAAACATGCCGGTTATTA
ACGAAGAAGATGATTTCCTGATATTCTTCAATCAGTCGACCCAACTGAGCGAGTCCC
AGCTTAAAGAGGAGGAGGAGGAAAAAGAGGAAGCGAATACCTCTACCTTGTCTCTG
AAAGGGGAGGACGAGGATGTCGACTCAGAGATTGTGATGTTTGTATCAGACGACGT
GCAAGAAGAGTCGATGAGGAATATTTCGAGAGAAAAGTCTGAGAAAAACCTCGAA
GTTGAGAGCAAGGAGAAAAGCGAATCGAGTGACAATGACGACGACAAGTCGGACA
GTTCGTCGAAAAACTCAAGTTGCCTCACCTCGAGTGACCAGAGAAGCAACGAAGAA
GCTGGTAGCTCTCTGAAAGAATCCGACGGCGCTTCAAAGGAGTCTGACTCTGGTTCT
AAAGAATCCGACAATGGAAGCGGGGAAGAAAACAAAGCTGACCAACGGCCGGTCA
TAGAGAAGGTCGATTACGCAAGCTTCCATGAGTTGTTCATTCCATTGACCTTGCGTA
TGAGCAAAAAACATGAGGAGGAACACAAGCTGGCAAAGCTTCCGCACTGGAGAAT
GGAGGCACATTTGACGAAGAACATAGAAATGAACTATCAACTCAGCTCCAAGGATT
TGAGCAATGTGCTTGAGGCTGACCGAAGGCGGATGACAGGCTTAGAACAACCAAGT
CTAGTTAAAGAACAATTACAGGTTCTCTTGAGTGAAATAAGCACTCAGGAGAACAC
GGATGCTGCATCTTTCATTGTAGCCGATAGCTGCTGCGGTGTTACTGGGTCTACAAC
CACATCGCTTTCAACTTCAGCATCCAAAGTCGATGATCAAAATGTTAAATCTTCGCA
TTCCCATTCTTTTCCGTTTCCCGCTGAATGTAAAACTTTGGCAGCATCATTCGAGTCA
ATGGATGTAGACATCGTATCGCACAAGAGTACAGAAACAACAAAGGACACTGAAAA
TGTTGTTATAGACTTTAAGAAAATTTGTCCCCCTCTACAGGATTCTGAGTCTGCTTTG
TGGGACCAGGAACCTGAAGAAGATGTTGTCATGTCATCGCCACACAATCCGAACAC
TACAATTGTTGCCGGGTCTTCTTTGCATGCCCCGGAATCTTCAAATATGGAAACGTC
ACAAACATGGACTTGCGAGTCAGCCATTTCTGAGTCCAAAGGTTCTGGAGATGCAA
GCACATCTTTACCAACCAAAACTACAGACTGTAAAGATACAACAACACTCCCACAC
CGATCTCACTTTGAGACTTCATCATTGCCAATGAGCACGACAGCGGAAACTTCTAGT
TCGTCAACTGCAAAAAATATGCCAGCTGCCAATGACTCTATTAAATTAAGCGTCAGT
CCAGAGATGGATGATGTATTTGAAAAACTTTTCACTACATCCACGGCAGAAGACATA
TCTACTTTCTAA

Figure B-2: Nucleotide sequence of EsPeriod. The sequence is shown 5'-3' and the putative start and stop codons are shown in red.

MTTHRQADAVACILLVTK**LRNSRKRKKRPTF**SKSNLWCRRPRSVAKKTGTLKALQHV
IDKLKNLKESKNESKFNSGDDSAAGSVSQYSGSSLAQSTEIERKPQKESFQVAVTLDCRV
ESVDSALLEYLGYPKDSWHGHLLTSFTSRKDIITVNNMLSKNESVFKRFTDPGGTANQK
EKVIYFRLRYYKHLNEGYGLKRPDRFCALQASVTTQVIDTPPSEKDRGDASGMKKTKHF
ILKCVPLHSAYIVGSLPKNFSFSTTHTLYCNLNYVSNSSIALLGFLPQDLIGLSVFDLYHPD
DLPYLYTAYQRIVSSKGKAFKSEPYRMRTRNQNWVYVETEFSGSVNHWSKWFEHISGQ
HTVVRVPENPNVFDEENSKASPILSDETQLQQQKLQRRIQDLLLQQTTSDDSAIITLPSKP
STSFDVATTAVMSAKETDATPNLGKKCEGKSKEALMTAGSFVEEVIRCQNDGNISPAVS
HSSSPQIIFDSDTSITYEQLNYSYNIKRFLLSQPKTYHSDNSDQEDAKLTSLKDVKEVLDA
KHPKLFSNSDVCGDADFASVDIPILNPPSFGSSTKVLVSDQEPRETTSPPADEYFEDFIIHK
ELSQPNQVFSDGQNLYQPVALTPEVLRMHTKFQERLYVQQATSDSSLFELDRGNSSDNS
GNSNVKRSKRHLPNSGEPDTYSHQLKVPRFEDPYMSASNLQQQQQQNTMSSSQTKPGS
YFNKQQSFFRPSIPVSMSYPKFSPQPNFQNIHNTFQQYQQPKLGLYSQAIPMLSYDTTIHM
TTNTTTSTTTQKNYSSNTTANSLSNTYWPCYTQTGMSFMPTQLVGGTQLMGGFYQPMP
GMFQTFATPIPYPTNLPSMANKTPGPVQNSTTPPSAMHLKTSISSNLNKHESLKQPSKISE
STGSTSSQEETSSSLLYLLETGSYNTTPSPPPDDIEKLRGSRRLPRDPFWLQSTNWSSNIR
MKYTVPQKSMKRVLKEDNEKLNSLYQPKPLLEQLKDLKTRNMPVINEEDDFLIFFNQST
QLSESQLKEEEEEKEEANTSTLSLKGEDEDVDSEIVMFVSDDVQEESMRNISREKSEKNL
EVESKEKSESSDNDDDKSDSSSKNSSCLTSSDQRSNEEAGSSLKESDGASKESDSGSKES
DNGSGEENKADQRPVIEKVDYASFHELFIPLTLRMSKKHEEEHKLAKLPHWRMEAHLT
KNIEMNYQLSSKDLSNVLEADRRRMTGLEQPSLVKEQLQVLLSEISTQENTDAASFIVAD
SCCGVTGSTTTSLSTSASKVDDQNVKSSHSHSFPFPAECKTLAASFESMDVDIVSHKSTE
TTKDTENVVIDFKKICPPLQDSESALWDQEPEEDVVMSSPHNPNTTIVAGSSLHAPESSN
METSQTWTCESAISESKGSGDASTSLPTKTTDCKDTTTLPHRSHFETSSLPMSTTAETSSS
STAKNMPAANDSIKLSVSPEMDDVFEKLFTTSTAEDISTF

Figure B-3: Amino acid sequence and domain structure of EsPeriod. PAS domains are yellow, a PAS C-terminal domain is green, and Period domains are highlighted in magenta. A putative nuclear localization signal is shown in red text.

EsTimeless

To identify Timeless in the light organ, we BLASTed the existing EST database (Chun *et al.*, 2006) and a recently published RNASeq database (Kremer *et al.*, 2013) using *D. melanogaster* Timeless as the subject. Once we identified a potential full-length transcript (Figure B-4) we determined the open reading frame using the ExPASy Translate tool (Figure B-5) and then used the NCBI BLAST utility to determine that the proteins with the highest BLAST hits were also confirmed period proteins. The top BLAST hit was *Clunio marinus* (midge) Timeless, with an E-value of $2e^{-62}$. Using InterProScan 4 (http://www.ebi.ac.uk/Tools/pfa/iprscan/), we identified a Timeless domain, which is a region that is found in Timeless proteins.

To determine if the *estimeless* transcript is expressed in a cyclical manner, we performed qRT-PCR on RNA extracts from wild-caught adult squid light organs collected at four different times over the day/night cycle (Chapter 2) using primers specific to *estimeless*. We found that *estimeless* transcription varies significantly over the day/night cycle with a four-fold upregulation between 2 and 14 h after dawn (Figure B-6). These data suggest that *escry1* is not the only circadian-associated gene to be differentially regulated over the day/night cycle in the light organ, and due to the fact that the time of maximum transcription is the same as what we described for *escry1* in Chapter 2, it is possible that Timeless is regulating the transcription of *escry1* as is shown in other systems. However, since circadian circuitry can vary drastically between even closely related invertebrate species (Tomioka and Matsumoto, 2010), it will be necessary to validate the role of both EsTimeless and EsPeriod in the circadian clock of the squid.

ATGAAATTTTTTGCTTTAATTCTAAAACTGCTGTCCAACTTGACTCAATCCCTTGACT
GCCTCTTTCCACAAAGTTTCCAGCAGAATTCAATGAATGCTGAAATCATGGAGAGCA
TAGTTAAACTTTTGCAAACAATTAAACTCCTTTTTTGCCAACAACAAAATCTCGACA
GATTATTCTACCTTGTTAAGCCGATCATTTACAAGGGAGAAGATAAAGAAATCATCA
ACCAATTCCTATTGCTCGTCCGAAACCTTTTATACATTCAAGTATGGGACAGAATGA
GTGGTCCGGCGGATATTCAGTGTAAATTTATTAAAAATATGTTTGAGTGTGAATTGG
ATGAGATACTGTTGTCACTGCTTGCCCACCCATCAAAGATATATTGGGGAGTGATCA
TCGTTCAGACGTTGTCGCTGCTTTTTACTGATCAGAGTGTTTTGGCTGGGCTGAATGT
TCCCGAAAGCAAAGTGTCTGAAGATATAATTTTCAATGCTGACAATTGTGAAGTGAT
CTCTGTGATGATGGAAGCCGACAGAAATATTGCAAGCCGGGCACCTGTCCGGGACC
ACATTCGGATGCAGTTAGTAGCCATTTTGAAGTCTTTTAATTCTCGATTCTTGATGAG
CGGCTTTAGCGGACTTGTTTCTGATTTGAAGGAGATTTTGATTTCCAAGGATTGTAAC
TTTGATGGATCCTACTTCATGTGGCTGGTCATGTTCTTTCTACGAATTTCTAGAGTTT
CAGAAATGAATTTTGTTTATATCAGAGACGTGATTTCCATTGATACTGTCGGTTTCTT
AGTTTACATGGGTGTCAGTACTCATGAGGAAATACTGATCGGAGAGCAGAAGAAAT
TGGACGTTAGTTCCAAAAAGATGAAGCTGCATTTTACTATTGCATCCATAAAGGAAC
TCTTGAAGACTCTAGAGACTTATGACAACCATTTGTGCCATTCTGTCTCTGCAGAAG
ATCGACACACAATCAAAGAACTCAAAAGAACGCTGATCAACATGACGGATCTCCGC
CAACTGTTTCTGTTCTTAATCCGCAACAGCCACAACCAGAGACTCTCTTTTGTCCGCG
ATGTGATTATCACCAATCGTGTGTATCTCTTATTGCTTGATCGATGGATCCGTGAAGA
AAATGACGTCTCCGTTAATTTTGAAATGGTGCAACATATAAACCAATTTGCTAGCAT
TTCTGCCATGCAACAGTACGCCCGCCTCTTGGAGAATTTTGACAACAACAGTCACGC
AGTAAATGACAGCATTTTTACAATGATGCATCATGTTGCAGGCGACTGCAACAATCC
CGAGGTCCTCATGCAAATGCCGATCCTAAAAATATTTACAGACCTTTGCGATGACAA
CAAATTCATTTCAAATGAAGCCGAGGATTTGATGGAGTACATAATTCACAAATTCAT
GACGACAGCAGCAGAAGATCCTGCCCTTTGTACTAAATATTTGTTCAGCATGGAAAT
GAGAAACATCCACACAGAAGATGAGGAAAGTTCTAATGACACTGATTCTGAGATGT
CGGCTTATTCAAACTCCGAGTTTTTACCGAGCAGCCCCAAAGATGAGAGAGCGAGTC
CACCTCCAAACGATGAGATGGAAGAAGTCGACGAAAGCGTAATAATGCAGGCGTTG
GAAAAACAACTTGAACACTTAAGCGAGGAAAGCATCATCAAATTCTGCATTCAAAA
ATTACACAATGACGGCATGGATTACCAGCTTCTTTGGCTCCAAACTGTTCTTCTTGAG
ACGTGCTTCATCAAATACGTTGGTACATCACCTGAAAGCAACCAGATTGAAGAGCC
GGTCCCGTTATATTATTCCTTACAAAACAGAGATATTCCACTTATTCCTTACAACGAT
CGGCAGGAGGCAGCTCTTGAAGACAAATTCTTCCATTTACTTCTTAAATATCTTGGA
TTTAAGTCTGGTGCAGAAGGCAACACAATTTACCCTAGAATTCCAGAAGATGTCACA
GCGGAACAACTTTTATCGAAAGCCCGGGAAATGGGAAATATTAAATTTGATATGGC
AGAGAGCAAAAGTCCAGAAAATCTACGTTATCAGCAGATGCAGTTGAAACGAGTCC
GTGGAGTGCATAGGAAATTAGTGGACGTGTTAGAAAATGGCGATGCATCCTCCAAA
CGATGGATTCATCGGATGATGTCGTTAAACAACATGGACATCTTTGAGGAAAAAGA
TAATGAAAGAAAACATATTGCAGAAGCGAAAATAGAATTGTCGCCTTTGAAGTCGT
TCAACAAGGATTCTCACCTTTTGGAAAACAAGGTCATTTCCATCATGGCTGACCGAG
CACAGTCTCAGTTGCCATATTGGTTAAATCAAGGCCAACAGGGGATGGTTGGATTCT
GA

Figure B-4: Nucleotide sequence of EsTimeless.

MKFFALILKLLSNLTQSLDCLFPQSFQQNSMNAEIMESIVKLLQTIKLLFCQQQNLDRLFY
LVKPIIYKGEDKEIINQFLLLVRNLLYIQVWDRMSGPADIQCKFIKNMFECELDEILLSLL
AHPSKIYWGVIIVQTLSLLFTDQSVLAGLNVPESKVSEDIIFNADNCEVISVMMEADRNIA
SRAPVRDHIRMQLVAILKSFNSRFLMSGFSGLVSDLKEILISKDCNFDGSYFMWLVMFFL
RISRVSEMNFVYIRDVISIDTVGFLVYMGVSTHEEILIGEQKKLDVSSKKMKLHFTIASIK
ELLKTLETYDNHLCHSVSAEDRHTIKELKRTLINMTDLRQLFLFLIRNSHNQRLSFVRDVI
ITNRVYLLLLDRWIREENDVSVNFEMVQHINQFASISAMQQYARLLENFDNNSHAVNDS
IFTMMHHVAGDCNNPEVLMQMPILKIFTDLCDDNKFISNEAEDLMEYIIHKFMTTAAED
PALCTKYLFSMEMRNIHTEDEESSNDTDSEMSAYSNSEFLPSSPKDERASPPPNDEMEEV
DESVIMQALEKQLEHLSEESIIKFCIQKLHNDGMDYQLLWLQTVLLETCFIKYVGTSPES
NQIEEPVPLYYSLQNRDIPLIPYNDRQEAALEDKFFHLLLKYLGFKSGAEGNTIYPRIPED
VTAEQLLSKAREMGNIKFDMAESKSPENLRYQQMQLKRVRGVHRKLVDVLENGDASS
KRWIHRMMSLNNMDIFEEKDNERKHIAEAKIELSPLKSFNKDSHLLENKVISIMADRAQS
QLPYWLNQGQQGMVGF

Figure B-5: Derived amino acid sequence and domain structure of EsTimeless. Timeless protein domain is shown in red.

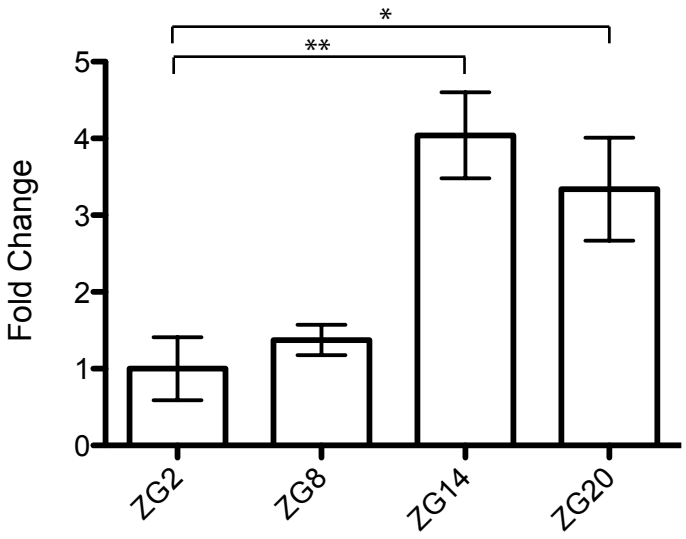

Figure B-6: Expression of *estimeless* in wild-caught adult light organs over the day/night cycle. Graphs indicate the relative expression of *estimeless* as measured by qRT-PCR ZG = Zeitgeber, or time after the onset of light in a 12h/12h day/night cycle. All data were normalized to the time point of lowest expression in each graph. Error bars represent the standard error of the mean. N= 2 to 6 biological replicates and 2 technical replicates per condition. * = Tukey's pairwise comparison $p < 0.05$, ** = Tukey's pairwise comparison $p < 0.01$.

MATERIALS AND METHODS:

Identification of Timeless and Period Sequences from Transcriptional Databases

A Timeless-like sequence was identified by a tblastn search against the EST database of the juvenile-host light organ (Chun *et al.*, 2006) and a tblastn search against the RNASeq library of the same organ (Kremer *et al.*, 2013) using *Drosophila* Timeless. Sequence for EsPeriod was identified in a 4-week transcriptional library (Kremer, unpublished) of the host light organ by a tblastn search using *Drosophila* Period. These sequences were used for primer design for subsequent sequence analysis.

RNA and cDNA Preparation

Whole juvenile animals were stored in RNALater RNA stabilization Reagent (Qiagen, Valencia, CA) for 24h at 4°C and then at -80°C until ready for RNA extraction. RNA was extracted from light organs, whole heads, or eyes using the RNeasy Fibrous Tissue Mini Kit (Qiagen, Valencia, CA) after homogenizing tissues in a TissueLyser LT (Qiagen, Valencia, CA). Three to six biological replicates were used per condition per experiment. The samples were treated with the Ambion TURBO DNA-*free* kit (Life Technologies, Grand Island, NY) to remove any contaminating DNA. The samples were then quantified using a Qubit 2.0 Fluorometer (Life Technologies, Grand Island, NY) and 5 μL were separated on a 1% agarose gel to ensure the quality of the RNA. If not used immediately, samples were aliquoted and then stored at -80°C. cDNA synthesis was performed with SMART MMLV Reverse Transcriptase (Clontech, Mountain View, CA) according to the manufacturer's instructions, and then reactions were diluted to a concentration of 2.08 ng/μL using nuclease-free water and stored at 4°C.

Quantitative Reverse Transcripase PCR

All qRT-PCR assays were performed in compliance with the MIQE Guidelines (Bustin *et al.*, 2009). Gene-specific primers were designed to *estimeless*, and the *Euprymna scolopes* 40S ribosomal RNA sequence was used as a control for equal well loading. Primers: *40S* F: AATCTCGGCGTCCTTGAGAA, *40S* R: GCATCAATTGCACGACGAGT, *estimeless* F: *estimeless* R: For each experiment, negative controls were run without template and with cDNA reactions run with no reverse transcriptase to ensure the absence of chromosomal DNA in the reaction wells. The efficiencies of all qRT-PCR primer sets were between 95 and 100%. Data were analyzed using the ΔΔCq method (Pfaffl, 2001). qRT-PCR was performed on *E.* scolopes cDNA using iQSYBR Green Supermix or SsoAdvanced SYBR Green Supermix (BioRad, Hercules, CA) in an iCycler Thermal Cycler or a CFX Connect Real-Time System (BioRad, Hercules, CA). Amplification was performed under the following conditions: 95°C for 5 min, followed by 45 cycles of 95°C for 15 sec, 60°C for 15 sec, and 72°C for 15 sec. Each reaction was performed in duplicate and contained 0.2 μM primers and 10.4 ng cDNA. To determine whether a single amplicon resulted from the PCR reactions, the presence of one optimal dissociation temperature for each PCR reaction was assayed by incrementally increasing the temperature every 10 sec from 60 to 89.5°C. Each reaction in this study had a single dissociation peak. Standard curves were created using a 10-fold dilution series of the PCR product with each primer set.

Statistics

All statistics were performed in GraphPad Prism.

REFERENCES:

Bustin, S.A., Benes, V., Garson, J.A., Hellemans, J., Huggett, J., Kubista, M., *et al.* (2009) The MIQE guidelines: minimum information for publication of quantitative real-time PCR experiments. *Clin Chem* **55**: 611–622.

Chang, D.C., and Reppert, S.M. (2003) A novel C-terminal domain of *Drosophila* PERIOD inhibits dCLOCK:CYCLE-mediated transcription. *Curr Biol* **13**: 758–762.

Chun, C.K., Scheetz, T.E., Bonaldo Mde, F., Brown, B., Clemens, A., Crookes-Goodson, W.J., *et al.* (2006) An annotated cDNA library of juvenile *Euprymna scolopes* with and without colonization by the symbiont *Vibrio fischeri*. *BMC genomics* **7**: 154.

Constance, C.M., Green, C.B., Tei, H., and Block, G.D. (2002) *Bulla gouldiana* period exhibits unique regulation at the mRNA and protein levels. *J Biol Rhythms* **17**: 413–427.

Kremer, N., Philipp, E.E., Carpentier, M.C., Brennan, C.A., Kraemer, L., Altura, M.A., *et al.* (2013) Initial Symbiont Contact Orchestrates Host-Organ-wide Transcriptional Changes that Prime Tissue Colonization. *Cell Host Microbe* **14**: 183–194.

Pfaffl, M.W. (2001) A new mathematical model for relative quantification in real-time RT-PCR. *Nucleic Acids Res* **29**: e45.

Tomioka, K., and Matsumoto, A. (2010) A comparative view of insect circadian clock systems. *Cell Mol Life Sci* **67**: 1397–1406.